GD | C-63-032

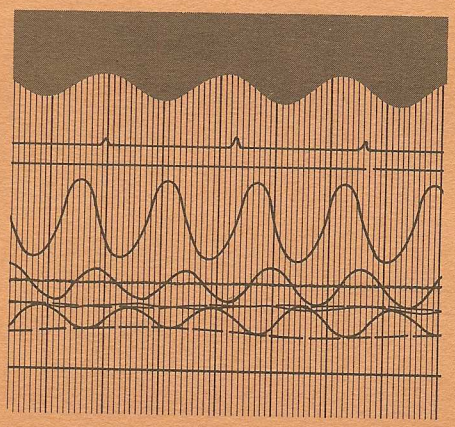

# FLAPPED HYDROFOILS IN WAVES, SUBCAVITATING FLOW

## TECHNICAL REPORT

**MAY 1963**

GENERAL DYNAMICS | CONVAIR
Post Office Box 1950, San Diego 12, California

GDC-63-032

# FLAPPED HYDROFOILS IN WAVES, SUBCAVITATING FLOW

Prepared by

A. C. Conolly

May 1963

Contract Nonr-3180(00)
Task No. NR062-252

# ABSTRACT

This report presents tank test data for a rectangular flapped hydrofoil mounted to the carriage by a single strut. Tests were carried out separately with flaps oscillating in smooth water, flaps fixed in regular waves, and then various combinations of conditions with flaps oscillating in regular waves. The separate effects of flap and wave on the force and moment coefficients for the hydrofoil were obtained, and compared with the results when both flap and wave were cycled together.

# CONTENTS

# TABLES

## ILLUSTRATIONS

# 1 | INTRODUCTION

The purpose of the test program described in this report was to experimentally determine the effects of wave and flap motions and possible intermittent ventilation on hydrofoil forces and moments. In order to do this, the program was divided into four test phases:

a. Tests in smooth water with flaps cycled at various frequencies.

b. Tests in regular waves with flaps fixed, running in both head and following seas.

c. Tests in regular waves with flaps cycled at various frequencies, in both head and following seas.

d. Tests with flaps driven through a 1/2 cycle at high frequency in smooth water, to determine the effect of sudden flap deflections on the hydrofoil forces and moments.

By comparison of the results of a, b and c it was possible to isolate and evaluate the force and moment variations caused by wave action and the variations caused by flap motion. The individual wave profiles were measured and correlated with the hydrofoil forces and moments.

The hydrofoil tested had an NACA 16-309 section and was capable of being fitted with four different flap sizes. It was the same hydrofoil model used in the tests reported in Reference 1. The measurements obtained during unsteady flow conditions were therefore compared with the results given in Reference 1.

Data is presented in coefficient form (in both tables and graphs) in this report. In certain cases time histories have been produced to bring out salient points and to show the effect of having two forcing functions (wave and flap) of different frequencies.

# 2 | MODEL DESCRIPTION AND INSTRUMENTATION

## 2.1 MODEL DESCRIPTION

The model used in this test program was the same as that used in tests reported in Reference 1; consequently, only a brief description will be given here. It exhibited a span of 24 inches, a chord of 4.0 inches, and a rectangular planform with a NACA 16-309 section. The model was fitted with simple flaps as follows:

| Flap Configuration | $c_f/c$ | $b_f/b$ |
|---|---|---|
| 1 | 0.3 | 0.6 |
| 2 | 0.3 | 0.8 |
| 3 | 0.2 | 0.6 |
| 4 | 0.2 | 0.8 |

The single center strut was enclosed in a double ogive fairing which did not touch the foil or strut, and thus strut drag was eliminated from the test results. Figure 1 shows the model with Flap Configuration No. 3. Figure 2 is a schematic drawing of the model and balances, and also shows the method of flap cycling.

The strain gages were waterproofed with Dijell wax, which was melted first and then brushed on. The gages were then coated with Ten-X waterproofing compound for mechanical protection.

## 2.2 INSTRUMENTATION

Forces were measured by means of strain gage balances mounted at the top of the strut (Figure 1). Data was recorded on a Consolidated Electrodynamics

Corp. (CEC) oscillograph, Type 5-114-P3-26. The circuit incorporated a CEC 3-kc amplifier with an output calibration circuit, and a variable attenuation and galvanometer damping circuit. This enabled amplifier output to be maintained within 1%.

Model velocity was obtained from a carriage-mounted photocell, whose signal on the oscillograph trace was deflected by interrupters placed every five feet along the carriage rails.

Wave contours were measured during each test by a sonic-type wave recorder developed and constructed by the University of Minnesota-St. Anthony Falls Hydraulics Laboratory (Reference 3). The wave recorder was mounted on the carriage to measure wave amplitudes at the foil 1/4-chord point.

Flap position was recorded continuously by a strain gage balance connected to the flap bell-crank. No readings were taken of flap forces and moments.

A 16-mm Eyemo motion picture camera was mounted on the carriage to document possible intermittent cavitation or ventilation on the foil and strut.

# 3 | TEST PROCEDURE

The test program was conducted in the 300-foot General Dynamics/Convair hydrodynamics towing tank (Reference 2). The model was tested at constant velocities between 18 and 32 ft/sec. approximately. It was run at fixed depths (1/4-chord point to smooth water level) of between 3 and 5 inches, and with fixed wing angles of attack between -5 and +10 deg. Flap oscillation frequencies which were constant for any given run, varied between 0.5 and 7.0 cycles per second. Regular waves from the paddle-type wavemaker, again constant for any run, were varied between 2 inches and 4 inches in height, and between 3.5 and 8.25 ft. in length (i.e., 20:1 to 24:1 approx.)

Flap angles were varied through the range -8 to +8 degrees during cycling tests, between -5 and +10 degrees for flaps fixed in wave tests, and between 0 and +16 degrees for 1/2 cycle tests. Positive values denote flaps deflected downward.

The procedure when testing with flaps cycling in waves was to choose a flap frequency, wave size and model velocity such that the frequency of encounter with a wave was almost the same as the frequency of oscillation of the flap. Usually, two runs were carried out under identical conditions in order to get instantaneous phase relationships between flap down and wave peak between $\pi$ radians lag, progressing through the "in-phase" condition to $\pi$ radians lead.

# 4 | METHOD OF ANALYSIS

## 4.1 TESTS IN SMOOTH WATER WITH FLAPS CYCLED AT VARIOUS FREQUENCIES

The purpose of this part of the program was to determine the frequency response of the system by sinusoidally moving the flaps.

Data from tests covered in Reference 1, with flap cycling frequencies of 0.50 to 1.66 cycles per second, were combined with more recent data with flap cycling frequencies between 3.0 and 7.0 cycles per second.

Average values of maximum and minimum trace readings for lift, drag, pitching moment and flap deflection were read from the oscillograph traces. The force and moment equations were programmed into the IBM 704 computer and $C_L$, $C_D$, and $C_M$ for the foil were read out.

The lift, drag, and moment traces were read at close intervals (i.e., as time histories) throughout the force cycles in order to determine the true maximum and minimum values of drag. Maximum and minimum drag could not be determined from inspection of the oscillograph traces because of the effects of balance interactions.

Phase relationships of the force coefficients were read as lead (positive) or lag (negative) in radians of the maximum values to the maximum flap down position. They were obtained by measuring from the oscillograph trace the time distance between the flap down and the force peak, and arithmetically solving for $\phi$ by the equation

$$\frac{\phi}{2\pi} = \frac{t}{T_1} \quad ,$$

where $T_1$ was the time distance from flap down to the next flap down (flap cycling period). If the force peak occurred later than maximum flap down position it was defined as lagging.

The frequency of flap oscillation was obtained from the oscillograph trace by measuring the time interval between successive peaks. Then

$$\omega_f = \frac{2\pi}{T_1} \text{ rads/sec.}$$

Force coefficient and flap amplitudes were defined as 1/2 (max. value - min. value). There was a tendency for the flapping mechanism to deflect slightly under heavy load, thus causing slight indentations in the sine traces of the almost simple harmonic motion of the flaps. However, the frequency of oscillation held very steady and was easily read from the traces.

## 4.2 TESTS IN REGULAR WAVES WITH FLAPS FIXED — HEAD AND FOLLOWING SEAS

The data was analyzed in the same manner as for flaps cycling in smooth water (described previously). Phase relationships of the force coefficients were read as lead, or lag, of the maximum values to the wave peak. Waves varied in size slightly during the course of each run, and thus average values of amplitude and phase angles were read from the oscillograph traces.

The frequency of wave encounter was obtained from the oscillograph trace by measuring the time interval between successive peaks, $T_2$ then,

$$\nu = \frac{2\pi}{T_2} \text{ rads/sec.}$$

Force coefficient and wave amplitudes were defined as 1/2 (max. value - min. value). Wave length was determined by solving the following simultaneous equations: The frequency of wave encounter

$$\nu = \frac{2\pi}{\lambda_K}\left(U_\infty \pm V_\omega\right), \tag{1}$$

where (+) indicates head seas and (-) indicates following seas.

The velocity of a trochoidal wave

$$V_\omega = \sqrt{\frac{g \cdot \lambda_K}{2\pi}} \quad . \tag{2}$$

a. Head Sea Case

From Equation (1)

$$V_\omega = \left(\frac{\nu\lambda_K}{2\pi} - U_\infty\right) .$$

Wave length

$$\lambda_K = \frac{2\pi V_\omega^2}{g}$$

$$= \frac{2\pi}{g}\left(\frac{\nu\lambda_K}{2\pi} - U_\infty\right)^2 .$$

$$\lambda_K = \frac{2\pi}{g}\left(\frac{\nu^2\lambda_K^2}{4\pi^2} + U_\infty^2 - \frac{U_\infty \nu \lambda_K}{\pi}\right)$$

$$= \frac{\nu^2\lambda_K^2}{2\pi g} + \frac{2\pi U_\infty^2}{g} - \frac{2U_\infty \nu\lambda_K}{g}$$

$$\therefore \quad \frac{\nu^2\lambda_K^2}{2\pi g} - \left(\frac{2U_\infty \nu}{g} + 1\right)\lambda_K + \frac{2\pi U_\infty^2}{g} = 0$$

$$\therefore \quad \lambda_K = \left\{\frac{\pi g\left(\frac{2U_\infty \nu}{g} + 1\right)}{\nu^2}\right\} \pm \left\{\frac{\pi g\sqrt{\left(\frac{2U_\infty \nu}{g} + 1\right)^2 - \frac{4\nu^2 U_\infty^2}{g^2}}}{\nu^2}\right\}$$

b. Following Sea Case

From Equation (1)

$$V_\omega = \left(U_\infty - \frac{\nu \lambda_K}{2\pi}\right)$$

$$\lambda_K = \frac{2\pi V_\omega^2}{g}$$

$$= \frac{2\pi}{g}\left(U_\infty - \frac{\nu \lambda_K}{2\pi}\right)^2$$

$$= \frac{2\pi}{g}\left(U_\infty^2 + \frac{\nu^2 \lambda_K^2}{4\pi^2} - \frac{U_\infty \nu \lambda_K}{\pi}\right)$$

Consequently, the expression for wavelength is the same for both head and following seas. Take second term in equation at the bottom of page 9 as positive for head seas and negative for following seas.

## 4.3 TESTS IN REGULAR WAVES WITH FLAPS CYCLING — HEAD AND FOLLOWING SEAS

Data was read from the oscillograph traces in exactly the same way as for the two previous cases. Phase relationships of the force coefficients were read as lead or lag of the maximum values to the wave peak. But in addition there was (at any time during a run) an instantaneous phase relationship between the flap position and the wave. This was defined as a lead if the maximum flap-down position occurred $\pi$ radians or less ahead of the wave peak. In order to obtain the phase in radians, the reference was taken as the encounter period of the wave in seconds — the same as for the force coefficient phase angles.

Because of the varying phase relationship between the flap and the wave, it was not possible to average the waves to take account of variations in wave size, and all values had to be read as close as possible to the times at which flap-wave phases were equal to $+\pi$, $+\pi/2$, $0$, $-\pi/2$ and $-\pi$. This meant that the results

for flaps cycling in waves could not be so accurate as for flaps fixed in waves. However, errors caused by this source were very much diminished by the fact that the flap is by far the more powerful forcing function.

Wave lengths were again calculated as for the flaps fixed in waves case.

## 4.4 DATA ANALYSIS ON TIME BASIS

The purpose of this part of the analysis was to get force and moment coefficients from 1) Steady-state data, flaps fixed in smooth water; 2) Data for flaps fixed in waves; and 3) Data for flaps cycling in smooth water. These three sets of data were added together in a time history and compared with the measured total as given by tests with flaps cycling in waves.

Because of the difference in frequency of the two forcing functions (wave and flap), there will be a "beating" of the resultant force and moment coefficients; i.e., the amplitudes of the oscillations will rise and fall periodically over a number of oscillations. The period of this "beating" will be of longer time duration as the frequencies of the two forcing functions come closer together. This effect was clearly observed on the oscillograph traces. See Figure 67 for a typical record, and Figures 34 through 37 for plots of the envelopes of $C_L$ with flap phase.

At any time from $t = 0$ $\begin{cases} \text{Wave amplitude } A_{K_t} = A_K \times \sin \nu t. \\ \text{Flap Deflection } = \delta_{f_t} = \delta_f \times \sin (\omega_f t + \phi_1). \end{cases}$

Adding wave and flap effects

$$\Delta C_{L_{(t)}} = \left(\frac{C_L}{A_K}\right)_\nu \times A_K \times \sin \left[\nu_t + \phi_{L_1}\right]$$

$$+ \left(\frac{C_L}{\delta_f}\right)_{\omega_f} \times \delta_f \times \sin \left[\left(\omega_f t + \phi_1\right) + \phi_{L_2}\right].$$

Similar expressions can be derived for $\Delta C_{D_{(t)}}$ and $\Delta C_{M_{(t)}}$. Values of force and moment amplitude ratio and phase relationships are read from Figures 3 through 20.

# 5 | DISCUSSION OF TEST RESULTS

## 5.1 GENERAL

The results of the tests are presented in coefficient form in Tables 2 through 17. $C_L$ and $C_D$ were obtained normal and parallel to the water surface respectively, and $C_M$ was measured at the 1/4-chord point. Total drag measurements were not corrected for interference effects due to the presence of the center strut, as this was found to be very small. (See Figure 25 of Reference 1.)

There was no evidence of cavitation or ventilation in any of the tests. The approximate test variables for which data has been obtained are summarized in Table 1. Not all combinations of the variables were tested; consequently, Table 1 must be read in conjunction with Tables 2 through 17.

## 5.2 FLAPS CYCLING IN SMOOTH WATER

Graphs have been plotted of

$\frac{\Delta C_{L_2}}{\Delta \delta_f}$ and $\phi_{L_2}$ ( the phase of maximum $C_L$ to the flap-down position) against a base of flap cycling frequency in radians/sec. Similar graphs have been plotted for

$$\frac{\Delta C_{D_2}}{\Delta \delta_f} \text{ and } \frac{\Delta C_{M_2}}{\Delta \delta_f} .$$

Figures 3 through 8 show these graphs for all four flap configurations.

Table 1. Summary of Approximate Test Variables

| Type of Test | Flaps Cycling in Smooth Water | Flaps Fixed in Waves | | Flaps Cycling in Waves | | Flaps Deflected 1/2 Cycle |
|---|---|---|---|---|---|---|
| | | Head Sea | Following Sea | Head Sea | Following Sea | |
| Flap Configuration | 1,2,3,4 | 1,2,3,4 | 1,2,3,4 | 1,2,3,4 | 1,2,3,4 | 1,2,3,4 |
| Depth of 1/4-Chord (Inches) | 4 | 4 | 3,4,5 | 4 | 4 | 4 |
| Wave Height - Trough to Crest (Inches) | - | 4 | 2,3,4 | 2,4 | 2,4 | - |
| Wavelength (Ft.) | - | 8 | 3.5 to 8.25 | 3.5 to 8.25 | 3.5 to 8.25 | - |
| Angle of Attack of Foil (Degrees) | 0, +5 | -5,0, +5,+10 | +5 | +5 | +5 | +5 |
| Flap Angle (Degrees) | 0 ± 8 | -5, 0 +5,+10 | +10 | 0 ± 8 | 0 ± 8 | 0 to +16 |
| Velocity (Ft./Sec.) | 30 | 18-32 | 18-32 | 20,30 | 20,30 | 30 |
| Flap Frequency (Cycles/Sec.) | .5 to 7.0 | - | - | 2.0 to 7.5 | 2.0 to 7.5 | 1.6 to 6.5 |

It will be noted that $\frac{\Delta C_{L_2}}{\Delta \delta_f}$

tends to increase with increase of flap cycling frequency, and this may mean that there is no flow separation at the higher frequencies. However, this possibility was not investigated.

With regard to

$$\frac{\Delta C_{D_2}}{\Delta \delta_f} ,$$

it will be noted that the flap cycling tests of Reference 1 (with the lowest cycling rates) were performed at foil angle of attack of zero degrees, whereas the later cycling tests at higher cycling rates were done at angle of attack of +5 degrees. Now the $C_D \sim \alpha$ curves for flaps fixed in smooth water are "trough" shaped with minimums for the different flap angles occurring at approximately $\alpha = 0°$. At $\alpha = 5°$, $C_D$ increases progressively when $\delta_f$ is moved from negative, through zero, to positive. However, at $\alpha = 0°$, $C_D$ may be greater at $\delta_f$ $-5°$, for example, than it is at $\delta_f = 0°$. This is probably the cause of the scatter in the tests points for

$$\frac{\Delta C_{D_2}}{\Delta \delta_f}$$

and drag phase angle at the lowest flap frequencies.

Force and moment phase lag increases with increase of cycling frequency, and would probably reach a value of $\pi$ at very high frequencies.

Average values of $C_{L_2}$, $C_{D_2}$ and $C_{M_2}$ were plotted against cycling frequency (Figures 21 through 25) and were found to be close (within limits of experimental error) to the steady-state values for $\alpha = 5°$. However, at $\alpha = 0°$ values of $C_{D_2}$ tended to be negative. No explanation is offered for this, but the data was carefully checked and is felt to be good. Negative drags did not occur in any other test.

## 5.3 FLAPS FIXED IN REGULAR WAVES

Graphs have been plotted of the non-dimensional coefficient

$$\frac{\triangle C_{L_1}}{A_K}\left(\frac{C}{2}\right)$$

and the phase of maximum $C_L$ to the wave peak, against a base of frequency of wave encounter in radians/sec. Similar graphs have been plotted for

$$\frac{\triangle C_{D_1}}{A_K}\left(\frac{C}{2}\right)$$

and

$$\frac{\triangle C_{M_1}}{A_K}\left(\frac{C}{2}\right)$$

These are shown in Figures 9 through 20 for all 4 flap configurations, and for both head and following sea conditions.

It was observed that there was a pronounced difference in the phase relationships between head and following seas. Because of the orbital velocity of the wave, the maximum lift occurs approximately $\pi/2$ radians ahead of the wave peak in a head sea, and approximately $\pi/2$ radians after the wave peak in a following sea. This is because of the change of effective angle of attack on the foil as it passes through the waves.

The frequency of wave encounter was defined as

$$\nu = \frac{2\pi}{\lambda_K}\left(U_\infty \pm V_\omega\right) \text{ radians/sec.}$$

The positive sign is taken with head seas, and the negative sign with following seas. Other experimenters, notably those discussed in Reference 5, have used a non-dimensional reduced frequency, which is useful where comparisons have to be made.

This is defined as:

$$\text{Reduced frequency} = \frac{\nu c}{2U_\infty},$$

$$= \frac{c}{2U_\infty} \times \frac{2\pi}{\lambda_K} \left(U_\infty \pm V_\omega\right),$$

$$= \frac{c\,\pi}{U_\infty \lambda_K} \left(U_\infty \pm V_\omega\right).$$

For head sea tests with flaps fixed,the same wave was used throughout, and therefore the reduced frequency remained almost the same even though the velocity changed. Consequently, it was not possible to use this form for graphical presentation of the results.

The oscillatory lift parameter decreases slowly with increase of $\nu$ for all four flap configurations in a head sea, and increases slowly for all configurations in a following sea. This is in agreement with Reference 4, Page 10, where it is noted that the unsteady lift effects are decreased in head seas with increasing velocity for the same range of wave conditions.

In general, it appears that the angle of attack of the foil, and flap angle, have little effect on the oscillatory lift coefficient in waves. (See Figures 9, 10, 15, 16.) Head sea tests were carried out at $\alpha = -5°$, $0°$, $5°$, $10°$, and $\delta_f = -5°$, $0°$, $5°$, $10°$, whereas following sea tests were all carried out at $\alpha = 5°$ and $\delta_f = 10°$.

The oscillatory drag parameter decreases slowly with increase of $\nu$ for all four flap configurations in a head sea, but is almost constant for all configurations in a following sea.

Drag is out of phase with lift in head seas. It has been suggested that this may be caused by leading edge suction. If the suction force increases with increase of instantaneous angle of attack in head seas as the foil approaches the

wave peak, then it would be expected to increase commensurately with increase of lift. This suction force would therefore act in complete opposition to the drag because of lift, and would tend to shift the phase angle of the drag relative to the wave.

In Reference 6, J. M. Wetzell gives another explanation of how lift and drag become out of phase, and also how it is possible for even negative drags to occur. To quote Reference 6, with explanations for Reference 4 that are applicable to this present report: "The lift and drag were measured perpendicular and parallel to the still water surface. As the instantaneous angle of attack was increased (up-wash) by the orbital velocity of the wave, the true lift and drag with respect to the instantaneous velocity vector also increased. However, the resultant force vector tilted forward, thereby increasing the measured lift and decreasing the measured drag. A downwash effect would decrease the measured lift and increase the measured drag. Thus, for quasi-steady conditions the lift and drag should be out of phase about 180 degrees, measurements in head seas (Figures 6 and 10 of Reference 4) indicate about 230 degrees. It may also be possible to obtain negative drags if the instantaneous angle of attack is sufficient to tilt the force vector forward of the vertical for part of the cycle, and if the steady drag is low. It should be mentioned that the drag reduction in an upwash can be expected only in a wetted, non-separated flow." These remarks are directly applicable to this present report, as flow was fully wetted, and lift and drag were also measured perpendicular and parallel to the water surface. In these tests lift and drag were out of phase in head seas by about 220 degrees.

There is considerable scatter in the test points for the oscillatory pitching moment parameter plotted against frequency of wave encounter in head seas, but there appears to be very little change in this parameter as frequency is increased (Figures 13, 14). In a following sea the oscillatory pitching moment parameter increases with increase of frequency for all four flap configurations (Figures 19, 20). The pitching moment oscillograph traces follow the lift traces

closely, and the maximum and minimum pitching moments occur at nearly the same phase angles as the lift maximum and minimums. In head seas the pitching moment leads the lift slightly, and in following seas it lags slightly.

Figures 26, 27, 28 and 29 show mean values of force coefficients for tests with flaps fixed in waves, for both head and following seas. Results indicate that within the range of frequencies tested there is slight decrease in both lift and drag as frequency of encounter increases. This is true for all positions of the wing and flap settings, and for all flap configurations, but particularly for Configurations 3 and 4.

Figure 30 shows mean values of pitching moment coefficient for all flap configurations in both head and following seas. Within the limits of experimental error there is very little change of mean pitching moment coefficients from the steady-state values of Reference 1.

## 5.4 FLAPS CYCLING IN REGULAR WAVES

The plotting of data from these tests is complicated because there are two forcing functions (flap and wave) of different frequencies. The forces and moments not only have phase relationships with the wave, but different phase relationships with the flap. Actually, all measured phases (which are instantaneous in this case) have been referred to the wave as the basic forcing function. The oscillatory force and moment coefficients would vary with both frequency of wave encounter and frequency of flap oscillation, as well as with the phase relationship of the flap to the wave. Consequently, the best way to analyze this data is in terms of continuous time histories (described in Paragraph 5.5). However, to cover all of the data in this way would be exceedingly lengthy and time consuming, and there are various other ways to plot in order to summarize and bring out the salient points. Figures 31, 32 and 33 present plots of average $C_L$, $C_D$ and $C_M$ respectively, against a combined frequency of flap and wave in radians per second. In general, there is a slight falling off in $C_L$ as frequency increases, $C_D$ remains sensibly constant and $C_M$ becomes slightly more

negative. The points for head and following seas fall very close to the same curves.

In Figures 34 through 37 instantaneous maximum and minimum lift coefficients have been plotted against the phase of the flap to the wave, for all flap configurations in head and following seas. The curves are really envelopes of the $\Delta C_L$ and show the harmonic "beating" of $\Delta C_L$ with change of phase between the two forcing functions. This effect can also be seen in the representative oscillograph trace in Figure 67, where there is a large frequency difference between the flap cycle and the wave cycle. It will be noted that in head seas $\Delta C_L$ is a maximum where the flap-down position leads the wave peak by $\pi/2$ radians, and that in following seas $\Delta C_L$ is a maximum where the flap lags the wave by $\pi/2$. This would be expected since these are the points where there is maximum disturbance input.

Figures 38, 39, 40, and 41 present curves of instantaneous maximum and minimum drag coefficients plotted against the phase of the flap to the wave, for all flap configurations in head and following seas. These curves do not exhibit so clearly as those of lift coefficient the change of drag with phase change between the forcing functions. Figures 42 and 43 show that there is little change of maximum instantaneous $C_M$ when plotted against the phase of the flap to the wave, in head or following seas.

Figure 54 is a summary plot that was prepared of an oscillatory lift parameter against frequency in radians per second. With this plot it is possible to compare on one sheet the tests with flaps cycling in waves, flaps cycling in smooth water and flaps fixed in waves for all four flap configurations in both head and following seas:

a. For flaps cycling in waves, the oscillatory lift parameter was taken as

$$\frac{\left(\Delta C_{L_3}\right)^2}{A_K \cdot \delta_f} \times \frac{C}{2} \quad ,$$

which brings in the effects of both flap and wave, and the frequency factor was taken as $\sqrt{\nu \cdot \omega_f}$ radians/sec.

b. For flaps cycling in smooth water, and flaps fixed in waves, a combined oscillatory lift parameter was taken as

$$\frac{\left(\Delta C_{L_1} + \Delta C_{L_2}\right)^2}{A_K \cdot \delta_f} \times \frac{C}{2} ,$$

which was again plotted against the combined frequency factor $\sqrt{\nu \cdot \omega_f}$ radians/sec.

Values of $\Delta C_{L_3}$ were read from the Summary Tables 14, 15, 16, and 17 as maximum values, at maximum flap down leading the wave peak by $\pi/2$ radians for head seas, and lagging by $\pi/2$ radians in following seas.

Figures 54 shows that for each flap configuration the oscillatory lift parameters for the different cases fall on the same curve for both head and following seas. Thus, the separate effects of flap and wave can be evaluated and then added together vectorially to give the combined effects with both flap and wave acting together.

Figure 55 is a summary diagram of flap and wave effectiveness in lift for all flap configurations in both head and following seas. It can be seen that for all flap configurations except No. 3 the flap is a very much more powerful forcing function than the wave and could easily cancel changes in $C_L$ caused by running through waves. Both Figures 54 and 55 show that much more flap effectiveness is derived from increase of flap chord than from increase of flap span. Phase relationships for flaps cycling in waves are presented in Figures 62 through 66. For Flap Configurations 1 and 2 in head seas, Figures 62 and 63 show that drag lags lift and that pitching moment lags drag fairly consistently by about 20 degrees each for all phase relationships between flap and wave. As the phase of flap to wave progresses from lag to lead, the phases of lift, drag and pitching moment become more leading. However, when the flap is in phase

with the wave, forces and moments are all lagging the wave. At a higher frequency of wave encounter and flap oscillation all forces and moments are more lagging to the wave than at a lower frequency. Considering Figures 64 and 65, for Flap Configurations 3 and 4 in head seas, roughly the same conclusions apply, but there is much more scatter in the data.

In following seas, the scatter was very bad, and made graph plotting impossible except for Flap Configuration 2 which had the largest flap. Figure 66 shows that Flap Configuration 2 in a following sea exhibited approximately the same characteristics as in a head sea.

## 5.5 TIME HISTORY ANALYSIS TO ISOLATE EFFECTS OF FLAP MOTIONS FROM EFFECTS OF WAVE MOTIONS

All comparisons were made with Flap Configuration No. 1 ($c_f/c = .3$, $b_f/b = .6$), but a variety of conditions was chosen to show that the method works for head and following seas, and for different instantaneous phase relationships between flap and wave. The results are shown in Figures 44 through 53.

Figures 44, 45 and 46 present lift, drag and pitching moment variation respectively, for Test Run 13191 through two complete cycles starting with $\pi/2$ radians flap lag and finishing with flap and wave in phase. The wave frequency of encounter was 4.72 cycles/sec. The wave height (trough to crest) was 1.73 inches and its length, 3.66 ft. The flap frequency was 6.30 cycles/sec. This was a following sea case.

$C_L$ variation with flaps cycling in waves agrees very closely with $C_L$ obtained by adding 1) components caused by flaps fixed in calm water (Reference 1), 2) components caused by flaps cycling in smooth water, and 3) components caused by flaps fixed in waves. Agreement is found in amplitude of oscillation, period and reduction in amplitude (i.e., beating) on going from flap "lag" to "in phase" conditions.

With $C_D$ it was found that there was good agreement in amplitude variation and period of oscillation, but the actual values of $C_D$ obtained by adding up separate components were an almost constant amount less than the values for flaps cycling in waves. This appears to be the result of an increase in the basic $C_D$ of the foil in going from steady to unsteady flow conditions. The same remarks apply to $C_M$, which was an almost constant amount more positive when made up of component parts.

Figure 47 shows the separate components of $\Delta C_L$ resulting from flap and $\Delta C_L$ caused by the wave for Run No. 13191. It can be seen that the flap is a very much more powerful forcing function than the wave, and could easily cancel out the variations of $C_L$ caused by the wave.

Figures 48, 49 and 50 present lift, drag and pitching moment variation respectively for Run No. 13157 at $\pi/2$ radians flap lead. Only one oscillation has been plotted since the two forcing functions were very nearly of the same frequency, and "beating" would be evident over a larger number of waves. The wave frequency of encounter was 3.42 cycles/sec. The wave height (trough to crest) was 3.77 inches and its length, 8.31 ft. The flap frequency was 3.22 cycles/sec. This was a head sea case.

There was good agreement for both lift and drag, but pitching moment was more positive by an almost constant amount when made up of component parts. Figures 51 and 53 present lift, drag and pitching moment variation for Test Run 13154, with flap lagging the wave by $\pi$ radians. Figure 52 and 53 present lift, drag and pitching moment variation for the same run, but with flap and wave in phase. The wave frequency of encounter was 7.88 cycles/sec. The wave height (trough to crest) was 1.51 inches and its length, 3.65 ft. The flap frequency was 7.35 cycles/sec. This again was a head sea case.

There was very close agreement in $C_L$ variation for both flap and wave, "out-of-phase" and "in-phase," and not much change in the actual values. $C_D$ again was a constant amount low when made up of component parts, for both

out-of-phase and in-phase conditions. $C_M$ showed very good agreement, both for actual values and for dimensions of the wave form.

It is felt that this detailed plotting of a small part of the experimental data obtained in the test program shows fairly conclusively that it is possible to isolate and evaluate the effects of flap motions from the effects of wave motion when running with flaps cycling in waves — if test results from flaps cycling in smooth water and flaps fixed in waves are available separately. It also shows that if a complicated wave of several superimposed sine waves is built up, it should be possible to obtain flap motions that would give a constant running $C_L$. This information would be useful to the hydrofoil boat designer but will require further analysis.

## 5.6 COMPARISONS WITH REFERENCE 1 SMOOTH WATER TESTS

Some of the figures that show comparisons with Reference 1 (flaps fixed in smooth water) were discussed previously in this section of the report. These are the plots of average force and moment coefficients against frequency of disturbance in radians per second (Figures 21 through 33). In general, these average force and moment coefficients show very good agreement, within the limits of experimental error, with the steady-state values. Sometimes average lift and drag coefficients are a little lower than steady state, and average pitching moment coefficients tend to be a little more negative. Figures 56 and 57 summarize some of the this data for average force coefficients. Figure 56 shows average values of lift coefficients for all four flap configurations at a constant angle of attack of 5° , and for flaps cycling in waves, flaps cycling in smooth water, and flaps fixed in waves (plotted against frequency in radians per second). The steady-state value of $C_L$ is 0.34. Figure 57 shows average values of drag coefficients at constant $\alpha = 5°$. The steady-state value of $C_D$ is 0.024. No particular trends are discernable from the curves, but it appears that there is not much change in the force coefficients from the steady-state value within the range of frequencies tested.

For the tests of flaps fixed in waves there was sufficient coverage of angle of attack to plot $C_L$ vs. $\alpha$ and $C_D$ vs. $\alpha$. These are compared with the steady-state curves from Reference 1, at a flap deflection of 10 degrees down in Figures 58 and 59. Two wave cases were evaluated: one where the wave encounter rate was 3 waves per second, and the other at 5 waves per second. Test points were plotted for head and following seas. The average force coefficients for flaps fixed in waves fall slightly below the steady-state curves, but are of the same form, and the lift curve slopes are the same. There is very little difference between the encounter rates of 3 or 5 waves per second, and these differences can probably be attributed to experimental scatter.

5.6.1 THE EFFECT OF DEPTH — In all of the tests described in this report the static depth of the 1/4-chord point of the foil was held steady at 1 chord, with the exception of tests with flaps fixed in waves in a following sea. Figure 60 presents values of the average lift coefficient plotted against the non-dimensional static depth of the foil (h/c) for all four flap configurations at $\alpha = 5°$ and $\delta_f = 10°$. As h/c drops from 1.25 to 0.75 the average $C_L$ falls about 10% for all four flap configurations. It is not possible to exactly compare this data with Figure 18 of Reference 1, because the Reference 1 plot is for Flap Configuration 2 only, at $\alpha = 2°$ and foil submergences (h/c) between 0.5 and 1.0. However, considering this case with a flap deflection of 10° down, as h/c drops from 1.0 to 0.5 the $C_L$ falls about 11%. Therefore, the foils running in waves exhibit approximately the same reduction in average lift on approaching the mean water surface as in the steady-state conditions.

## 5.7 COMPARISONS WITH REFERENCE 4

In Reference 4 (hydrofoils in regular waves tests) oscillatory lift parameter was plotted against wave length in feet, and oscillatory drag parameter against wave height. The plotting of the lift parameter against wave length had a theoretical basis, but the plotting of the drag parameter against wave height was arbitrarily adopted, since this parameter had little dependence on wave length.

In this report the only data obtained at a sufficiently large number of wave sizes was for flaps fixed in waves in a following sea. From Reference 4:

$$\text{Oscillatory lift parameter} = \frac{L_m}{ab\rho V^2} \quad \text{(Reference 4 symbols)},$$

$$= \frac{\Delta C_L \rho V^2 bc}{2A_K \cdot c\rho V^2} \quad \text{(symbols used in this report), and}$$

$$= \frac{\Delta C_L}{A_K}\left(\frac{b}{2}\right).$$

Similarly, oscillatory drag parameter

$$= \frac{\Delta C_D}{A_K}\left(\frac{b}{2}\right).$$

Figure 61 presents plots of

$$\left(\frac{\Delta C_{L_1}}{A_K}\right)\frac{b}{2}$$

against wave length $\lambda_K$ feet, and

$$\left(\frac{\Delta C_{D_1}}{A_K}\right)\frac{b}{2}$$

against wave height in feet (trough to crest), for Flap Configuration 1 at two speeds: 21 and 30 feet per second, and $\alpha = 5°$, $\delta_f = 10°$. As in Reference 4, the oscillatory lift parameter is fairly constant, falling slowly with increase of wave length. The actual values are lower, since the 16-309 is a low-lift, high-speed section when compared with the Wright 1903 tested in Reference 4. The oscillatory drag parameter falls with increase of wave-height; this is in opposition to Figure 10 of Reference 4. However, the drag change with wave is greater at the lower speed, which agrees with Reference 4.

## 5.8 ONE-HALF CYCLE TESTS IN SMOOTH WATER

Figures 68 through 76 present results of tests in which the flaps were driven through one-half of one cycle at various frequencies to determine the effect of sudden flap deflections on the hydrofoil forces and moments. Figure 77 presents a case where the flaps were driven through one complete cycle at 6.3 cycles/sec. These tests simulate sudden control motions which may occur during the operation of a full-scale hydrofoil vehicle.

It is noted from the curves that there is always considerable over-swing of $C_L$ and $C_M$, and to a much lesser extend of $C_D$. The maximum $C_L$ usually occurs just before the maximum flap-down position, and the maximum $C_D$ and $C_M$ just after maximum flap down. $C_M$ in particular does not become steady until about 100% of the flap deflection time has elapsed, after the flap is fully down. The overswing in $C_M$ may be up to 100% of the change resulting from steady flap deflection.

Except for the very low cycling rate of 1.6 cycles/sec., phase relationships between the flap, and the hydrofoil forces and moments, do not seem to be much affected by flap cycling rate within the range of frequencies tested. In the case where the flap was moved through one complete cycle (see Figure 77 for results on Flap Configuration 4), the peak values of $C_L$, $C_D$ and $C_M$ all occurred after the flap was in the full down position. As the flap returned to its original neutral position, $C_L$ and $C_D$ returned smoothly to their original values without overswing, but with $C_M$ there was again some overswing.

# 6 | RELIABILITY AND ACCURACY OF DATA

In general, the accuracy of the test points can be taken as ±5%. However, the accuracy of faired curves may be considerably better. The maximum frequency of the transient loads and moments obtained in waves was approximately 7 cycles/sec. The natural frequency of the complete model system was about 10 times this value; consequently, the force and moment variations could be read with good accuracy. Waves sometimes varied slightly both in height and length during any one run; therefore, the data had to be averaged over three or more waves.

Because the flap and its drive mechanism deflected slightly under very heavy loads, the flap deflection trace departed slightly at such times from a pure sinusoidal form. However, its frequency did not appear to vary. Flaps cycling in wave tests gave oscillograph traces which were essentially transitory in nature because of the different frequencies of the flap and the wave; consequently, this data is probably less accurate than that obtained from the other tests. It was read later, however, with the experience gained from reading all the earlier data, and so this may have increased its accuracy somewhat. Also, the flap was the stronger forcing function, and the flap trace was of more constant form than the wave trace — giving greater overall accuracy.

Of all the traces, the pitching moment was the worst one from the standpoint of harmonic distortion, especially with long waves in following seas. The lift trace exhibited good sinusoidal form (as did the wave), but the drag trace was masked by gage interactions. (See paragraph 4.1, Section 4.)

On page 11 of Reference 4 it is stated that an investigation was made of the wave profile used as the forcing function in the experiments. A harmonic analysis was made of several typical wave forms and a distortion of about 8 to 12% was found in most cases. In Reference 4 a harmonic analysis was also made on the lift traces.

No harmonic analysis was made on any of the data in this report. Consequently, the values presented for lift, drag and pitching moment represent peak-to-peak measurements taken directly from the records, rather than the maximum amplitude of the fundamental. Average values are $\left(\frac{\text{Max. Value + Min. Value}}{2}\right)$

In measuring phase angles it was found to be more difficult to measure drag phase angles in following seas than in head seas because the peak position fluctuated between waves. Therefore, it was rather difficult to select an average value. Also, the peaks were not sharply defined, but spanned a considerable length on the trace, and the midpoint fluctuated on each peak. In general, all phase angles were found to be difficult to measure accurately because the peaks were often not too clearly defined, and in flaps cycling in waves tests, phase relationships were transitory. This is illustrated in Figure 67, which presents a typical oscillograph record for flaps cycling in waves in a following sea. Note that the wave trace is inverted in Figure 67. This is a case where the flap frequency is considerably different from the wave frequency, and in three complete wave cycles the phase of the flap to the wave has changed from "in phase" to "$\pi$ lag" and back again to "in phase".

# 7 | CONCLUSIONS

a. The oscillatory lift coefficients and the oscillatory drag coefficients are not apparently affected by flap deflection or angle of attack within the range -5 degrees to +10 degrees.

b. The average values of lift, drag and pitching moment coefficients in unsteady flow do not vary much from the equivalent steady-state conditions.

c. It is possible to isolate and evaluate the separate effects of flap and wave motion, and then add these vectorially to get the combined effects of flap and wave acting together.

d. For the range of flap sizes and waves tested, the flap is by far the more powerful forcing function. Increase of flap chord has more effect than increase of flap span.

e. Flap 1/2-cycle tests show overswing of the force and moment coefficients, with center of pressure still moving up to 100% of the flap movement time beyond flap steady. There are varying phase relationships between force and moment coefficients and the flap.

f. No cavitation or intermittent ventilation was observed at any time.

# 8 | REFERENCES


1. Convair Report No. GDC-ZH-153, Flapped Hydrofoils in Smooth Water — Subcavitating Flow, C. E. Jones, Jr., November 1961.

2. Convair Report No. ZH-114, General Dynamics/Convair Hydrodynamics Laboratory.

3. St. Anthony Falls Hydraulic Laboratory (University of Minnesota) Memorandum No. M-74, The Sonic Surface-Wave Transducer, J. M. Killen, February 1959.

4. St. Anthony Falls Hydraulic Laboratory Project Report No. 64, Lift and Drag on Surface-Piercing Dihedral Hydrofoils in Regular Waves, J. M. Wetzel and F. R. Schiebe, September 1960.

5. St. Anthony Falls Hydraulic Laboratory Technical Paper No. 37-B, Longitudinal Motions and Stability of Two Hydrofoil Systems Free to Heave and Pitch in Regular Waves, J. M. Wetzel and W. H. Maxwell, December 1961.

6. Letter from J. M. Wetzel, Research Fellow, St. Anthony Falls Hydraulic Laboratory, to C. E. Jones, dated 12 April 1962.

ASSOCIATED REPORTS:

7. D. T. M. B. Report No. 1140, Experimental and Theoretical Studies of Hydrofoil Configurations in Regular Waves, P. Leehey and J. M. Steele, Jr., October 1957.

8. Work Sponsored by O.N.R., Contract No. N62-558-2236, On Oscillating Hydrofoils, Part I; S. Schuster and H. Schwanecke; December 1960, Part II; S. Schuster and H. Schwanecke; June 1962.

9. National Luchtvaartlab, Amsterdam Reports F-101, F-102, F-103, F-104; Experimental Determination of the Aerodynamic Coefficients of an Oscillating Wing in Incompressible, 2-Dimensional Flow; H. Greidanus and B. D. Van Vooren; 1952.

10. NACA Report No. 1108, Experimental Aerodynamic Derivatives of a Sinusoidally Oscillating Airfoil in 2-Dimensional Flow; R. L. Halfman, 1952.

11. NACA Technical Note No. 1372, Some Considerations on an Airfoil in an Oscillating Stream; J. M. Greenberg, 1947.

12. Dent. Luftfahrt-Forsch UM 1207, Results of Wind Tunnel Tests for the Determination of the Moments of the Aerodynamic Forces on an Oscillating Control Surface; F. Walter and W. Heger; 1944.

13. Journal of Aeronautical Sciences, 16; Readers Forum, p. 511; "Oscillating Aileron"; 1949.

14. Journal of Aeronautical Sciences, 15, p. 565-568, 1948; Journal of Aeronautical Sciences Errata,16, Oscillating Flap, p. 442-443, 1949.

# 9 | NOMENCLATURE

| | |
|---|---|
| $U_\infty$ | Model Velocity (Ft./Sec.). |
| $\alpha$ | Foil Angle of Attack (Degrees). |
| $\delta_f$ | Flap Angle (Degrees). |
| $\delta_{f_\tau}$ | Flap Angle (Radians). |
| $\triangle\delta_f$ | Flap, 1/2 Amplitude of Oscillation (Radians). |
| $A_K$ | Wave, 1/2 Amplitude (Ft.) |
| $\lambda_K$ | Wave Length (Ft.) |
| $\nu$ | Frequency of Wave Encounter (Rad./Sec.). |
| $V_\omega$ | Wave Velocity (Ft./Sec.). |
| $\omega_f$ | Frequency of Flap Oscillation (Rad./Sec.). |
| c | Hydrofoil Chord (Ft.). |
| b | Hydrofoil Span (Ft.). |
| $c_f$ | Flap Chord (Ft.). |
| $b_f$ | Flap Span (Ft.). |
| h | Depth of Foil 1/4-Chord Pt. (Ft.). |
| $H_0$ | Depth of Foil 1/4-Chord Pt. (In.). |
| L | Foil Lift Normal to Water Surface (Lb.). |
| D | Foil Drag Parallel to Water Surface (Lb.). |
| P. M. | Pitching Moment About Foil, 1/4-Chord Point, Positive Leading Edge Up (Lb./Ft.) |

$\rho$ Water Density (Slugs/Ft.$^3$).

$C_{L_1}$ Average Lift Coefficient, Flaps Fixed in Waves = $\dfrac{L}{1/2\rho\, U_\infty^2\, cb.}$

$C_{D_1}$ Average Drag Coefficient, Flaps Fixed in Waves = $\dfrac{D}{1/2\rho\, U_\infty^2\, cb.}$

$C_{M_1}$ Average Pitching Moment Coefficient, Flaps Fixed in Waves = $\dfrac{P.M.}{1/2\rho\, U_\infty^2\, c^2b.}$

$C_{L_2}$ Average Lift Coefficient, Flaps Cycling in Smooth Water.

$C_{D_2}$ Average Drag Coefficient, Flaps Cycling in Smooth Water.

$C_{M_2}$ Average Pitching Moment Coefficient, Flaps Cycling in Smooth Water.

$C_{L_3}$ Average Lift Coefficient, Flaps Cycling in Waves.

$C_{D_3}$ Average Drag Coefficient, Flaps Cycling in Waves.

$C_{M_3}$ Average Pitching Moment Coefficient, Flaps Cycling in Waves.

$\triangle C_{L_1}$ 1/2 Amplitude of $C_{L_1}$ Fluctuation, Flaps Fixed in Waves.

$\triangle C_{D_1}$ 1/2 Amplitude of $C_{D_1}$ Fluctuation, Flaps Fixed in Waves.

$\triangle C_{M_1}$ 1/2 Amplitude of $C_{M_1}$ Fluctuation, Flaps Fixed in Waves.

$\triangle C_{L_2}$ 1/2 Amplitude of $C_{L_2}$ Fluctuation, Flaps Cycling in Smooth Water.

$\triangle C_{D_2}$ 1/2 Amplitude of $C_{D_2}$ Fluctuation, Flaps Cycling in Smooth Water.

$\triangle C_{M_2}$ 1/2 Amplitude of $C_{M_2}$ Fluctuation, Flaps Cycling in Smooth Water.

$\triangle C_{L_3}$ 1/2 Amplitude of $C_{L_3}$ Fluctuation, Flaps Cycling in Waves.

$\Delta C_{D_3}$ 1/2 Amplitude of $C_{D_3}$ Fluctuation, Flaps Cycling in Waves.

$\Delta C_{M_3}$ 1/2 Amplitude of $C_{M_3}$ Fluctuation, Flaps Cycling in Waves.

$\phi_{L_1}$ Phase Lag or Lead Angle of Max. $C_{L_1}$ to Wave Peak (Radians).

$\phi_{D_1}$ Phase (negative lag) or (positive lead) Angle of Max. $C_{D_1}$ to Wave Peak (Radians).

$\phi_{M_1}$ Phase (negative lag) or (positive lead) Angle of Max. $C_{M_1}$ to Wave Peak (Radians).

$\phi_{L_2}$ Phase (negative lag) or (positive lead) Angle of Max. $C_{L_2}$ to Max. Flap Down (Radians).

$\phi_{D_2}$ Phase (negative lag) or (positive lead) Angle of Max. $C_{D_2}$ to Max. Flap Down (Radians).

$\phi_{M_2}$ Phase (negative lag) or (positive lead) Angle of Max. $C_{M_2}$ to Max. Flap Down (Radians).

$\phi_{L_3}$ Phase (negative lag) or (positive lead) Angle of Max. $C_{L_3}$ to Wave Peak (Radians).

$\phi_{D_3}$ Phase (negative lag) or (positive lead) Angle of Max. $C_{D_3}$ to Wave Peak (Radians).

$\phi_{M_3}$ Phase (negative lag) or (positive lead) Angle of Max. $C_{M_3}$ to Wave Peak (Radians).

$\phi_f$ Phase (negative lag) or (positive lead) Angle of Max. Flap Down to Wave Peak (Radians).

$\phi_1$ Instantaneous Phase of Flap to Wave, Referenced to Flap Frequency, and Measured at $t = 0$.

$t$ Time on Oscillograph Trace from Start of Time History (Seconds).

$\left(\frac{C_L}{A_K}\right)_\nu$ Lift Amplitude Ratio, Flaps Fixed in Waves.

$\left(\frac{C_D}{A_K}\right)_\nu$ Drag Amplitude Ratio, Flaps Fixed in Waves.

$\left(\frac{C_M}{A_K}\right)_\nu$ P. M. Amplitude Ratio, Flaps Fixed in Waves.

$\left(\frac{C_L}{\delta_f}\right)_{\omega_f}$ Lift Amplitude Ratio, Flaps Cycling in Smooth Water.

$\left(\frac{C_D}{\delta_f}\right)_{\omega_f}$ Drag Amplitude Ratio, Flaps Cycling in Smooth Water.

$\left(\frac{C_M}{\delta_f}\right)_{\omega_f}$ P. M. Amplitude Ratio, Flaps Cycling in Smooth Water.

Table 2. Flap Configuration 1; $c_f/c = 0.3, b_f/b = 0.6$; Tests in Smooth Water, Flaps Oscillating, Static h/c = 1.0

| Run No. | $U_\infty$ Ft./Sec. | $\Delta\delta_f$ Rad. | $\omega_f$ Rad./Sec. | $C_{L_2}$ | $C_{D_2}$ | $C_{M_2}$ | $\frac{\Delta C_{L_2}}{\Delta\delta_f}$ | $\phi_{L_2}$ Rad. | $\frac{\Delta C_{D_2}}{\Delta\delta_f}$ | $\phi_{D_2}$ Rad. | $\frac{\Delta C_{M_2}}{\Delta\delta_f}$ | $\phi_{M_2}$ Rad. | $\alpha°$ |
|---|---|---|---|---|---|---|---|---|---|---|---|---|---|
| 13128 | 29.40 | .1466 | 13.95 | 0.32 | 0.0282 | -0.046 | 0.955 | -.134 | 0.0689 | -0.403 | 0.259 | -0.376 | 5 |
| 13130 | 28.70 | .1449 | 28.53 | 0.34 | 0.0240 | -0.056 | 1.173 | -.441 | 0.0821 | -0.523 | 0.386 | -0.688 | |
| 13132 | 29.85 | .1452 | 33.49 | 0.34 | 0.0238 | -0.060 | 1.102 | -.478 | 0.0751 | -0.683 | 0.413 | -1.127 | 5 |
| 11359 | 30.30 | .1374 | 4.99 | 0.06 | 0.0030 | -0.079 | 0.873 | 0 | 0.0073 | 0 | 0.342 | 0 | 0 |
| 11355 | 31.25 | .1352 | 3.48 | 0.07 | -0.0005 | -0.068 | 0.814 | 0 | 0.0059 | +0.487 | 0.325 | 0 | |
| 11349 | 30.08 | .1431 | 8.10 | 0.08 | 0.0014 | -0.077 | 0.804 | -.081 | 0.0444 | +1.135 | 0.328 | -0.081 | |
| 11326 | 30.77 | .1256 | 8.32 | 0.17 | 0.0039 | -0.099 | 0.796 | 0 | 0.0163 | +0.666 | 0.330 | +0.374 | |
| 11322 | 30.77 | .1108 | 3.51 | 0.16 | 0.0036 | -0.088 | 0.722 | 0 | 0.0226 | +0.457 | 0.289 | 0 | |
| 11317 | 31.25 | .1248 | 5.19 | 0.15 | 0.0041 | -0.109 | 0.681 | -.171 | 0.0132 | -0.748 | 0.353 | -0.239 | 0 |

Table 3. Flap Configuration 2; $c_f/c = 0.3$, $b_f/b = 0.8$; Tests in Smooth Water, Flaps Oscillating, Static h/c = 1.0

| Run No. | $U_\infty$ Ft./Sec. | $\Delta\delta_f$ Rad. | $\omega_f$ Rad./Sec. | $C_{L_2}$ | $C_{D_2}$ | $C_{M_2}$ | $\frac{\Delta C_{L_2}}{\Delta\delta_f}$ | $\phi_{L_2}$ Rad. | $\frac{\Delta C_{D_2}}{\Delta\delta_f}$ | $\phi_{D_2}$ Rad. | $\frac{\Delta C_{M_2}}{\Delta\delta_f}$ | $\phi_{M_2}$ Rad. | $\alpha°$ |
|---|---|---|---|---|---|---|---|---|---|---|---|---|---|
| 13232 | 28.10 | .1632 | 17.34 | 0.30 | 0.0245 | -0.030 | 1.195 | -.259 | 0.0705 | 0 | 0.334 | -0.190 | 5 |
| 13234 | 27.70 | .1579 | 31.92 | 0.30 | 0.0245 | -0.039 | 1.470 | -.317 | 0.0766 | -.253 | 0.481 | -0.952 | |
| 13236 | 27.40 | .1579 | 41.59 | 0.29 | 0.0240 | -0.037 | 1.654 | -.620 | 0.0735 | -.413 | 0.441 | -1.530 | 5 |
| 11270 | 30.76 | .1152 | 8.67 | 0.06 | -0.0012 | -0.084 | 1.215 | 0 | 0.1180 | +.607 | 0.443 | 0 | 0 |
| 11263 | 29.20 | .1099 | 3.44 | 0.07 | 0.0053 | -0.072 | 1.365 | 0 | 0.0746 | +.275 | 0.464 | +0.275 | |
| 11257 | 31.25 | .1326 | 5.32 | 0.07 | -0.0053 | -0.084 | 1.131 | +.186 | 0.0837 | 0 | 0.430 | +0.160 | |
| 11309 | 31.50 | .1396 | 5.11 | 0.17 | 0.0022 | -0.109 | 1.218 | +.179 | 0.0057 | +.245 | 0.358 | +0.204 | |
| 11305 | 29.85 | .1222 | 3.51 | 0.17 | 0.0001 | -0.115 | 0.982 | 0 | 0.0074 | +.562 | 0.385 | +0.070 | |
| 11301 | 29.85 | .1396 | 8.38 | 0.17 | -0.0039 | -0.118 | 0.931 | +.335 | 0.0473 | +.503 | 0.358 | +0.251 | 0 |

Table 4. Flap Configuration 3; $c_f/c = 0.2$, $b_f/b = 0.6$; Tests in Smooth Water, Flaps Oscillating, Static $h/c = 1.0$

| Run No. | $U_\infty$ Ft./Sec. | $\Delta\delta_f$ Rad. | $\omega_f$ Rad./Sec. | $C_{L_2}$ | $C_{D_2}$ | $C_{M_2}$ | $\frac{\Delta C_{L_2}}{\Delta\delta_f}$ | $\phi_{L_2}$ Rad. | $\frac{\Delta C_{D_2}}{\Delta\delta_f}$ | $\phi_{D_2}$ Rad. | $\frac{\Delta C_{M_2}}{\Delta\delta_f}$ | $\phi_{M_2}$ Rad. | $\alpha°$ |
|---|---|---|---|---|---|---|---|---|---|---|---|---|---|
| 12859 | 30.30 | .1304 | 20.92 | 0.310 | 0.0227 | -0.044 | 0.615 | -.383 | 0.0346 | -0.745 | 0.238 | -1.065 | 5 |
| 12861 | 30.80 | .1300 | 31.60 | 0.310 | 0.0227 | -0.041 | 0.692 | -.330 | 0.0338 | -0.826 | 0.269 | -1.289 | |
| 12863 | 31.30 | .1287 | 39.52 | 0.310 | 0.0248 | -0.036 | 0.698 | -.445 | 0.0372 | -1.134 | 0.132 | -1.417 | 5 |
| 11552 | 32.26 | .0925 | 8.06 | 0.035 | 0.0004 | -0.069 | 0.595 | -.201 | 0.0346 | +0.161 | 0.308 | 0 | 0 |
| 11544 | 31.25 | .1283 | 4.78 | 0.035 | 0.0014 | -0.070 | 0.429 | -.144 | 0.0207 | +0.119 | 0.218 | 0 | |
| 11572 | 31.75 | .1475 | 3.21 | 0.070 | 0.0031 | -0.097 | 0.339 | 0 | 0.0115 | +0.546 | 0.207 | 0 | |
| 11568 | 30.77 | .1475 | 3.22 | 0.050 | 0.0023 | -0.061 | 0.203 | 0 | 0.0047 | +0.371 | 0.125 | 0 | |
| 11566 | 32.79 | .1457 | 4.76 | 0.080 | 0.0007 | -0.093 | 0.412 | 0 | 0.0045 | +0.476 | 0.209 | 0 | |
| 11560 | 32.79 | .1492 | 7.95 | 0.080 | 0.0003 | -0.092 | 0.335 | -.238 | 0.0174 | +0.318 | 0.191 | 0 | 0 |

Table 5. Flap Configuration 4; $c_f/c = 0.2$, $b_f/b = 0.8$; Tests in Smooth Water, Flaps Oscillating, Static $h/c = 1.0$

| Run No. | $U_\infty$ Ft./Sec. | $\Delta\delta_f$ Rad. | $\omega_f$ Rad./Sec. | $C_{L_2}$ | $C_{D_2}$ | $C_{M_2}$ | $\frac{\Delta C_{L_2}}{\Delta\delta_f}$ | $\phi_{L_2}$ Rad. | $\frac{\Delta C_{D_2}}{\Delta\delta_f}$ | $\phi_{D_2}$ Rad. | $\frac{\Delta C_{M_2}}{\Delta\delta_f}$ | $\phi_{M_2}$ Rad. | $\alpha°$ |
|---|---|---|---|---|---|---|---|---|---|---|---|---|---|
| 12911 | 33.70 | .1300 | 29.47 | 0.30 | 0.0235 | -0.053 | 0.923 | -.364 | 0.0438 | -.728 | 0.331 | -0.910 | 5 |
| 12913 | 34.85 | .1309 | 32.23 | 0.29 | 0.0224 | -0.048 | 0.840 | -.324 | 0.0397 | -.809 | 0.336 | -0.971 | |
| 12915 | 35.40 | .1300 | 41.91 | 0.30 | 0.0212 | -0.040 | 1.000 | -.586 | 0.0415 | -.753 | 0.215 | -1.422 | 5 |
| 11491 | 31.25 | .1012 | 9.82 | 0.025 | -0.0008 | -0.048 | 0.642 | -.393 | 0.0553 | +.196 | 0.346 | -0.393 | 0 |
| 11487 | 28.99 | .0777 | 3.73 | 0.020 | 0.0021 | -0.064 | 0.901 | 0 | 0.0766 | 0 | 0.541 | 0 | |
| 11481 | 29.41 | .0899 | 5.76 | 0.030 | 0.0004 | -0.049 | 0.667 | -.230 | 0.0300 | +.288 | 0.445 | -0.173 | |
| 11520 | 32.26 | .1230 | 4.80 | 0.075 | -0.0026 | -0.070 | 0.610 | -.239 | 0.0358 | +.240 | 0.317 | -0.384 | |
| 11512 | 29.41 | .1335 | 8.06 | 0.070 | -0.0069 | -0.086 | 0.524 | -.177 | 0.0479 | +.403 | 0.281 | -0.177 | 0 |

Table 6. Flap Configuration 1; $c_f/c = 0.3$, $b_f/b = 0.6$; Tests in Regular Head Seas, Flaps Fixed, Static $h/c = 1.0$

| Run No. | $\lambda_K$ Ft. | $A_K$ Ft. | $\alpha$ Deg. | $\delta_f$ Deg. | $U_\infty$ Ft./Sec. | $\nu$ Rad./Sec. | $C_{L_1}$ | $C_{D1}$ | $C_{M_1}$ | $\frac{\Delta C_{L_1}}{A_K}\frac{c}{2}$ | $\phi_{L_1}$ Rad. | $\frac{\Delta C_{D_1}}{A_K}\frac{c}{2}$ | $\phi_{D_1}$ Rad. | $\frac{\Delta C_{M_1}}{A_K}\frac{c}{2}$ | $\phi_{M_1}$ Rad. |
|---|---|---|---|---|---|---|---|---|---|---|---|---|---|---|---|
| 12162 | 8.04 | .206 | 5 | -5 | 21.74 | 22.02 | .230 | .0136 | -.00545 | .0874 | 1.277 | .00101 | -2.33 | -.00510 | 0.793 |
| 12164 | 8.23 | .207 | 5 | -5 | 31.75 | 29.20 | .228 | .0157 | +.00105 | .0674 | 1.314 | .00137 | -3.22 | -.00758 | 0.759 |
| 12166 | 7.80 | .198 | 5 | 0 | 21.51 | 22.40 | .335 | .0201 | -.0103 | .0840 | 1.411 | .00169 | -1.61 | -.00758 | 1.030 |
| 12168 | 7.56 | .178 | 5 | 0 | 29.85 | 29.20 | .340 | .0201 | -.0073 | .0750 | 1.110 | .00069 | -1.05 | -.00308 | 0.730 |
| 12156 | 7.84 | .197 | 5 | 5 | 22.73 | 23.30 | .388 | .0273 | -.0389 | .0734 | 1.584 | .00267 | -2.47 | -.00162 | 1.281 |
| 12158 | 7.99 | .187 | 5 | 5 | 30.77 | 29.20 | .393 | .0285 | -.0496 | .0476 | 1.080 | .00128 | -2.63 | -.00696 | 0.818 |
| 12160 | 8.01 | .194 | 5 | 10 | 31.75 | 29.90 | .443 | .0397 | -.0629 | .0504 | 0.927 | .00126 | -2.09 | -.00642 | 0.419 |
| 12136 | 7.96 | .202 | 5 | 10 | 22.47 | 22.80 | .305 | .0474 | -.0559 | .0806 | 1.140 | .00300 | -1.09 | -.00372 | 0.958 |
| 12120 | 8.03 | .187 | 0 | 10 | 31.25 | 29.45 | .209 | .0232 | -.0844 | .0816 | 1.355 | .00270 | -0.88 | -.00836 | 0.795 |
| 12118 | 8.28 | .182 | 0 | 10 | 22.47 | 22.00 | .202 | .0262 | -.0821 | .0958 | 1.188 | .00395 | -0.88 | -.00491 | 1.188 |
| 12132 | 7.94 | .207 | 10 | 10 | 25.31 | 25.10 | .693 | .0793 | -.0609 | .0870 | 1.004 | .00118 | -2.89 | -.00706 | 0.276 |
| 12130 | 7.82 | .201 | 10 | 10 | 20.62 | 21.65 | .659 | .0803 | -.0701 | .0820 | 0.909 | .00349 | -1.30 | -.01010 | 0.693 |
| 12126 | 8.11 | .207 | -5 | 10 | 30.30 | 28.50 | .062 | .0271 | -.0890 | .0772 | 1.710 | .00901* | -0.14 | -.00406 | 1.197 |
| 12124 | 7.99 | .205 | -5 | 10 | 18.51 | 19.60 | -.080 | .0320 | -.0893 | .1122 | 1.823 | .01016* | -0.39 | -.00646 | 1.333 |

* Wild Points.

Table 7. Flap Configuration 2; $c_f/c = 0.3$, $b_f/b = 0.8$: Tests in Regular Head Seas, Flaps Fixed, Static $h/c = 1.0$

| Run No. | $\lambda_K$ Ft. | $A_K$ Ft. | $\alpha$ Deg. | $\delta_f$ Deg. | $U_\infty$ Ft./Sec. | $\nu$ Rad./Sec. | $C_{L_1}$ | $C_{D_1}$ | $C_{M_1}$ | $\frac{\Delta C_{L_1}}{A_K}\frac{c}{2}$ | $\phi_{L1}$ Rad. | $\frac{\Delta C_{D_1}}{A_K}\frac{c}{2}$ | $\phi_{D1}$ Rad. | $\frac{\Delta C_{M_1}}{A_K}\frac{c}{2}$ | $\phi_{M1}$ Rad. |
|---|---|---|---|---|---|---|---|---|---|---|---|---|---|---|---|
| 12050 | 8.21 | .211 | 5 | 10 | 20.80 | 20.93 | .509 | .0369 | -.04331 | .1024 | 1.298 | .00438 | -1.15 | -.00548 | 1.005 |
| 12054 | 8.10 | .203 | 5 | 10 | 31.25 | 29.22 | .519 | .0472 | -.05975 | .0518 | 1.023 | .00193 | -1.81 | -.01030 | 0.701 |
| 12056 | 8.06 | .174 | 5 | -5 | 20.40 | 20.93 | .244 | .0179 | -.01089 | .1014 | 1.298 | .00103 | -1.19 | -.00800 | 0.963 |
| 12058 | 8.20 | .190 | 5 | -5 | 31.70 | 29.22 | .242 | .0186 | -.01154 | .0696 | 1.110 | .00155 | -2.40 | -.00542 | 0.643 |
| 12062 | 7.86 | .203 | 5 | 0 | 21.70 | 22.43 | .393 | .0282 | -.04954 | .0738 | 1.480 | .00145 | -1.41 | -.00648 | 1.077 |
| 12064 | 8.20 | .192 | 5 | 0 | 31.70 | 29.22 | .368 | .0239 | -.01709 | .0688 | 1.052 | .00115 | +0.76 | -.00822 | 0.438 |
| 12066 | 7.71 | .193 | 5 | 5 | 22.20 | 23.25 | .436 | .0370 | -.05379 | .0876 | 1.349 | .00321 | -1.33 | -.00482 | 1.023 |
| 12068 | 7.99 | .187 | 5 | 5 | 30.80 | 29.22 | .427 | .0306 | -.05660 | .0538 | 1.227 | .00098 | -2.40 | -.00892 | 0.877 |
| 12108 | 8.12 | .191 | -5 | 10 | 20.20 | 20.61 | -.075 | .0299 | -.06988 | .1012 | 1.546 | .01024* | -0.80 | -.01024 | 1.113 |
| 12100 | 7.87 | .206 | -5 | 10 | 30.30 | 29.22 | -.074 | .0356 | -.12230 | .0664 | 1.812 | .00742* | -0.88 | -.00712 | 1.344 |
| 12046 | 8.16 | .194 | 0 | 10 | 21.70 | 21.68 | .258 | .0240 | -.08060 | .1106 | 1.019 | .00221 | -0.65 | -.00508 | 0.759 |
| 12048 | 8.34 | .203 | 0 | 10 | 32.30 | 29.22 | .279 | .0156 | -.04761 | .0676 | 0.935 | .00213 | -1.05 | -.00536 | 0.643 |
| 12102 | 7.86 | .188 | 10 | 10 | 21.70 | 22.43 | .704 | .0839 | -.03893 | .1084 | 0.942 | .00415 | -1.79 | +.00380* | 0.718 |
| 12104 | 8.02 | .192 | 10 | 10 | 25.00 | 24.63 | .747 | .0951 | -.06361 | .0976 | 1.010 | .00625 | -1.97 | -.00728 | 0.616 |

* Wild points.

Table 8. Flap Configuration 3; $c_f/c = 0.2$, $b_f/b = 0.6$; Tests in Regular Head Seas, Flaps Fixed, Static $h/c = 1.0$

| Run No. | $\lambda_K$ Ft. | $A_K$ Ft. | $\alpha$ Deg. | $\delta_f$ Deg. | $U_\infty$ Ft./Sec. | $\nu$ Rad./Sec. | $C_{L_1}$ | $C_{D_1}$ | $C_{M_1}$ | $\frac{\Delta C_{L_1}}{A_K}\frac{c}{2}$ | $\phi_{L_1}$ Rad. | $\frac{\Delta C_{D_1}}{A_K}\frac{c}{2}$ | $\phi_{D_1}$ Rad. | $\frac{\Delta C_{M_1}}{A_K}\frac{c}{2}$ | $\phi_{M_1}$ Rad. |
|---|---|---|---|---|---|---|---|---|---|---|---|---|---|---|---|
| 12328 | 8.21 | .166 | 5 | 10 | 18.90 | 19.52 | .380 | .0327 | -.0608 | .0980 | 1.483 | .00273 | -1.04 | -.00194 | 0.683 |
| 12330 | 8.28 | .191 | 5 | 10 | 32.80 | 29.64 | .413 | .0304 | -.0477 | .0492 | 1.363 | .00089 | -2.30 | -.00176 | 0.237 |
| 12334 | 7.99 | .175 | 5 | -5 | 23.00 | 23.02 | .209 | .0192 | -.0427 | .0996 | 1.312 | .00207 | -1.65 | -.00442 | 0.736 |
| 12336 | 8.26 | .175 | 5 | -5 | 31.70 | 29.22 | .223 | .0164 | -.0161 | .0724 | 1.315 | .00103 | -0.525 | -.00316 | 0.701 |
| 12338 | 8.13 | .207 | 5 | 0 | 22.70 | 22.68 | .294 | .0235 | -.0459 | .0628 | 1.270 | .00267 | -1.74 | -.00582 | 0.749 |
| 12340 | 8.22 | .196 | 5 | 0 | 32.30 | 29.78 | .292 | .0219 | -.0480 | .0634 | 1.131 | .00063 | -0.99 | -.00628 | 0.536 |
| 12342 | 7.95 | .188 | 5 | 5 | 21.70 | 22.12 | .334 | .0284 | -.0733 | .0826 | 1.372 | .00242 | -0.84 | -.00354 | 0.885 |
| 12344 | 8.17 | .193 | 5 | 5 | 32.80 | 30.21 | .330 | .0233 | -.0480 | .0498 | 1.239 | .00037 | -0.30 | -.00062 | 0.363 |
| 12318 | 7.47 | .176 | -5 | 10 | 21.50 | 22.28 | -.173 | .0343 | -.0673 | .0986 | 1.872 | .01121* | -1.12 | -.00872 | 1.337 |
| 12320 | 8.12 | .158 | -5 | 10 | 31.25 | 29.78 | -.166 | .0322 | -.0770 | .0904 | 1.965 | .01045* | -1.11 | -.00526 | 1.013 |
| 12310 | 7.73 | .160 | 0 | 10 | 20.20 | 21.59 | .117 | .0155 | -.0434 | .1026 | 1.252 | .00408 | -1.32 | -.00780 | 0.950 |
| 12312 | 8.12 | .174 | 0 | 10 | 32.30 | 29.78 | .117 | .0148 | -.0751 | .0766 | 1.370 | .00274 | -1.23 | -.00034 | 0.745 |
| 12306 | 8.18 | .182 | 10 | 10 | 22.00 | 22.05 | .598 | .0611 | -.0484 | .1102 | 1.058 | .00268 | -1.73 | -.00352 | 0.684 |
| 12308 | 8.12 | .186 | 10 | 10 | 26.00 | 24.93 | .593 | .0603 | -.0490 | .0878 | 1.147 | .00088 | -0.40 | -.00468 | 0.339 |

* Wild Points.

Table 9. Flap Configuration 4; $c_f/c = 0.2$, $b_f/b = 0.8$; Tests in Regular Head Seas, Flaps Fixed, Static h/c = 1.0

| Run No. | $\lambda_K$ Ft. | $A_K$ Ft. | $\alpha$ Deg. | $\delta_f$ Deg. | $U_\infty$ Ft./Sec. | $\nu$ Rad./Sec. | $C_{L_1}$ | $C_{D_1}$ | $C_{M_1}$ | $\frac{\Delta C_{L_1}}{A_K}\frac{c}{2}$ | $\phi_{L1}$ Rad. | $\frac{\Delta C_{D_1}}{A_K}\frac{c}{2}$ | $\phi_{D1}$ Rad. | $\frac{\Delta C_{M_1}}{A_K}\frac{c}{2}$ | $\phi_{M1}$ Rad. |
|---|---|---|---|---|---|---|---|---|---|---|---|---|---|---|---|
| 12228 | 8.27 | .186 | 5 | 10 | 21.10 | 20.94 | .395 | .0299 | -.0742 | .0802 | 1.236 | .00410 | -1.28 | -.00103 | 0.796 |
| 12230 | 8.21 | .189 | 5 | 10 | 30.30 | 27.92 | .438 | .0344 | -.0644 | .0414 | 1.117 | .00140 | -1.56 | -.00426 | 0 |
| 12238 | 8.29 | .187 | 5 | -5 | 19.40 | 19.94 | .200 | .0126 | -.0043 | .1204 | 1.476 | .00237 | -0.59 | -.00476 | 0.638 |
| 12240 | 8.07 | .207 | 5 | -5 | 29.40 | 27.56 | .207 | .0138 | +.0082 | .0696 | 1.185 | .00137 | +0.29 | -.00492 | 0.689 |
| 12242 | 8.17 | .210 | 5 | 0 | 19.80 | 20.27 | .273 | .0192 | -.0326 | .1014 | 1.480 | .00155 | -1.14 | +.00362* | 0.892 |
| 12244 | 8.27 | .193 | 5 | 0 | 30.80 | 28.82 | .263 | .0181 | -.0296 | .0614 | 0.980 | .00073 | +0.43 | -.00480 | 0.576 |
| 12246 | 8.20 | .203 | 5 | 5 | 21.30 | 21.30 | .321 | .0240 | -.0486 | .0890 | 1.448 | .00123 | -0.94 | -.00098 | 1.022 |
| 12248 | 8.09 | .177 | 5 | 5 | 31.30 | 29.22 | .337 | .0238 | -.0398 | .0658 | 1.227 | .00082 | -1.79 | -.00288 | 0.438 |
| 12288 | 8.15 | .187 | -5 | 10 | 20.80 | 20.94 | -.155 | .0406 | -.1173 | .1132 | 1.654 | .01112* | -0.77 | -.00672 | 1.424 |
| 12290 | 7.88 | .187 | -5 | 10 | 30.30 | 29.36 | -.135 | .0317 | -.0854 | .0806 | 1.585 | .00807* | -1.17 | -.00478 | 0.998 |
| 12294 | 8.09 | .201 | 0 | 10 | 20.80 | 21.16 | .136 | .0206 | -.0799 | .1156 | 1.142 | .00388 | -0.73 | -.00338 | 0.825 |
| 12296 | 8.32 | .200 | 0 | 10 | 30.30 | 28.31 | .149 | .0168 | -.0784 | .0760 | 0.991 | .00253 | -1.06 | -.00311 | 0.396 |
| 12298 | 8.02 | .177 | 10 | 10 | 20.60 | 21.23 | .621 | .0684 | -.1011 | .1060 | 1.061 | .00343 | -2.04 | -.00380 | 0.531 |
| 12300 | 8.12 | .162 | 10 | 10 | 26.70 | 25.96 | .621 | .0677 | -.0800 | .1122 | 0.831 | .00278 | +0.13 | -.00880 | 0.363 |

* Wild points.

Table 10. Flap Configuration 1; $c_f/c = 0.3$, $b_f/b = 0.6$; Tests in Following Seas, Flaps Fixed

| Run No. | $\lambda_K$ Ft. | $A_K$ Ft. | $H_o$ In. | $\alpha$ Deg. | $\delta_f$ Deg. | $U_\infty$ Ft./Sec. | $\nu$ Rad./Sec. | $C_{L_1}$ | $C_{D_1}$ | $C_{M_1}$ | $\frac{\triangle C_{L_1}}{A_K}\frac{c}{2}$ | $\phi_{L_1}$ Rad. | $\frac{\triangle C_{D_1}}{A_K}\frac{c}{2}$ | $\phi_{D_1}$ Rad. | $\frac{\triangle C_{M_1}}{A_K}\frac{c}{2}$ | $\phi_{M_1}$ Rad. |
|---|---|---|---|---|---|---|---|---|---|---|---|---|---|---|---|---|
| 12186 | 3.58 | .079 | 4 | 5 | 10 | 21.2 | 29.90 | .451 | .0442 | -.0894 | .1098 | -2.080 | .00570 | +0.150 | .0045 | -3.498 |
| 12188 | 3.53 | .058 | 4 | | | 30.3 | 46.50 | .427 | .0411 | -.0690 | .1218 | -2.230 | .00490 | -1.628 | .0098 | -3.162 |
| 12182 | 5.10 | .098 | 4 | | | 21.3 | 19.92 | .427 | .0431 | -.0868 | .0818 | -1.733 | .00582 | -0.040 | .0044 | -2.092 |
| 12184 | 4.94 | .131 | 4 | | | 30.3 | 32.20 | .435 | .0424 | -.0738 | .0750 | -1.739 | .00262 | -0.644 | .0012 | -3.091 |
| 12204 | 8.40 | .198 | 3 | | | 21.7 | 11.30 | .452 | .0429 | -.0432 | .0702 | -1.650 | .00458 | +0.339 | .0023 | -1.831 |
| 12206 | 8.21 | .168 | 3 | | | 30.8 | 18.63 | .435 | .0399 | -.0461 | .0616 | -1.435 | .00163 | +0.317 | .0073 | -1.900 |
| 12200 | 8.35 | .186 | 5 | | | 21.7 | 11.47 | .459 | .0405 | -.0377 | .0642 | -1.812 | .00384 | +0.574 | .0049 | -1.893 |
| 12202 | 8.31 | .188 | 5 | | | 30.8 | 18.30 | .450 | .0417 | -.0551 | .0434 | -1.867 | .00124 | -0.988 | .0069 | -2.086 |
| 12194 | 8.40 | .179 | 4 | | | 21.7 | 11.37 | .424 | .0400 | -.0720 | .0778 | -1.819 | .00428 | +0.728 | .0067 | -1.944 |
| 12196 | 8.26 | .195 | 4 | 5 | 10 | 30.8 | 18.45 | .429 | .0392 | -.0555 | .0506 | -1.476 | .00260 | +0.793 | .0037 | -1.919 |

Table 11. Flap Configuration 2; $c_f/c = 0.3$, $b_f/b = 0.8$; Tests in Following Seas, Flaps Fixed

| Run No. | $\lambda_K$ Ft. | $A_K$ Ft. | $H_o$ In. | $\alpha$ Deg. | $\delta_f$ Deg. | $U_\infty$ Ft./Sec. | $\nu$ Rad./Sec. | $C_{L_1}$ | $C_{D_1}$ | $C_{M_1}$ | $\frac{\Delta C_{L_1}}{A_K}\frac{c}{2}$ | $\phi_{L_1}$ Rad. | $\frac{\Delta C_{D_1}}{A_K}\frac{c}{2}$ | $\phi_{D_1}$ Rad. | $\frac{\Delta C_{M_1}}{A_K}\frac{c}{2}$ | $\phi_{M_1}$ Rad. |
|---|---|---|---|---|---|---|---|---|---|---|---|---|---|---|---|---|
| 12086 | 3.63 | .058 | 4 | 5 | 10 | 22.5 | 31.42 | .507 | .0481 | -.0533 | .1078 | -2.199 | .00446 | -0.566 | .0078 | -3.236 |
| 12088 | 3.76 | .065 | 4 | | | 28.6 | 40.53 | .490 | .0482 | -.0587 | .1126 | -1.945 | .00426 | -1.783 | .0107 | -2.553 |
| 12090 | 5.45 | .124 | 4 | | | 21.4 | 18.47 | .473 | .0512 | -.0767 | .0860 | -1.718 | .00494 | +0.277 | .0090 | -2.013 |
| 12092 | 5.04 | .091 | 4 | | | 30.2 | 31.42 | .514 | .0482 | -.0455 | .0876 | -1.917 | .00540 | +0.314 | .0086 | -2.514 |
| 12080 | 8.07 | .190 | 3 | | | 20.4 | 10.81 | .474 | .0482 | -.0599 | .0652 | -1.924 | .00592 | +0.627 | .0090 | -2.011 |
| 12082 | 8.27 | .175 | 3 | | | 27.9 | 16.53 | .491 | .0436 | -.0473 | .0430 | -1.537 | .00472 | +0.661 | .0079 | -1.769 |
| 12076 | 8.17 | .223 | 5 | | | 18.4 | 8.99 | .505 | .0523 | -.0602 | .0776 | -2.104 | .00478 | +1.025 | .0039 | -2.122 |
| 12078 | 7.84 | .203 | 5 | | | 29.5 | 18.47 | .522 | .0473 | -.0481 | .0436 | -2.143 | .00284 | +1.108 | .0043 | -2.327 |
| 12072 | 8.27 | .180 | 4 | | | 19.6 | 9.99 | .462 | .0473 | -.0647 | .0950 | -1.858 | .00522 | +0.999 | .0080 | -1.998 |
| 12074 | 8.04 | .193 | 4 | 5 | 10 | 27.1 | 16.09 | .497 | .0481 | -.0551 | .0614 | -1.979 | .00372 | +1.078 | .0051 | -2.156 |

Table 12. Flap Configuration 3; $c_f/c = 0.2$, $b_f/b = 0.6$; Tests in Following Seas, Flaps Fixed

| Run No. | $\lambda_K$ Ft. | $A_K$ Ft. | $H_o$ In. | $\alpha$ Deg. | $\delta_f$ Deg. | $U_\infty$ Ft./Sec. | $\nu$ Rad./Sec. | $C_{L_1}$ | $C_{D_1}$ | $C_{M_1}$ | $\frac{\Delta C_{L_1}}{A_K}\frac{c}{2}$ | $\phi_{L_1}$ Rad. | $\frac{\Delta C_{D_1}}{A_K}\frac{c}{2}$ | $\phi_{D_1}$ Rad. | $\frac{\Delta C_{M_1}}{A_K}\frac{c}{2}$ | $\phi_{M_1}$ Rad. |
|---|---|---|---|---|---|---|---|---|---|---|---|---|---|---|---|---|
| 12356 | 3.53 | .149 | 4 | 5 | 10 | 21.0 | 29.78 | .399 | .0373 | -.0711 | .0534 | -2.025 | .00280 | -0.893 | .0031 | -2.114 |
| 12358 | 3.55 | .054 | 4 | | | 30.4 | 46.20 | .387 | .0321 | -.0624 | .1124 | -1.848 | .00956 | -0.924 | .0078 | -3.142 |
| 12360 | 5.00 | .133 | 4 | | | 21.4 | 20.60 | .380 | .0321 | -.0793 | .0850 | -1.813 | .00352 | +1.030 | .0022 | -2.802 |
| 12364 | 5.05 | .106 | 4 | | | 30.7 | 31.89 | .376 | .0298 | -.0545 | .0662 | -1.818 | .00524 | -0.797 | .0073 | -2.041 |
| 12352 | 8.53 | .158 | 4 | | | 21.3 | 10.83 | .387 | .0345 | -.0799 | .0684 | -1.516 | .00468 | +0.237 | .0026 | -1.949 |
| 12354 | 8.45 | .159 | 4 | | | 30.4 | 17.70 | .357 | .0308 | -.0612 | .0608 | -1.947 | .00298 | +0.531 | .0038 | -2.425 |
| 12370 | 8.11 | .187 | 3 | | | 21.25 | 11.44 | .368 | .0324 | -.0761 | .0782 | -1.659 | .00426 | +0.641 | .0038 | -2.002 |
| 12372 | 8.17 | .167 | 3 | | | 30.5 | 18.48 | .349 | .0311 | -.0524 | .0688 | -1.552 | .00336 | +0.869 | .0106 | -1.903 |
| 12376 | 8.25 | .183 | 5 | | | 21.4 | 11.36 | .397 | .0400 | -.1163 | .0838 | -2.124 | .00276 | +1.216 | .0059 | -2.272 |
| 12378 | 7.85 | .158 | 5 | 5 | 10 | 30.5 | 19.33 | .419 | .0365 | -.0780 | .0622 | -1.991 | .00194 | +0.251 | .0048 | -2.204 |

Table 13. Flap Configuration 4; $c_f/c = 0.2$, $b_f/b = 0.8$; Tests in Following Seas, Flaps Fixed

| Run No. | $\lambda_K$ Ft. | $A_K$ Ft. | $H_o$ In. | $\alpha$ Deg. | $\delta_f$ Deg. | $U_\infty$ Ft./Sec. | $\nu$ Rad./Sec. | $C_{L_1}$ | $C_{D_1}$ | $C_{M_1}$ | $\frac{\Delta C_{L_1}}{A_K}\frac{c}{2}$ | $\phi_{L_1}$ Rad. | $\frac{\Delta C_{D_1}}{A_K}\frac{c}{2}$ | $\phi_{D_1}$ Rad. | $\frac{\Delta C_{M_1}}{A_K}\frac{c}{2}$ | $\phi_{M_1}$ Rad. |
|---|---|---|---|---|---|---|---|---|---|---|---|---|---|---|---|---|
| 12274 | 3.75 | .104 | 4 | 5 | 10 | 21.1 | 27.92 | .369 | .0388 | -.0828 | .0658 | -1.954 | .00364 | -0.670 | .0063 | -3.239 |
| 12278 | 3.53 | .101 | 4 | | | 30.4 | 46.54 | .399 | .0344 | -.0657 | .0850 | -2.048 | .00264 | -1.629 | .0070 | -2.327 |
| 12280 | 5.62 | .122 | 4 | | | 21.0 | 17.46 | .395 | .0355 | -.0688 | .0784 | -1.484 | .00146 | +0.890 | .0060 | -1.658 |
| 12282 | 5.51 | .132 | 4 | | | 30.2 | 28.43 | .405 | .0354 | -.0626 | .0640 | -1.308 | .00452 | +0.284 | .0053 | -1.535 |
| 12252 | 8.20 | .173 | 4 | | | 21.4 | 11.55 | .384 | .0383 | -.0919 | .0856 | -1.790 | .00344 | +1.016 | .0049 | -1.986 |
| 12254 | 8.03 | .158 | 4 | | | 30.4 | 18.76 | .400 | .0347 | -.0703 | .0636 | -1.538 | .00294 | 0 | .0031 | -1.932 |
| 12264 | 8.37 | .167 | 3 | | | 21.3 | 11.14 | .392 | .0395 | -.0869 | .0774 | -1.582 | .00294 | +0.334 | .0005 | -1.827 |
| 12266 | 8.25 | .170 | 3 | | | 30.6 | 18.37 | .383 | .0340 | -.0627 | .0572 | -1.396 | .00412 | +0.184 | .0041 | -2.094 |
| 12256 | 8.40 | .175 | 5 | | | 21.4 | 11.22 | .420 | .0400 | -.0832 | .0678 | -2.020 | .00328 | +0.449 | .0049 | -2.435 |
| 12258 | 8.12 | .199 | 5 | 5 | 10 | 30.8 | 18.81 | .413 | .0368 | +.0733 | .0568 | -1.599 | .00210 | +0.564 | .0076 | -2.389 |

Table 14. Flap Configuration 1; $c_f$
and Following Seas, Fla

| Run No. | Head Following Sea | $\phi_f$ Rads. | $C_{L_{Max.}}$ | $C_{L_{Min.}}$ | $\Delta C_{L_3}$ | $C_{L_3}$ | $\phi_{L_3}$ Rads. | $C_{D_{Max.}}$ | $C_{D_{Min.}}$ | $\Delta C_{D_3}$ | $C_{D_3}$ |
|---|---|---|---|---|---|---|---|---|---|---|---|
| 13154 | Head | $-\pi/2$ | .52 | .20 | .16 | .36 | -2.36 | .0400 | .0131 | .0134 | .0266 |
| | | $-\pi$ | .58 | .15 | .22 | .36 | +2.24 | .0386 | .0156 | .0115 | .0271 |
| | | $+\pi/2$ | .60 | .10 | .25 | .35 | + .883 | .0371 | .0177 | .0097 | .0274 |
| 13157 | Head | $+\pi$ | .49 | .18 | .16 | .33 | +2.375 | .0366 | .0134 | .0116 | .0250 |
| | | $+\pi/2$ | .57 | .06 | .26 | .31 | +1.41 | .0350 | .0155 | .0098 | .0232 |
| 13160 | Head | $-\pi$ | .44 | .19 | .13 | .32 | +2.50 | .0410 | .0109 | .0150 | .0260 |
| | | $-\pi/2$ | .43 | .27 | .08 | .35 | -1.06 | .0433 | .0146 | .0144 | .0289 |
| 13167 | Following | $+\pi/2$ | .35 | .27 | .04 | .31 | -2.52 | .0412 | .0197 | .0107 | .0305 |
| | | $+\pi$ | .51 | .09 | .21 | .30 | -1.94 | .0437 | .0215 | .0111 | .0326 |
| 13182 | Following | $-\pi$ | .48 | .07 | .21 | .28 | -2.07 | .0410 | .0216 | .0097 | .0313 |
| | | $-\pi/2$ | .55 | .10 | .23 | .32 | -1.89 | .0417 | .0216 | .0101 | .0316 |
| 13191 | Following | $-\pi$ | .50 | .16 | .17 | .33 | +1.23 | .0418 | .0207 | .0105 | .0313 |
| | | $+\pi/2$ | .53 | .20 | .16 | .36 | +1.23 | .0428 | .0204 | .0112 | .0316 |
| | | $-\pi/2$ | .60 | .17 | .21 | .38 | -1.70 | .0435 | .0200 | .0117 | .0318 |

$c = 0.3$, $b_f/b = 0.6$; Tests in Regular Head
s Oscillating; Static $h/c = 1.0$, $\alpha = 5°$

| $\phi D_3$ Rads. | $C_{M_{Max.}}$ | $C_{M_{Min.}}$ | $\Delta C_{M_3}$ | $C_{M_3}$ | $\phi M_3$ Rads. | $U_\infty$ Ft./Sec. | $\nu$ Rads./Sec. | $\omega_f$ Rads./Sec. | $\lambda_K$ Ft. | $A_K$ Ft. | $\Delta\delta_f$ Rads. |
|---|---|---|---|---|---|---|---|---|---|---|---|
| -2.78 | -.061 | -.005 | -.028 | -.033 | -3.14 | 23.80 | 49.4 | 46.1 | 3.65 | .0628 | .148 |
| +1.96 | -.063 | -.003 | -.030 | -.033 | +1.354 | 23.90 | | | | | |
| + .748 | -.069 | -.005 | -.032 | -.037 | 0 | 24.40 | | | | | |
| -2.085 | -.083 | -.028 | -.027 | -.056 | +2.375 | 22.10 | 21.5 | 20.2 | 8.32 | .157 | .149 |
| +1.09 | -.101 | -.007 | -.047 | -.054 | +1.15 | 21.70 | | | | | |
| +3.06 | -.097 | -.026 | -.035 | -.062 | +2.68 | 23.30 | 22.1 | 23.2 | 8.53 | .163 | .149 |
| -1.90 | -.114 | -.021 | -.046 | -.068 | -1.193 | 23.31 | | | | | |
| +2.68 | -.104 | -.009 | -.047 | -.057 | -2.57 | 20.83 | 10.45 | 12.17 | 8.58 | .157 | .149 |
| -2.90 | -.080 | -.021 | -.029 | -.051 | -1.965 | | | | | | |
| -2.79 | -.090 | -.019 | -.035 | -.055 | +2.78 | 20.80 | 10.57 | 11.57 | 8.46 | .154 | .148 |
| +1.32 | -.081 | -.016 | -.032 | -.049 | -2.06 | | | | | | |
| +1.04 | -.114 | -.012 | -.051 | -.063 | +0.44 | 21.57 | 29.6 | 39.5 | 3.66 | .072 | .145 |
| +2.11 | -.116 | -.005 | -.055 | -.061 | +0.44 | | | | | | |
| -1.88 | -.100 | -.006 | -.047 | -.053 | -2.38 | | | | | | |

Table 15. Flap Configuration 2; $c_f/$
and Following Seas, Fla

| Run No. | Head or Following Sea | $\phi_f$ Rads. | $C_{L_{Max.}}$ | $C_{L_{Min.}}$ | $\triangle C_{L_3}$ | $C_{L_3}$ | $\phi_{L_3}$ Rads. | $C_{D_{Max.}}$ | $C_{D_{Min.}}$ | $\triangle C_{D_3}$ | $C_{D_3}$ |
|---|---|---|---|---|---|---|---|---|---|---|---|
| 13240 | Head | $-\pi/2$ | .55 | .04 | .25 | .30 | -1.98 | .0372 | .0131 | .0120 | .0252 |
| 13248 | Head | $+\pi$ | .59 | 0 | .29 | .30 | +2.36 | .0385 | .0136 | .0125 | .0260 |
| | | $+\pi/2$ | .63 | -.05 | .34 | .29 | + .83 | .0400 | .0142 | .0129 | .0271 |
| 13256 | Head | $-\pi/2$ | .39 | .17 | .11 | .28 | -1.13 | .0376 | .0136 | .0120 | .0256 |
| 13260 | Head | $+\pi$ | .48 | .02 | .23 | .25 | +2.74 | .0340 | .0147 | .0096 | .0244 |
| | | $+\pi/2$ | .58 | -.05 | .32 | .26 | +1.33 | .0365 | .0131 | .0117 | .0248 |
| 13284 | Following | $-\pi/2$ | .51 | .01 | .25 | .26 | -1.79 | .0357 | .0194 | .0082 | .0275 |
| | | $-\pi$ | .49 | .02 | .24 | .25 | -2.07 | .0401 | .0204 | .0098 | .0303 |
| 13302 | Following | $+\pi/2$ | .39 | .18 | .10 | .29 | +1.63 | .0441 | .0178 | .0132 | .0309 |
| 13308 | Following | $-\pi/2$ | .58 | -.01 | .29 | .29 | -1.79 | .0311 | .0131 | .0090 | .0221 |
| 13310 | Following | $-\pi$ | .57 | .04 | .27 | .30 | +1.87 | .0375 | .0136 | .0119 | .0256 |
| | | $+\pi/2$ | .52 | .07 | .22 | .30 | +1.23 | .0396 | .0143 | .0126 | .0270 |

: = 0.3, $b_f/b$ = 0.8; Tests in Regular Head
s Oscillating; Static h/c = 1.0, $\alpha$ = 5°

| $\phi_{D_3}$ Rads. | $C_{M_{Max.}}$ | $C_{M_{Min.}}$ | $\Delta C_{M_3}$ | $C_{M_3}$ | $\phi_{M_3}$ Rads. | $U_\infty$ Ft./Sec. | $\nu$ Rads./Sec. | $\omega_f$ Rads./Sec. | $\lambda_K$ Ft. | $A_K$ Ft. | $\Delta\delta_f$ Rads. |
|---|---|---|---|---|---|---|---|---|---|---|---|
| -2.125 | -.105 | -.001 | -.052 | -.053 | -3.18 | 23.12 | 46.9 | 45.2 | 3.67 | .066 | .160 |
| +2.325 | -.106 | -.011 | -.047 | -.059 | +1.56 | 22.73 | 46.5 | 44.8 | 3.66 | .063 | .159 |
| + .472 | -.117 | -.003 | -.057 | -.060 | - .28 | | | | | | |
| -1.775 | -.124 | +.012 | -.068 | -.056 | -1.80 | 22.64 | 22.4 | 27.2 | 8.16 | .165 | .160 |
| +2.54 | -.126 | -.081 | -.023 | -.103 | +2.85 | 22.02 | 22.1 | 23.5 | 8.11 | .167 | .160 |
| + .942 | -.136 | -.010 | -.063 | -.073 | +1.16 | | | | | | |
| -1.214 | -.093 | -.006 | -.043 | -.050 | -1.74 | 21.38 | 11.31 | 10.46 | 8.27 | .166 | .162 |
| +2.46 | -.091 | -.002 | -.045 | -.046 | -2.67 | | | | | | |
| +1.315 | - .119 | -.009 | -.055 | -.064 | +1.47 | 21.74 | 11.73 | 12.55 | 8.15 | .140 | .163 |
| -1.10 | - .137 | +.012 | -.075 | -.062 | -2.44 | 21.83 | 30.0 | 35.8 | 3.67 | .075 | .158 |
| +2.80 | - .138 | +.025 | -.082 | -.056 | +1.24 | 21.33 | 30.3 | 34.9 | 3.54 | .068 | .158 |
| + .868 | - .143 | +.021 | -.082 | -.061 | + .54 | | | | | | |

Table 16. Flap Configuration 3; $c_f$
and Following Seas, Fla

| Run No. | Head or Following Sea | $\phi_f$ Rads. | $C_{L_{Max.}}$ | $C_{L_{Min.}}$ | $\Delta C_{L_3}$ | $C_{L_3}$ | $\phi_{L_3}$ Rads. | $C_{D_{Max.}}$ | $C_{D_{Min.}}$ | $\Delta C_{D_3}$ | $C_{D_3}$ |
|---|---|---|---|---|---|---|---|---|---|---|---|
| 12702 | Head | $-\pi$ | .35 | .22 | .06 | .29 | +1.955 | .0282 | .0171 | .0056 | .0226 |
| 12704 | Head | $-\pi/2$ | .39 | .19 | .10 | .29 | + .116 | .0261 | .0172 | .0044 | .0217 |
| 12706 | Head | $+\pi/2$ | .44 | .17 | .14 | .30 | +1.529 | .0287 | .0162 | .0063 | .0224 |
| 12760 | Head | $+\pi/2$ | .47 | .14 | .17 | .30 | + .911 | .0267 | .0181 | .0043 | .0224 |
| 12762 | Head | $-\pi/2$ | .39 | .21 | .09 | .30 | +2.710 | .0264 | .0132 | .0066 | .0198 |
| | | $-\pi$ | .48 | .16 | .16 | .32 | +1.657 | .0323 | .0211 | .0056 | .0267 |
| 12778 | Following | $+\pi/2$ | .30 | .26 | .02 | .28 | +2.074 | .0301 | .0167 | .0067 | .0234 |
| 12784 | Following | $+\pi$ | .39 | .17 | .11 | .28 | -2.154 | .0254 | .0199 | .0028 | .0226 |
| 12824 | Following | $+\pi/2$ | .35 | .24 | .05 | .30 | - .347 | .0318 | .0175 | .0072 | .0246 |
| 12849 | Following | $-\pi/2$ | .42 | .16 | .13 | .29 | -2.079 | .0276 | .0156 | .0060 | .0216 |
| | | $-\pi$ | .41 | .17 | .12 | .29 | +3.095 | .0263 | .0194 | .0035 | .0228 |
| | | $+\pi/2$ | .37 | .24 | .07 | .30 | +1.032 | .0253 | .0206 | .0024 | .0229 |

/c = 0.2; $b_f/b$ = 0.6; Tests in Regular Head
ıps Oscillating; Static h/c = 1.0; $\alpha$ = 5°

| $\phi_{D_3}$ Rads. | $C_{M_{Max.}}$ | $C_{M_{Min.}}$ | $\triangle C_{M_3}$ | $C_{M_3}$ | $\phi_{M_3}$ Rads. | $U_\infty$ Ft./Sec. | $\nu$ Rads./Sec. | $\omega_f$ Rads./Sec. | $\lambda_K$ Ft. | $A_K$ Ft. | $\Delta\delta_f$ Rads. |
|---|---|---|---|---|---|---|---|---|---|---|---|
| +2.89 | -.031 | -.014 | -.009 | -.022 | +2.066 | 30.77 | 28.4 | 29.75 | 8.24 | .157 | .169 |
| -1.40 | -.068 | +.013 | -.040 | -.028 | - .781 | 30.46 | 26.7 | 29.9 | 8.74 | .150 | .167 |
| +1.39 | -.044 | +.003 | -.024 | -.020 | +1.119 | 29.26 | 27.65 | 29.6 | 8.11 | .164 | .169 |
| +1.57 | -.058 | -.015 | -.022 | -.036 | - .288 | 22.90 | 46.8 | 47.2 | 3.65 | .065 | .127 |
| -2.365 | -.047 | -.032 | -.007 | -.040 | -1.892 | 21.71 | 43.3 | 47.5 | 3.79 | .064 | .124 |
| +2.02 | -.040 | -.020 | -.010 | -.030 | + .741 | | | | | | |
| + .415 | -.067 | -.016 | -.025 | -.042 | +1.566 | 30.48 | 18.3 | 18.95 | 8.25 | .158 | .127 |
| +1.632 | -.065 | -.013 | -.026 | -.039 | -2.428 | 30.61 | 18.85 | 19.0 | 8.07 | .150 | .128 |
| + .316 | -.073 | -.025 | -.024 | -.049 | + .539 | 30.50 | 19.0 | 20.7 | 7.99 | .161 | .124 |
| -2.44 | -.060 | -.015 | -.022 | -.038 | -2.800 | 30.37 | 43.3 | 42.0 | 3.77 | .066 | .126 |
| +2.41 | -.066 | -.019 | -.024 | -.042 | +1.705 | | | | | | |
| - .698 | -.061 | -.020 | -.021 | -.040 | 0 | | | | | | |

Table 17. Flap Configuration 4; $c_f/c$ and Following Seas, Flap

| Run No. | Head or Following Sea | $\phi_f$ Rads. | $C_{L_{Max.}}$ | $C_{L_{Min.}}$ | $\Delta C_{L_3}$ | $C_{L_3}$ | $\phi_{L_3}$ Rads. | $C_{D_{Max.}}$ | $C_{D_{Min.}}$ | $\Delta C_{D_3}$ | $C_{D_3}$ |
|---|---|---|---|---|---|---|---|---|---|---|---|
| 12996 | Head | $+\pi/2$ | .47 | .13 | .17 | .30 | +1.174 | .0268 | .0198 | .0035 | .0233 |
| 12999 | Head | $-\pi/2$ | .36 | .26 | .05 | .31 | -1.011 | .0277 | .0189 | .0044 | .0233 |
| 13002 | Head | $-\pi$ | .41 | .17 | .12 | .29 | +1.708 | .0264 | .0132 | .0066 | .0198 |
| 13012 | Head | $+\pi/2$ | .50 | .13 | .18 | .32 | +1.024 | .0269 | .0157 | .0056 | .0213 |
| | | $+\pi$ | .47 | .14 | .17 | .30 | +1.714 | .0291 | .0146 | .0073 | .0218 |
| | | $-\pi/2$ | .42 | .21 | .11 | .31 | -2.405 | .0263 | .0160 | .0052 | .0211 |
| 13005 | Head | $-\pi/2$ | .39 | .24 | .07 | .32 | -2.173 | .0286 | .0203 | .0042 | .0244 |
| 13008 | | $+\pi/2$ | .50 | .11 | .20 | .30 | + .879 | .0341 | .0208 | .0066 | .0275 |
| 12965 | Following | $-\pi/2$ | .45 | .15 | .15 | .30 | -1.294 | .0292 | .0199 | .0046 | .0246 |
| 12967 | Following | $-\pi$ | .39 | .17 | .11 | .28 | -2.261 | .0317 | .0206 | .0055 | .0262 |
| 12990 | Following | $+\pi/2$ | .41 | .22 | .10 | .31 | - .320 | .0359 | .0175 | .0092 | .0267 |
| 12947 | Following | $-\pi/2$ | .45 | .13 | .16 | .29 | -2.003 | .0322 | .0188 | .0067 | .0255 |
| | | $+\pi$ | .39 | .18 | .10 | .29 | +2.493 | .0292 | .0196 | .0048 | .0244 |
| 12952 | Following | $+\pi/2$ | .41 | .19 | .11 | .30 | + .553 | .0333 | .0191 | .0071 | .0262 |

$c = 0.2$, $b_f = 0.8$; Tests in Regular Head
s Oscillating; Static $h/c = 1.0$, $\alpha = 5°$

| $\phi_{D_3}$ Rads. | $C_{M_{Max.}}$ | $C_{M_{Min.}}$ | $\Delta C_{M_3}$ | $C_{M_3}$ | $\phi_{M_3}$ Rads. | $U_\infty$ Ft./Sec. | $\nu$ Rads./Sec. | $\omega_f$ Rads./Sec. | $\lambda_K$ Ft. | $A_K$ Ft. | $\Delta\delta_f$ Rads. |
|---|---|---|---|---|---|---|---|---|---|---|---|
| +..328 | -.088 | 0 | -.044 | -.044 | + .411 | 34.20 | 31.4 | 32.2 | 8.41 | .173 | .124 |
| -2.01 | -.072 | -.017 | -.027 | -.045 | -2.173 | 34.50 | 30.2 | 33.4 | 8.55 | .173 | .120 |
| +2.28 | -.069 | -.010 | -.029 | -.040 | +1.130 | 32.60 | 28.9 | 34.1 | 8.53 | .176 | .119 |
| + .752 | -.058 | -.038 | -.010 | -.048 | + .578 | 20.93 | 43.3 | 49.0 | 3.66 | .068 | .120 |
| +1.99 | -.066 | -.048 | -.009 | -.057 | +1.218 | | | | | | |
| -3.47 | -.062 | -.054 | -.004 | -.058 | +2.229 | | | | | | |
| -3.46 | -.065 | -.040 | -.012 | -.053 | -3.303 | 21.90 | 45.2 | 46.9 | 3.64 | .064 | .120 |
| + .72 | -.068 | -.032 | -.018 | -.050 | + .259 | 22.70 | 48.0 | 46.2 | 3.53 | .073 | .119 |
| -2.68 | -.072 | -.012 | -.030 | -.042 | -1.595 | 30.60 | 17.6 | 17.4 | 8.53 | .161 | .127 |
| +1.57 | -.082 | -.012 | -.035 | -.047 | +2.744 | 31.30 | 18.3 | 20.3 | 8.49 | .160 | .124 |
| + .274 | -.033 | -.005 | -.014 | -.019 | - .553 | 29.80 | 17.7 | 13.6 | 8.27 | .163 | .124 |
| -2.295 | -.073 | -.010 | -.031 | -.042 | -3.184 | 29.65 | 39.0 | 39.2 | 4.04 | .065 | .128 |
| +1.385 | -.081 | +.001 | -.041 | -.040 | +1.532 | | | | | | |
| + .128 | -.073 | -.021 | -.026 | -.047 | 0 | 29.10 | 44.5 | 39.7 | 3.51 | .065 | .124 |

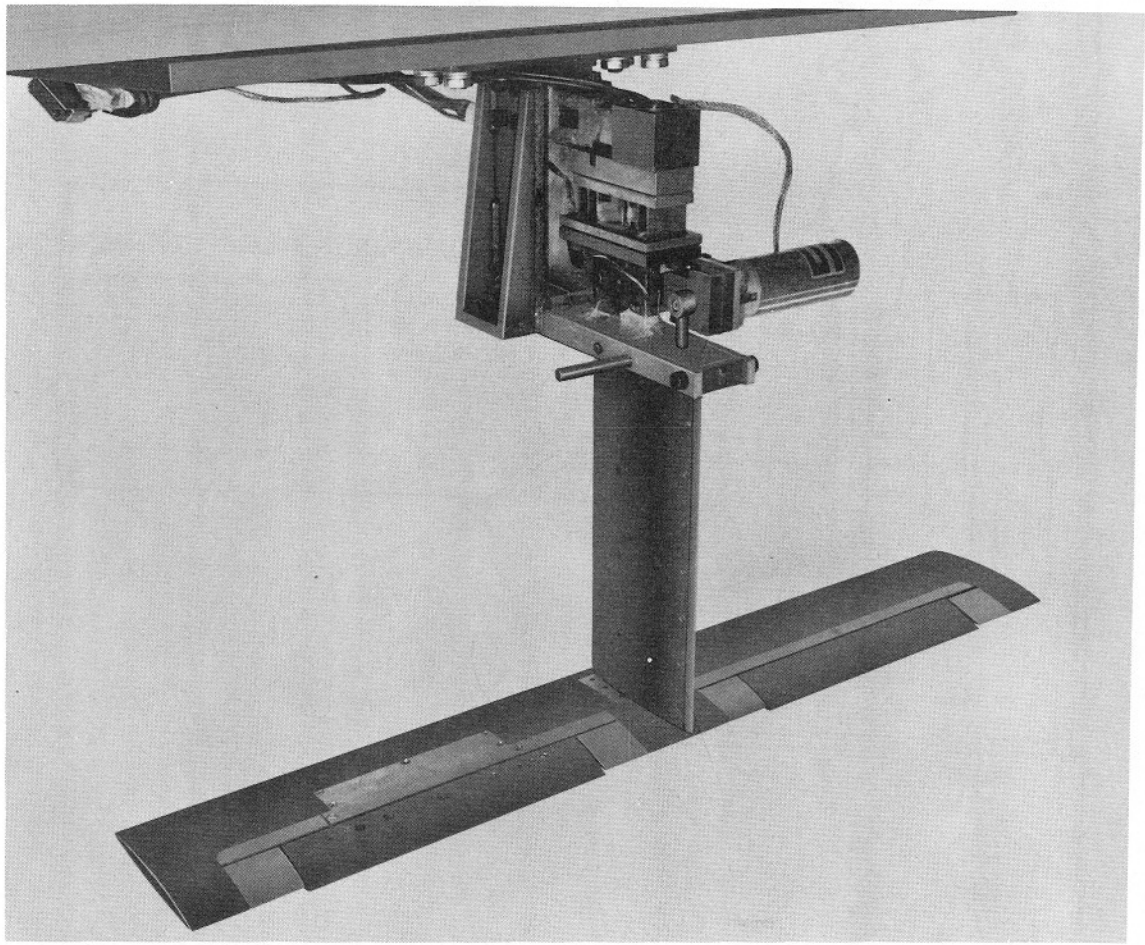

Figure 1. MODEL WITH $c_f/c = 0.2$, $b_f/b = 0.6$, FLAPS INSTALLED

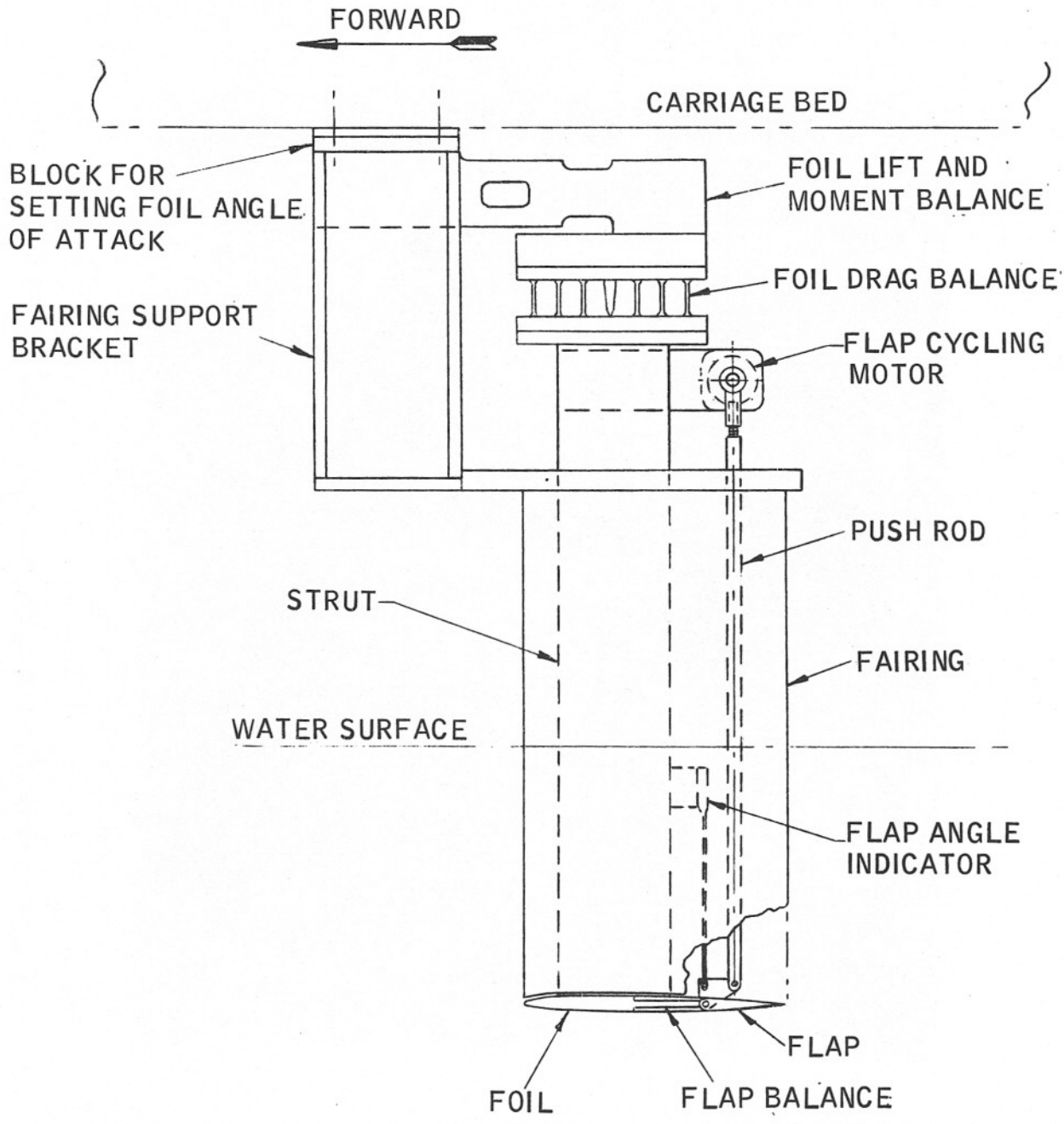


Figure 2. Model and Balances

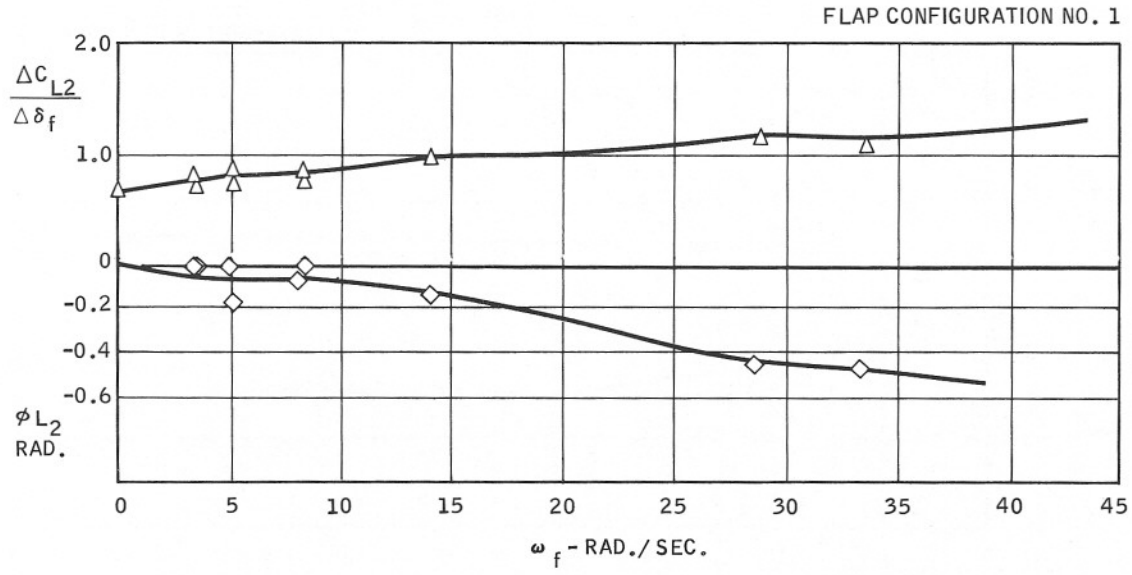


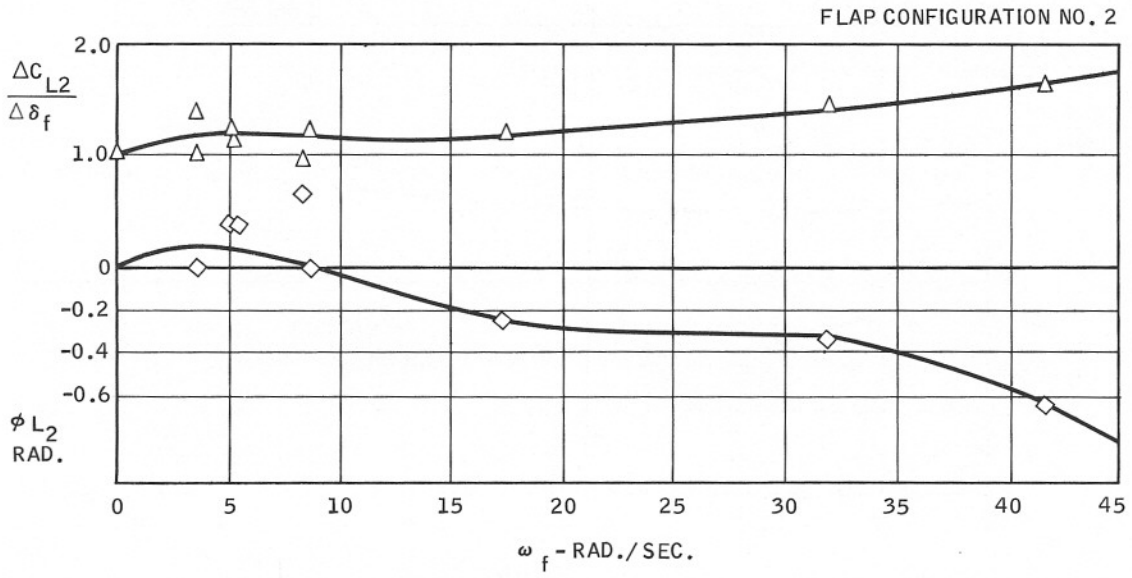


Figure 3. Lift Frequency Response, Flaps Oscillating, Smooth Water

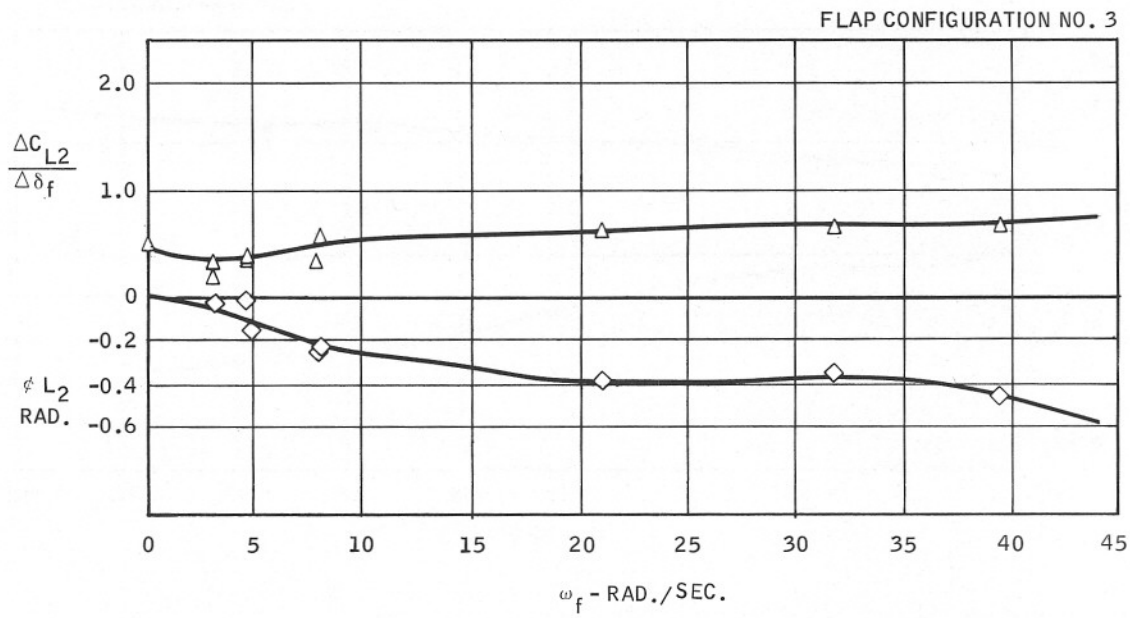


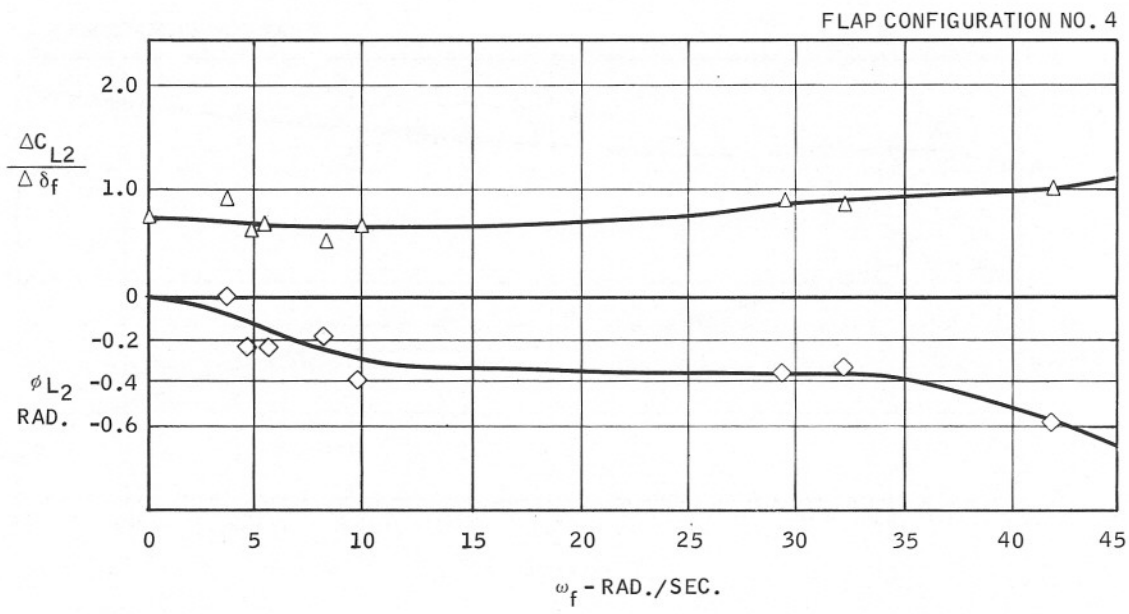


Figure 4. Lift Frequency Response, Flaps Oscillating, Smooth Water

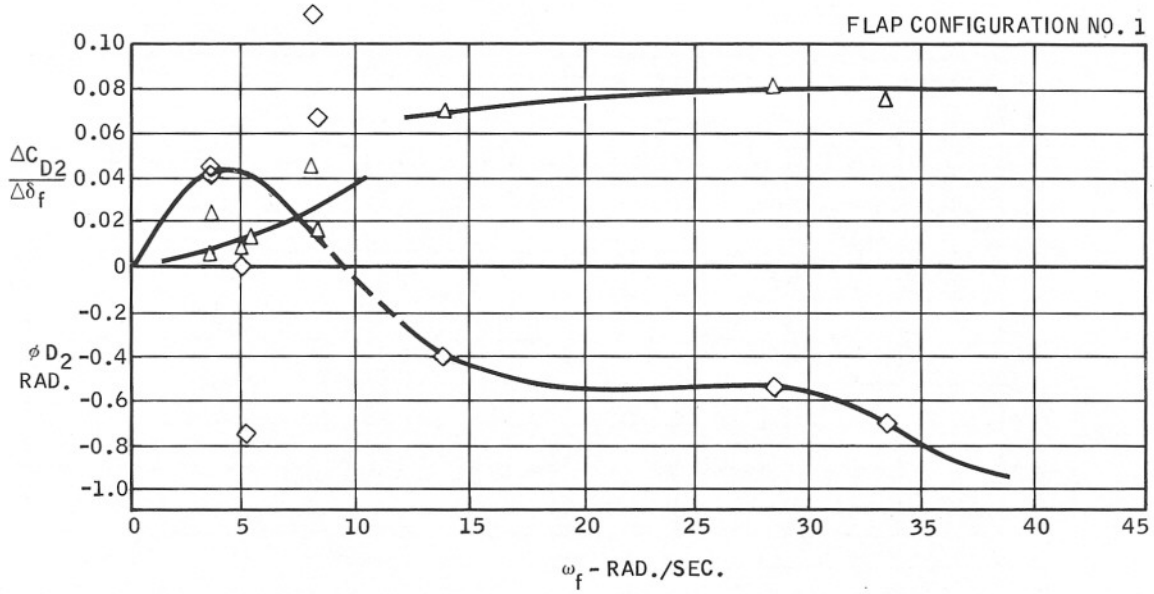


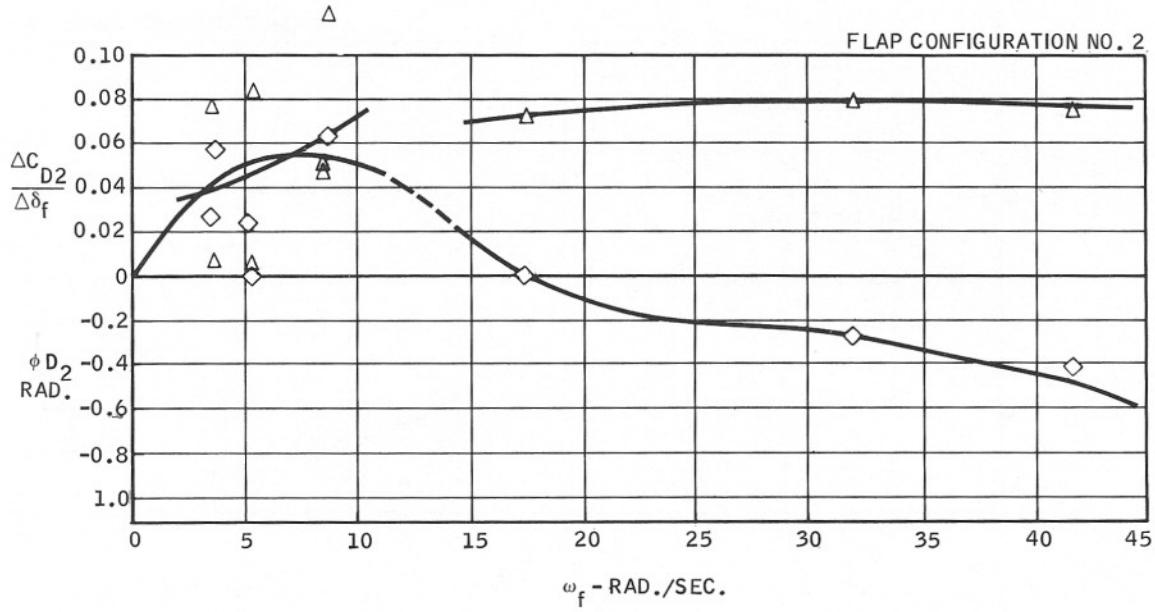


Figure 5. Drag Frequency Response, Flaps Oscillating, Smooth Water

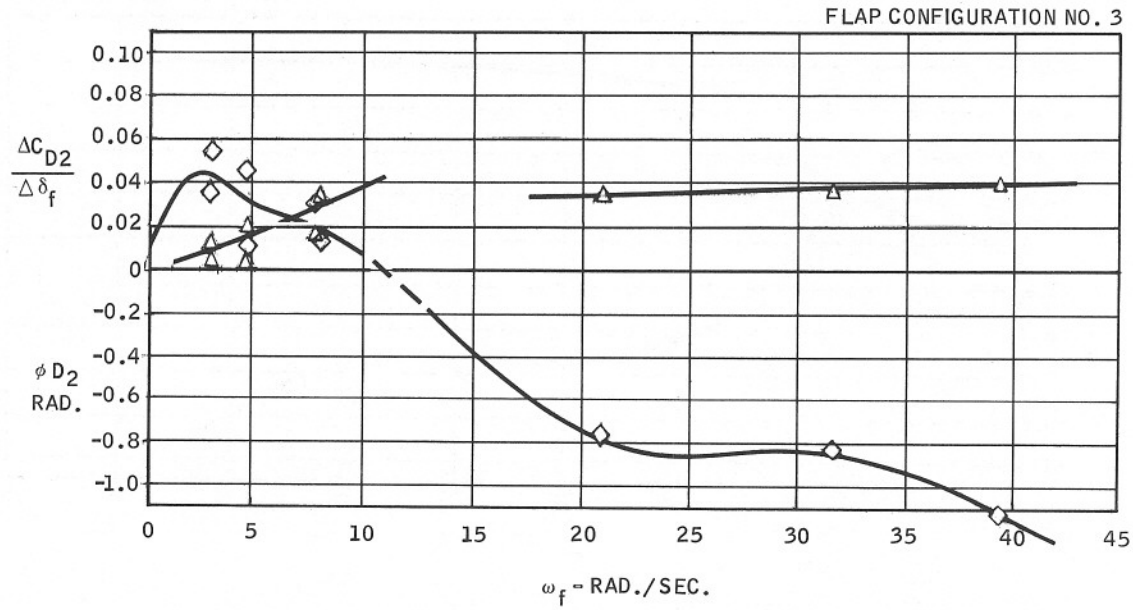


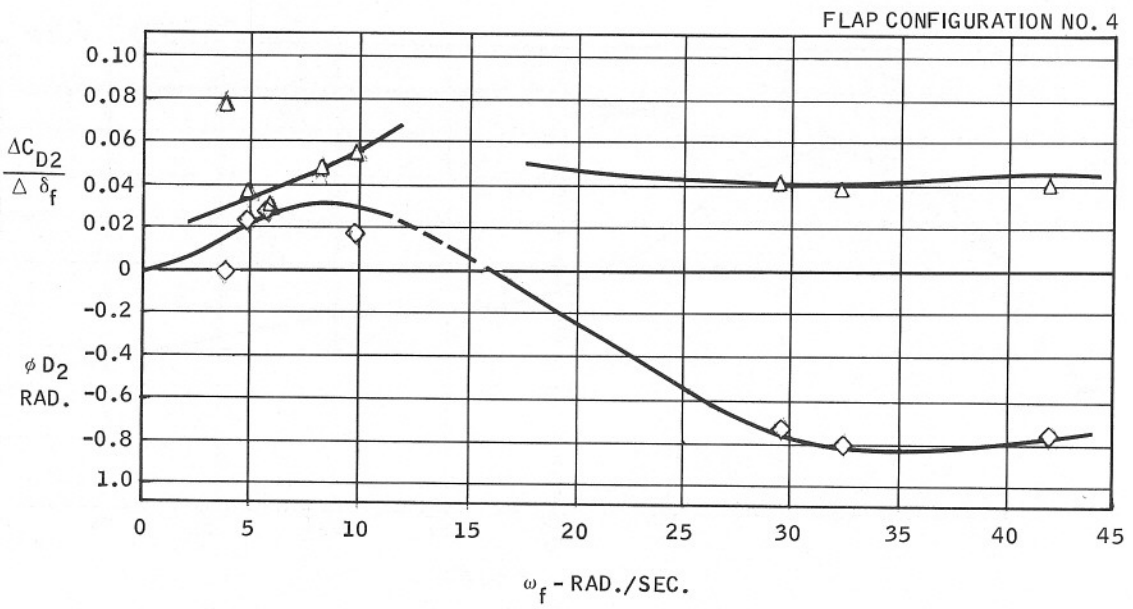


Figure 6. Drag Frequency Response, Flaps Oscillating, Smooth Water

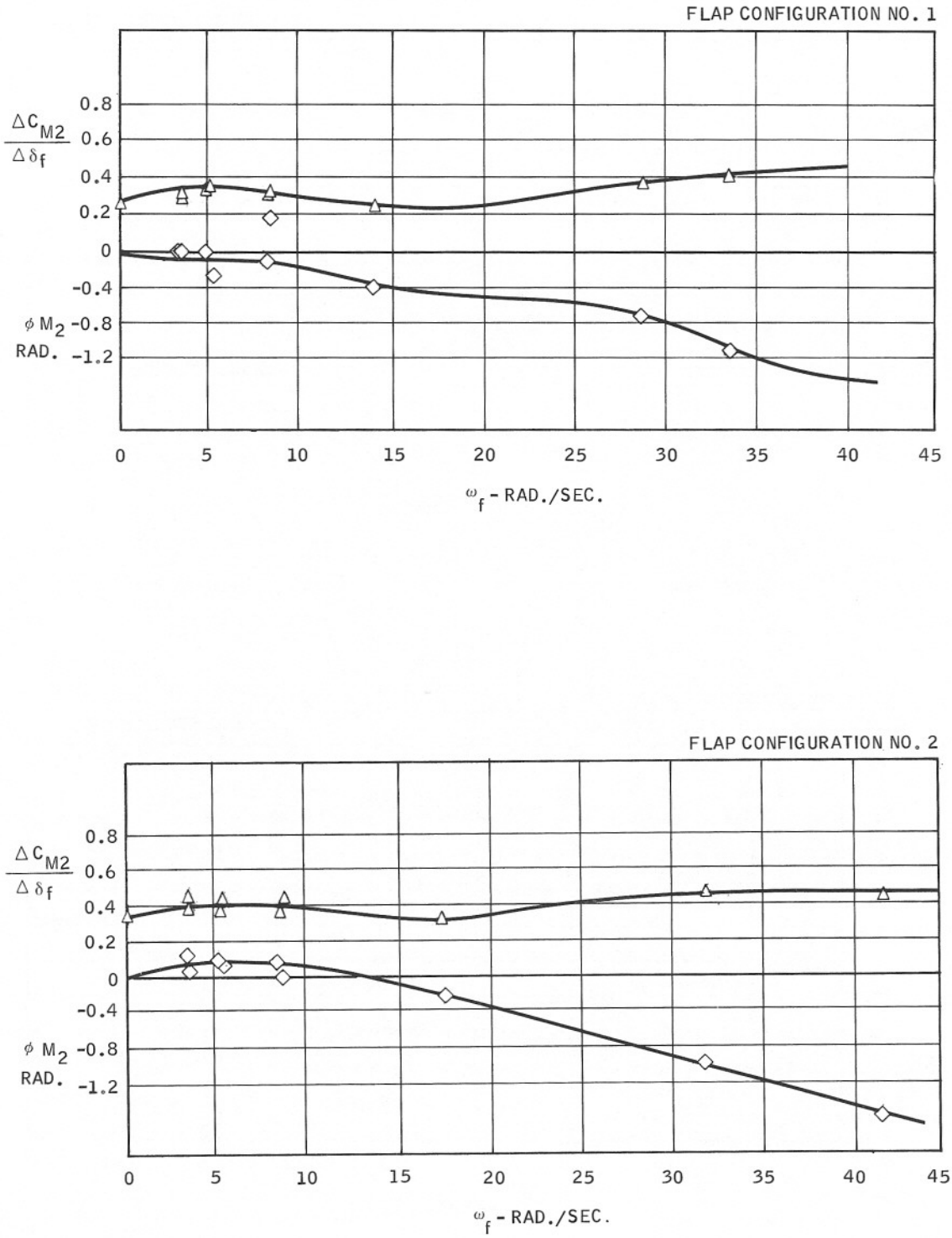


Figure 7. Pitching Moment Frequency Response, Flaps Oscillating, Smooth Water

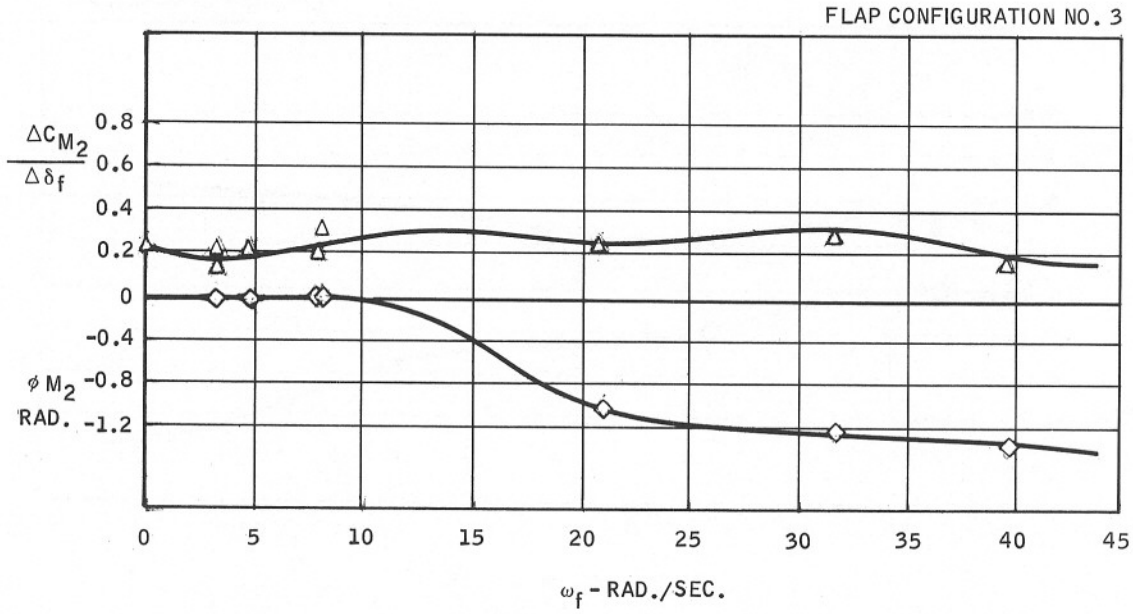


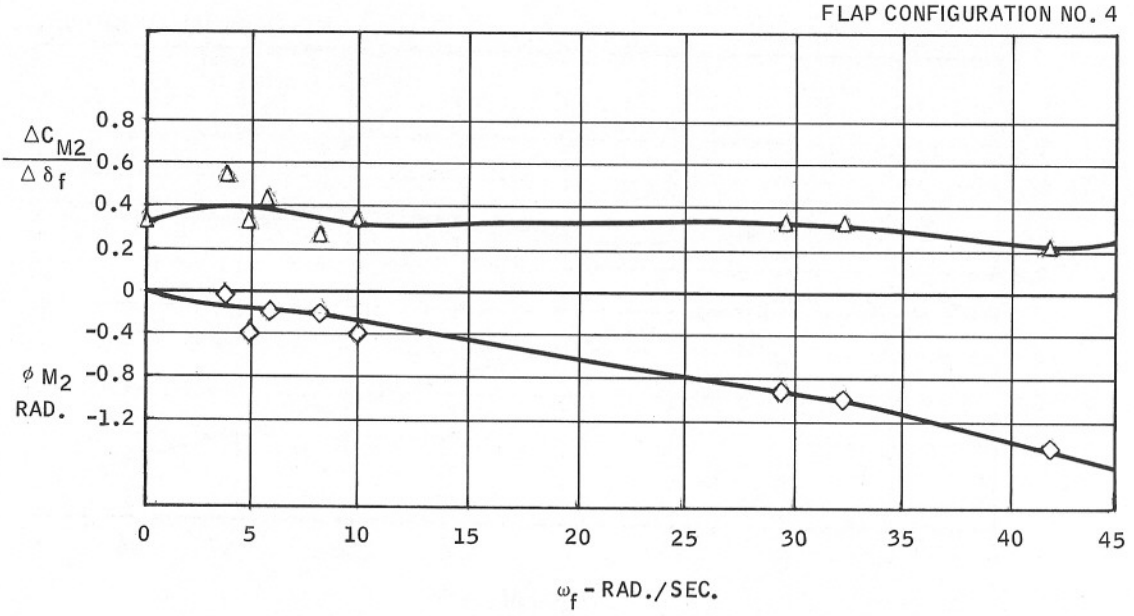


Figure 8. Pitching Moment Frequency Response, Flaps Oscillating, Smooth Water

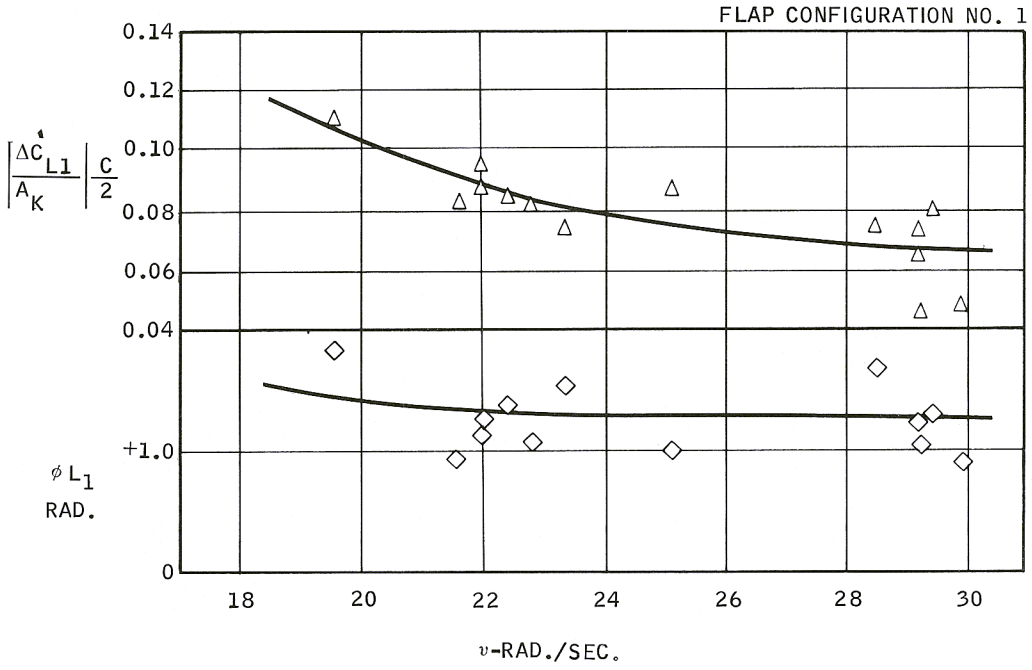


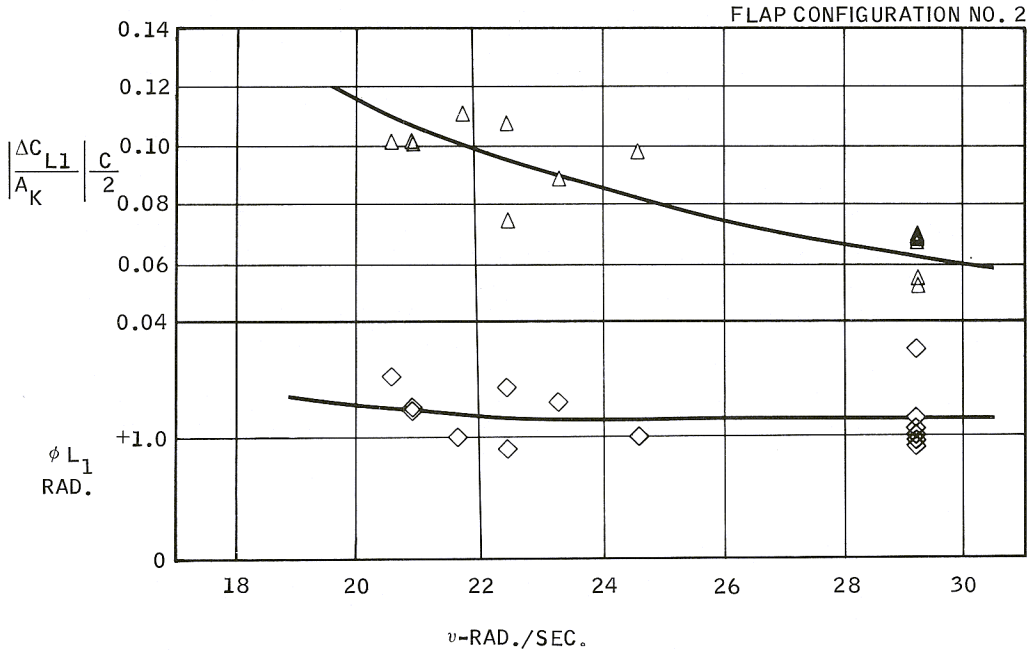


Figure 9. Lift Frequency Response, Head Seas, Flaps Fixed

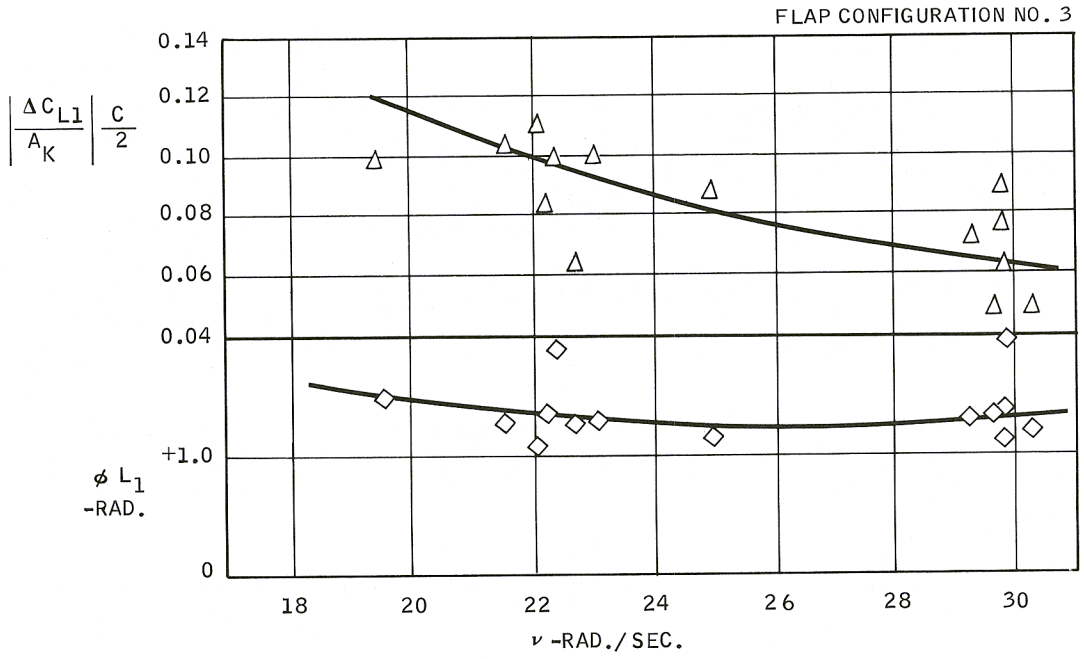


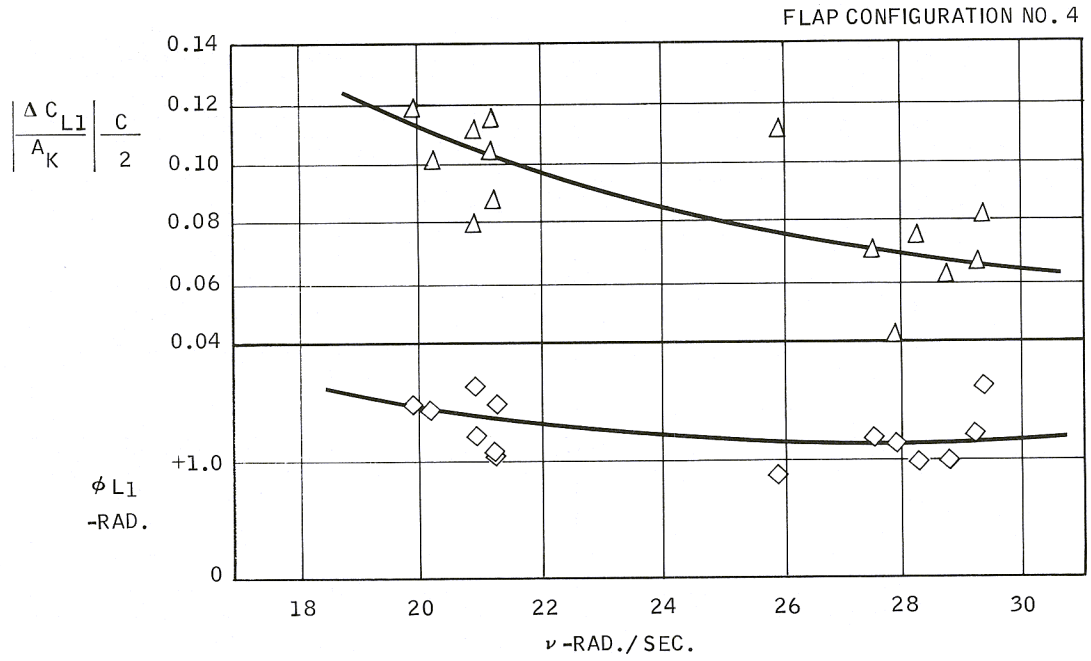


**Figure 10. Lift Frequency Response, Head Seas, Flaps Fixed**

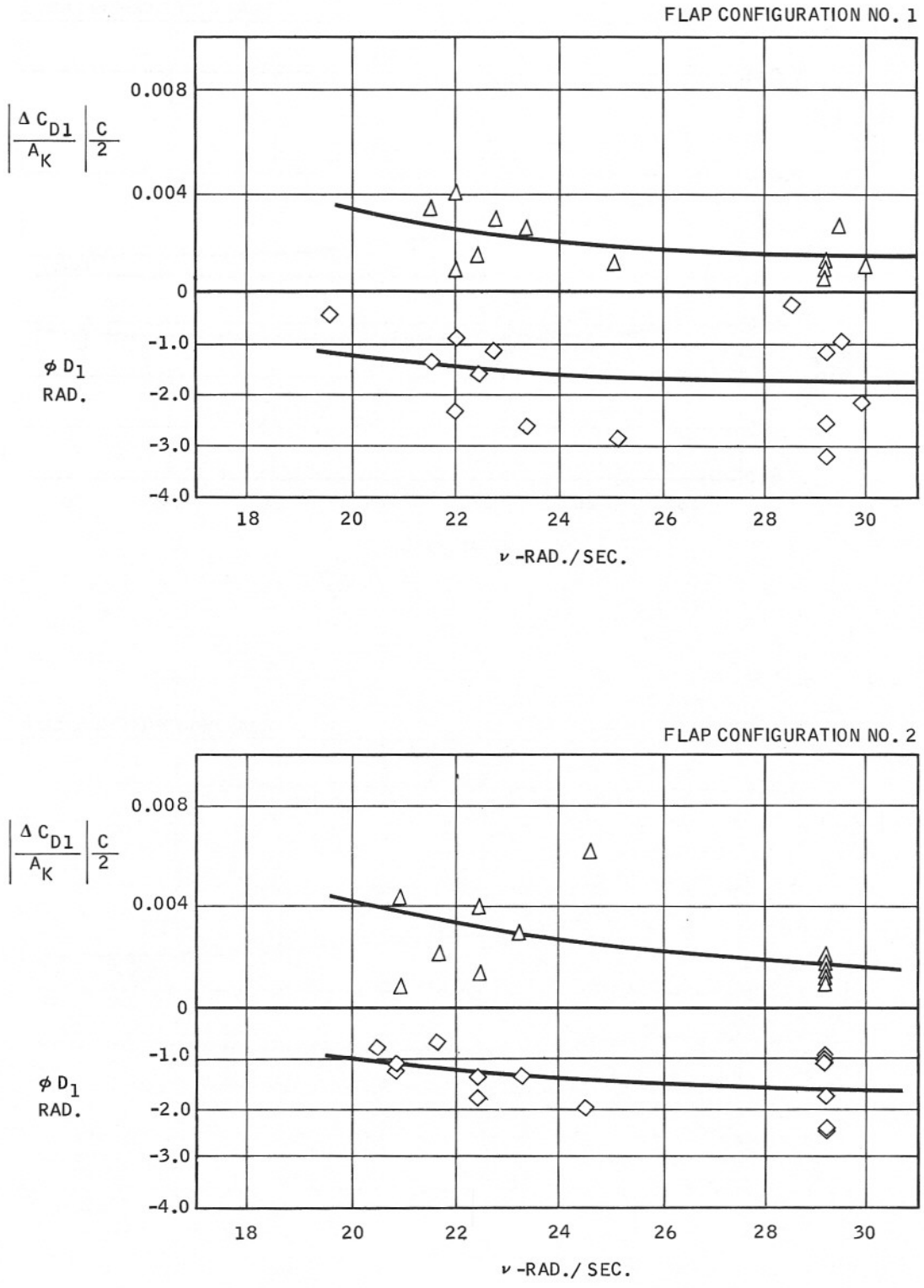


**Figure 11. Drag Frequency Response, Head Seas, Flaps Fixed**

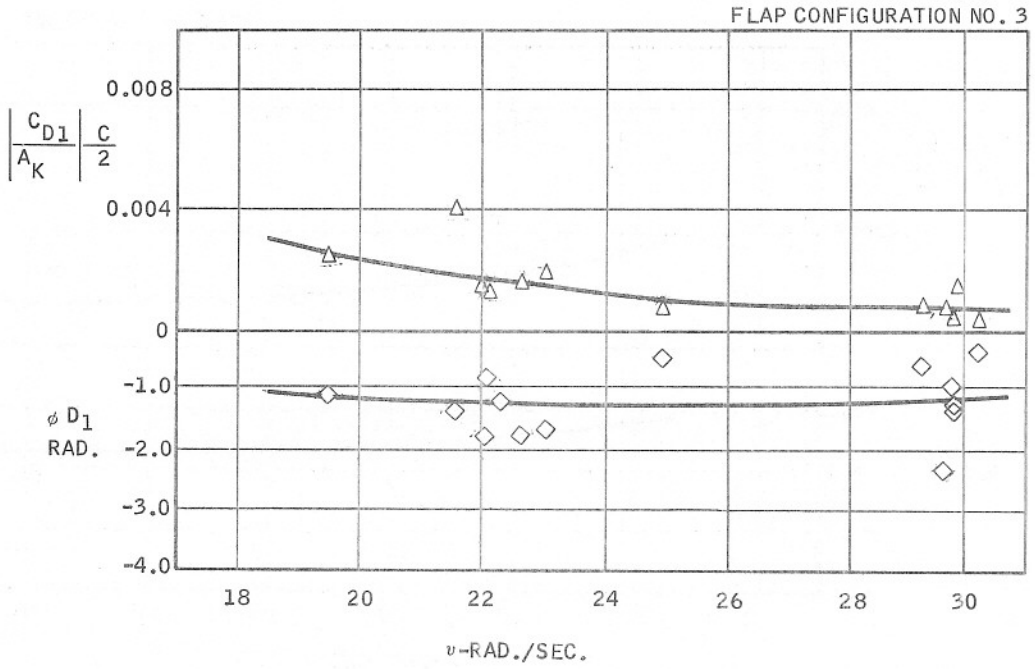


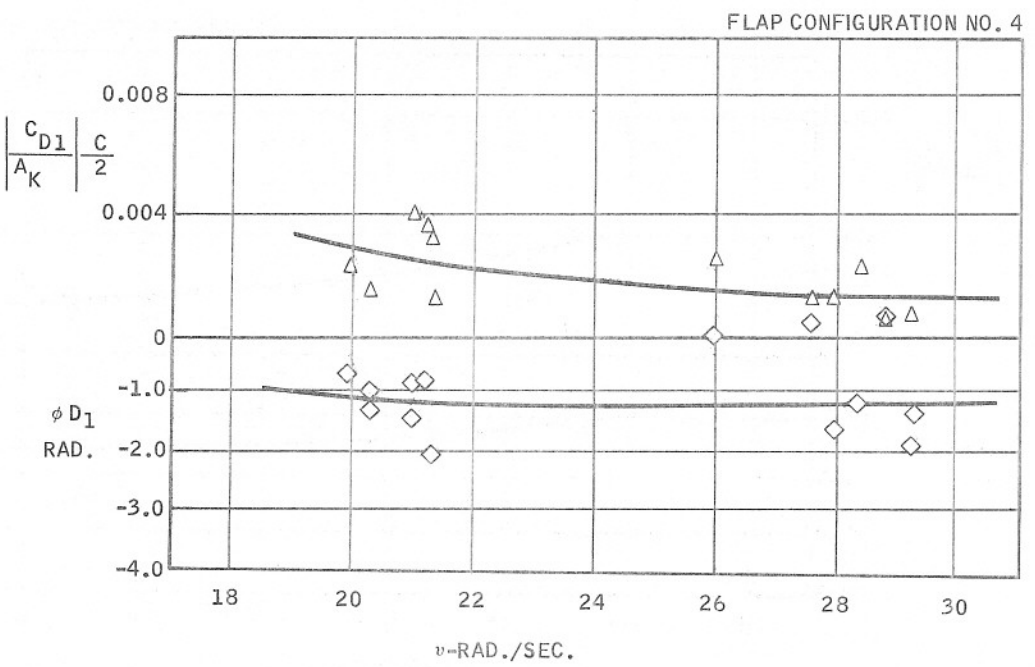


**Figure 12.** Drag Frequency Response, Head Seas, Flaps Fixed

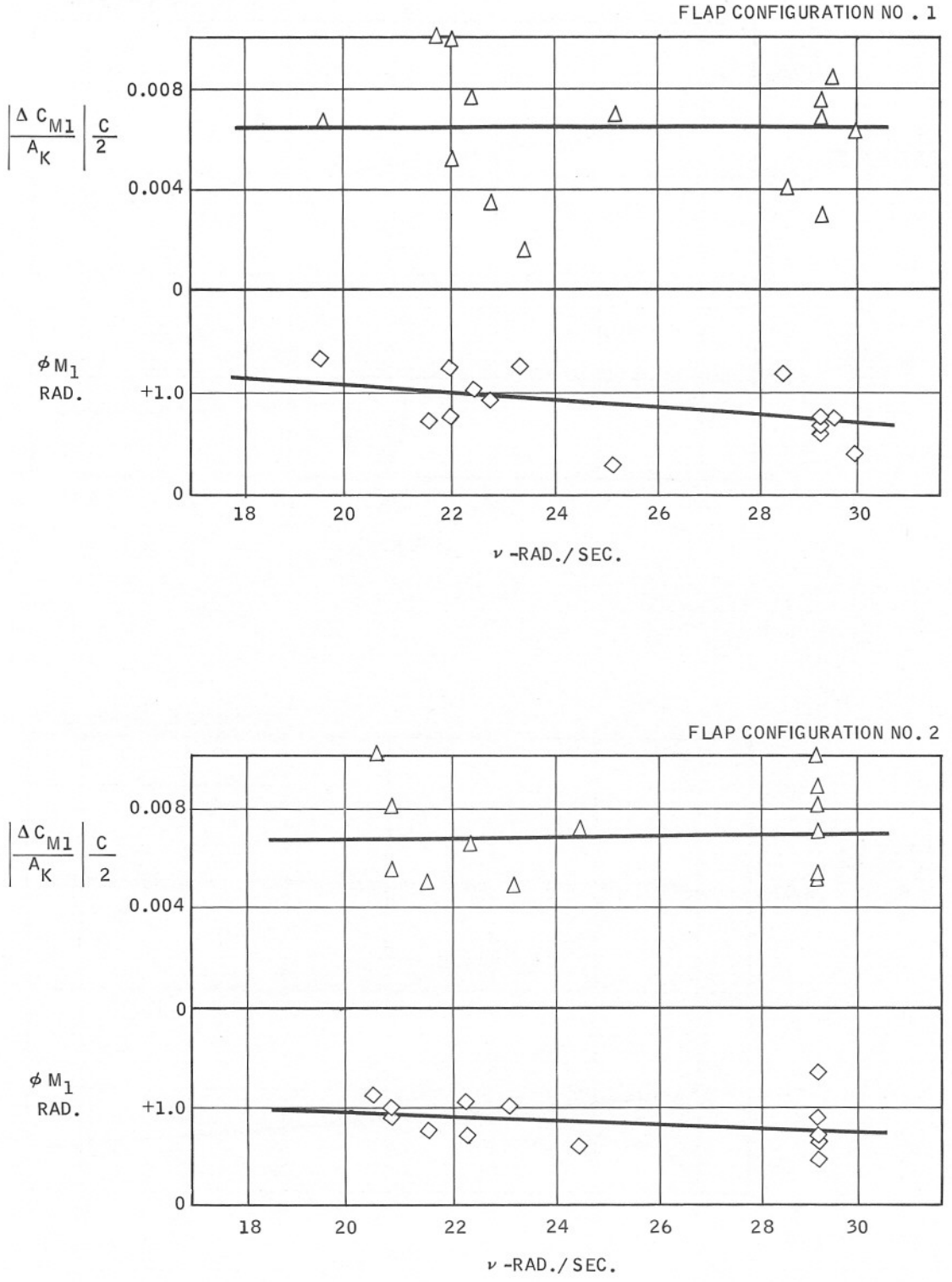


Figure 13. Pitching Moment Frequency Response, Head Seas, Flaps Fixed

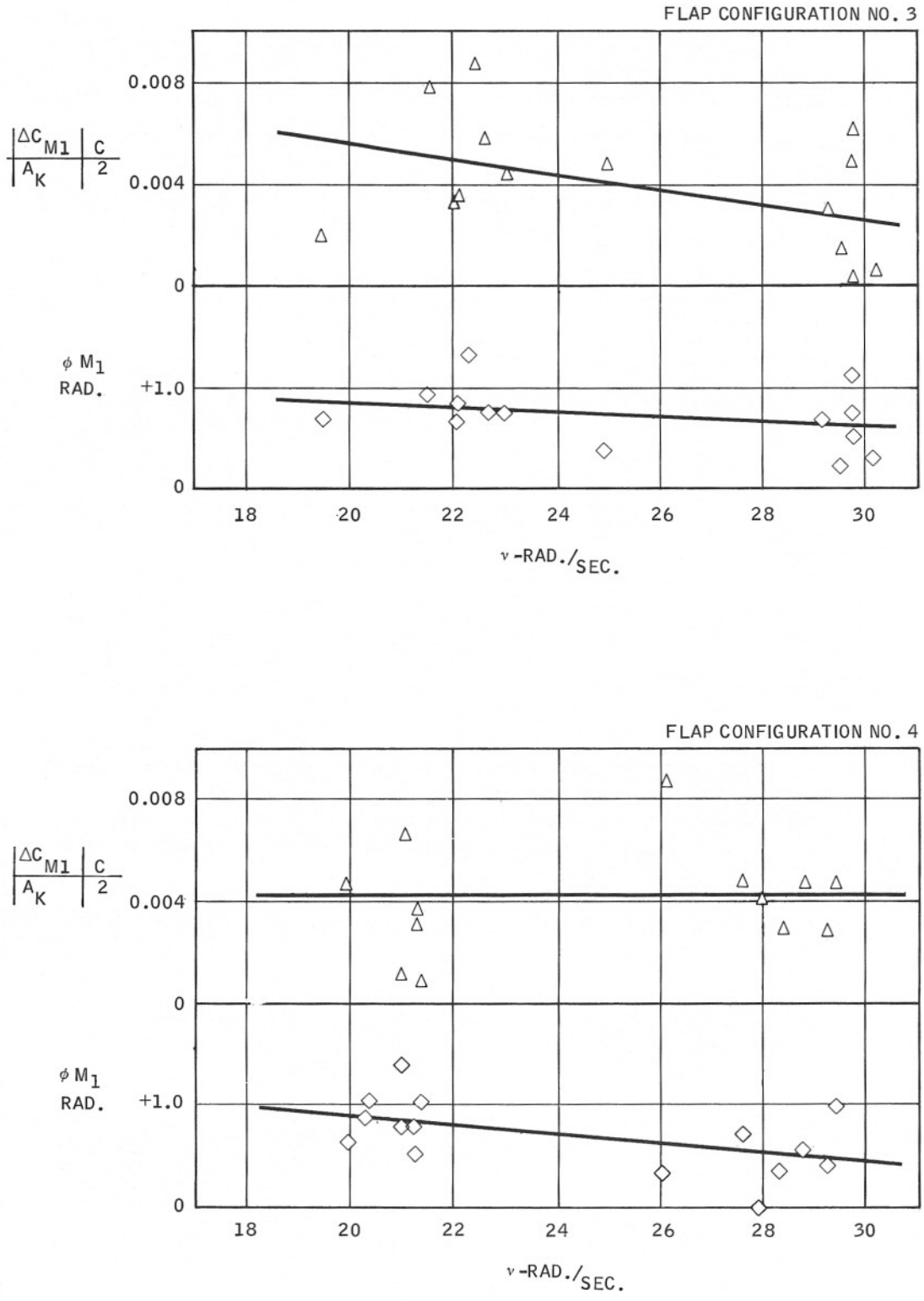


**Figure 14. Pitching Moment Frequency Response, Head Seas, Flaps Fixed**

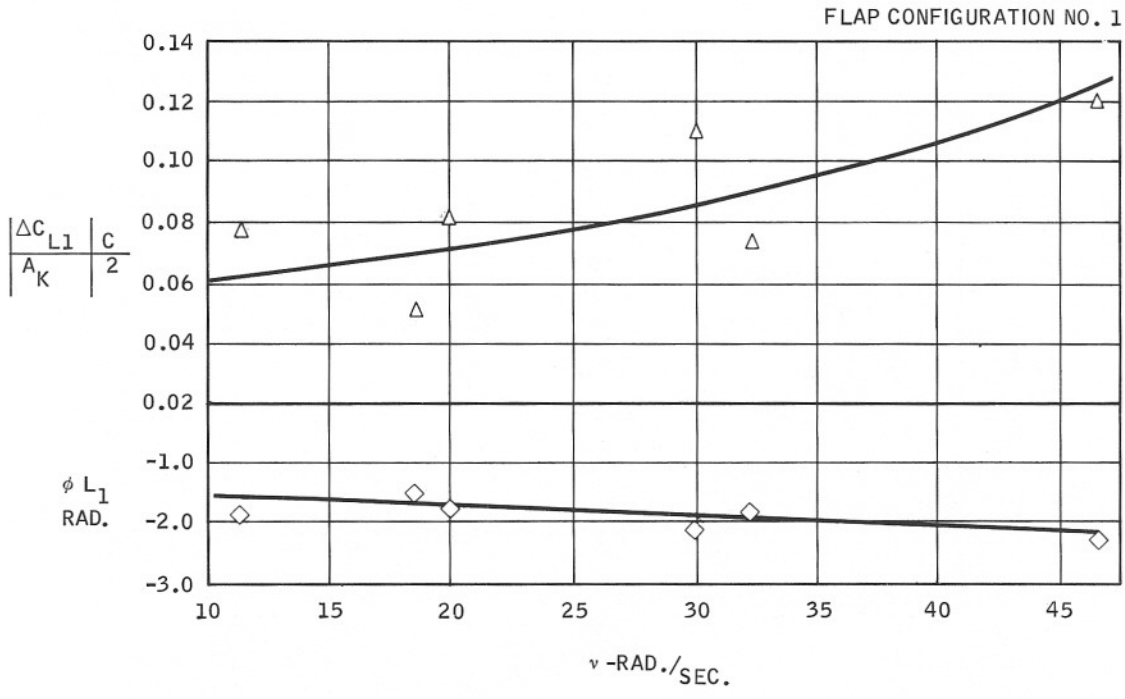


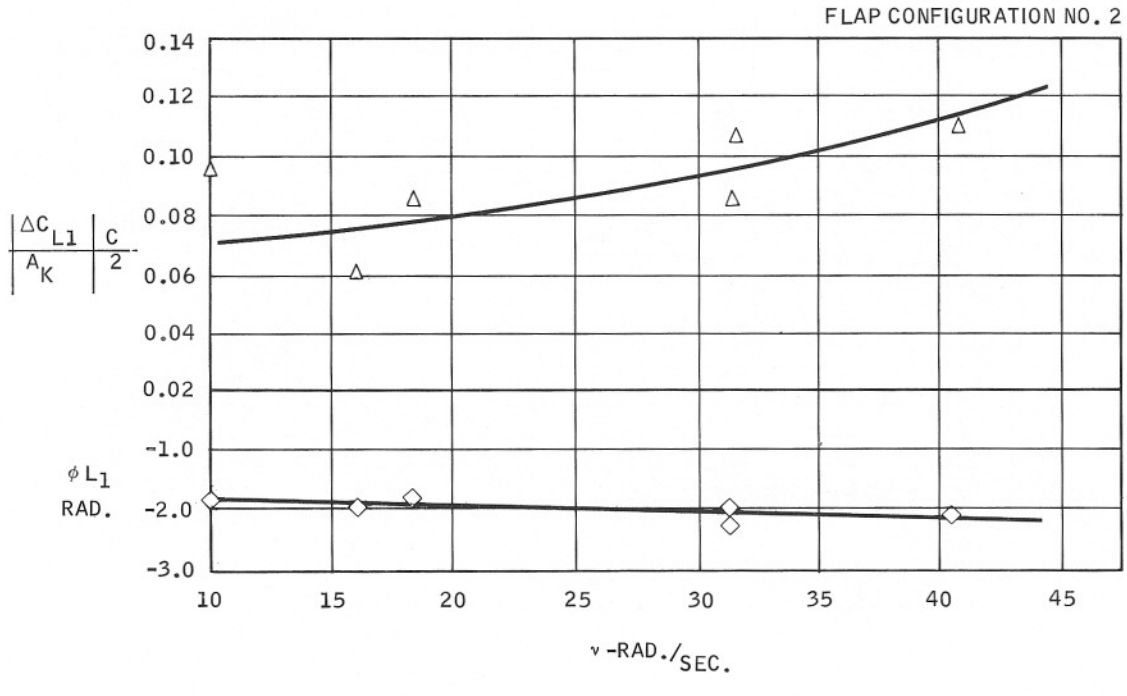


Figure 15. Lift Frequency Response, Following Seas, Flaps Fixed

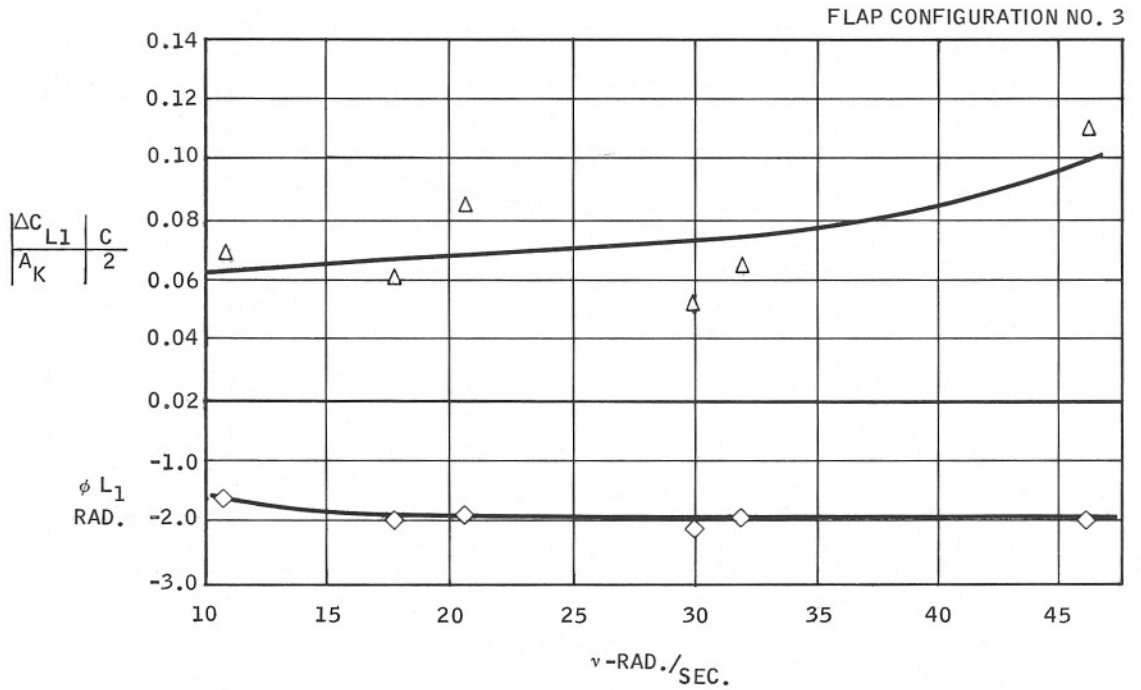


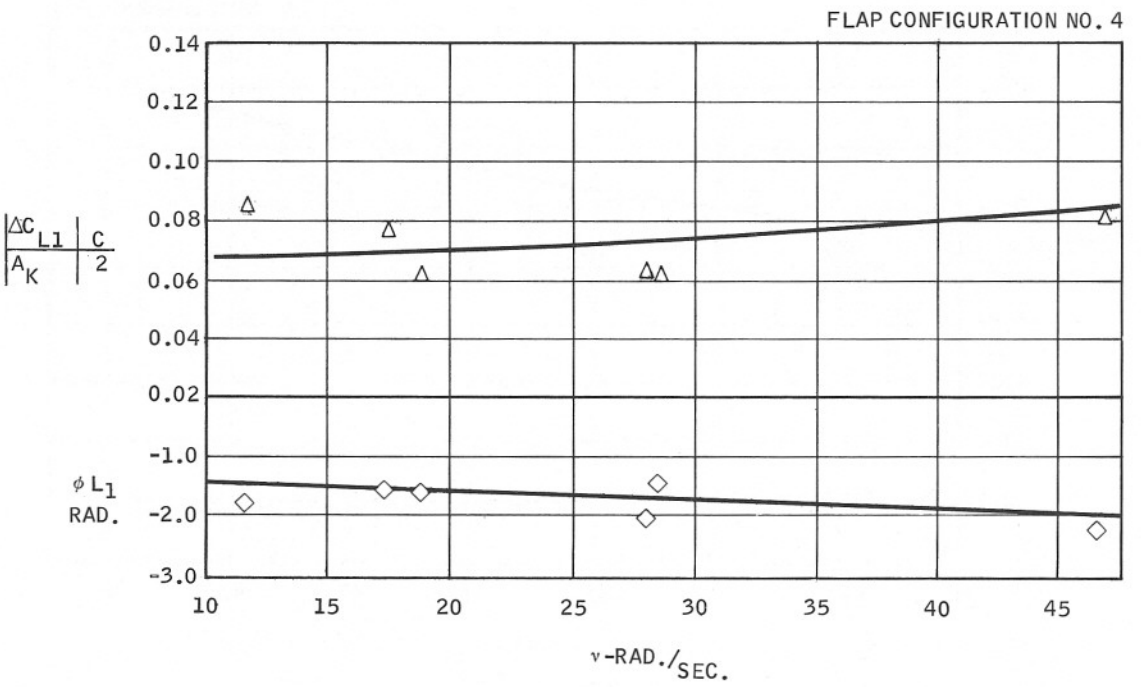


Figure 16. Lift Frequency Response, Following Seas, Flaps Fixed

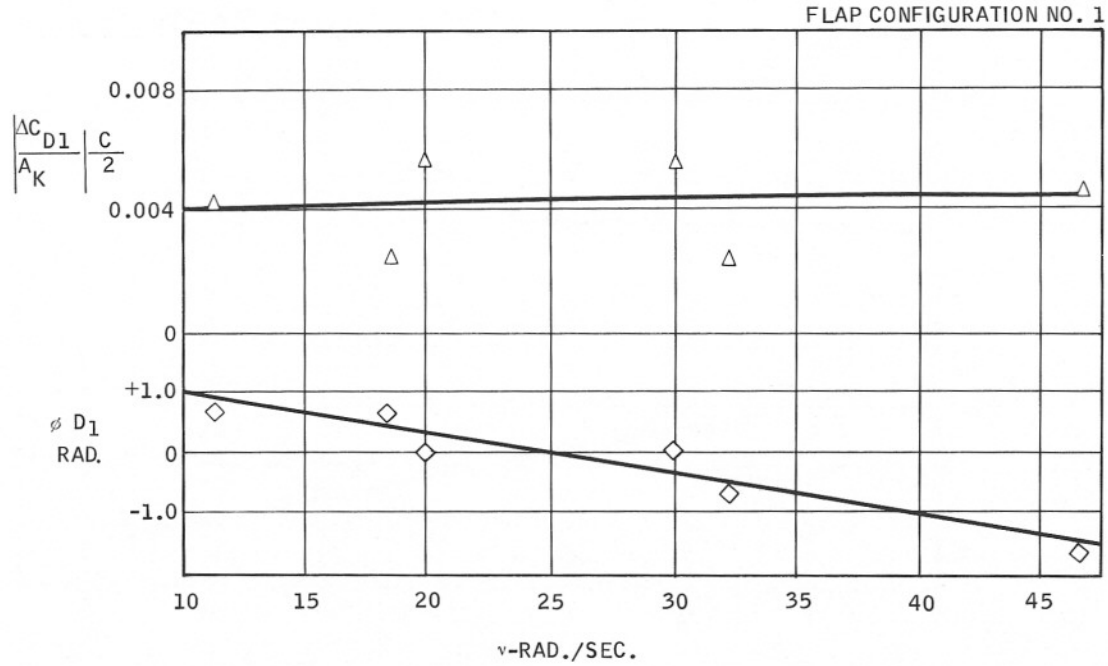


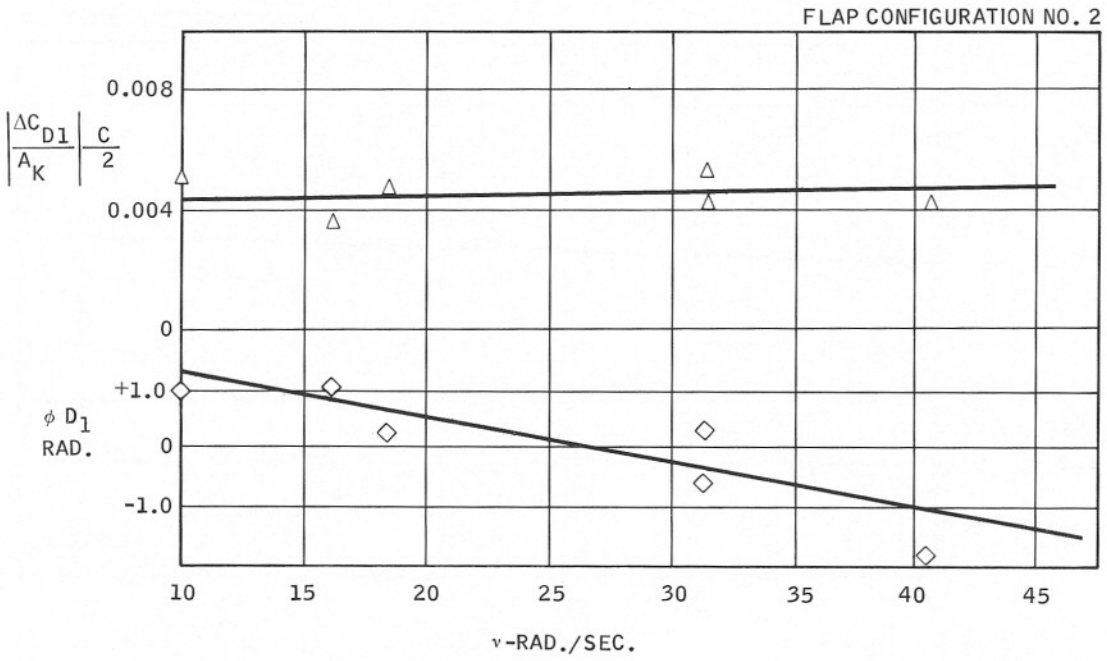


Figure 17. Drag Frequency Response, Following Seas, Flaps Fixed

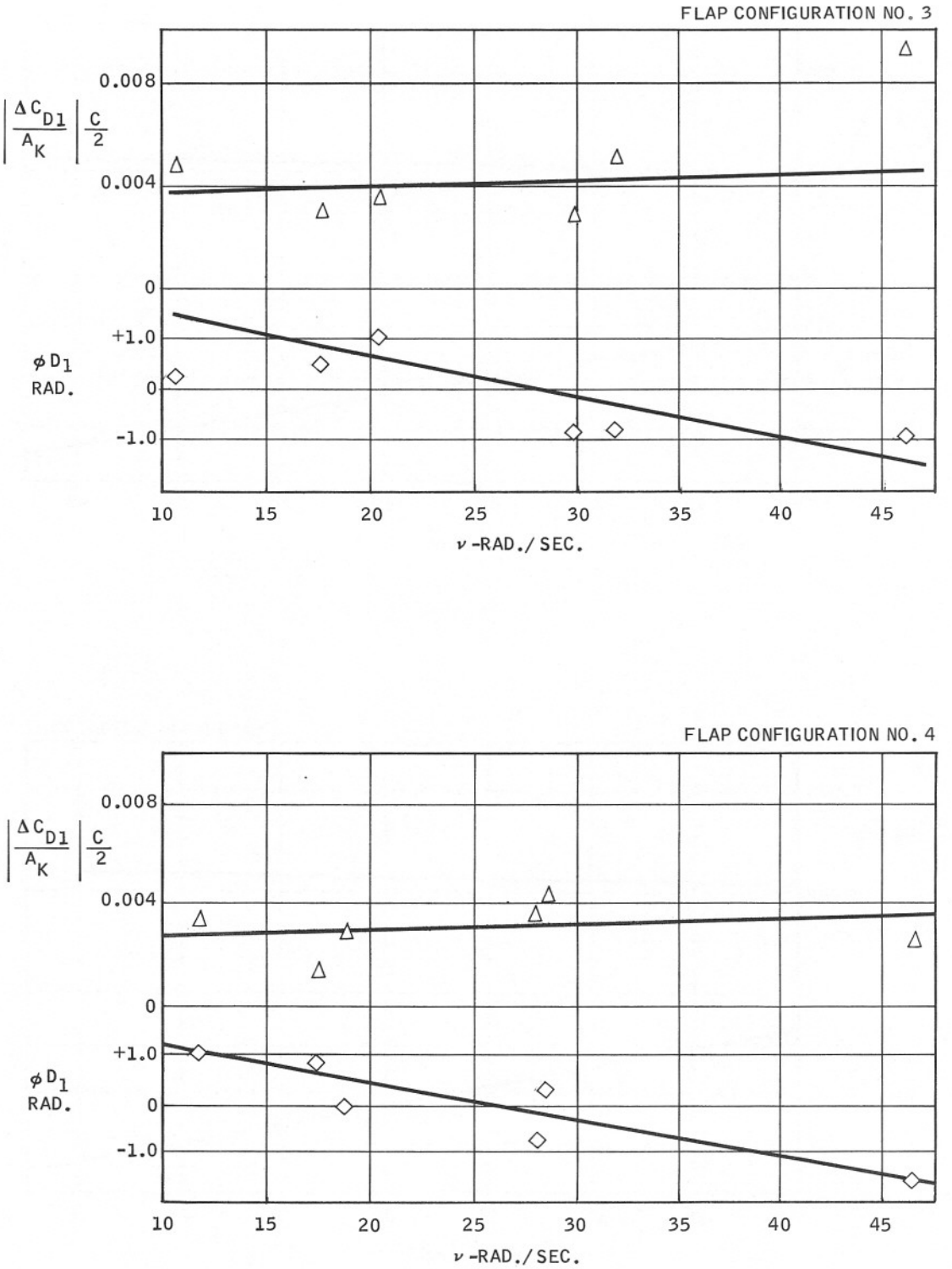


Figure 18. Drag Frequency Response, Following Seas, Flaps Fixed

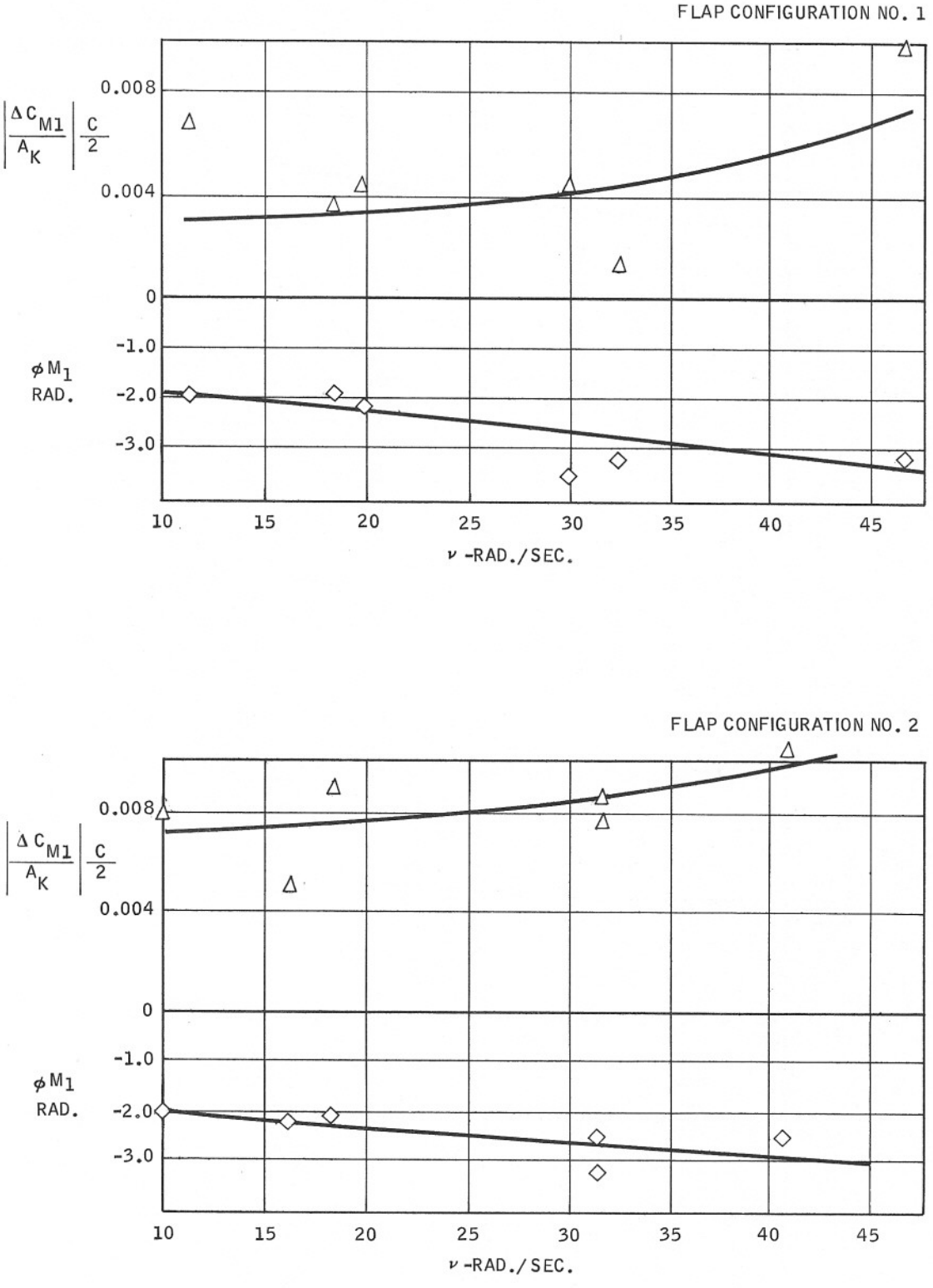


Figure 19. Pitching Moment Frequency Response, Following Seas, Flaps Fixed

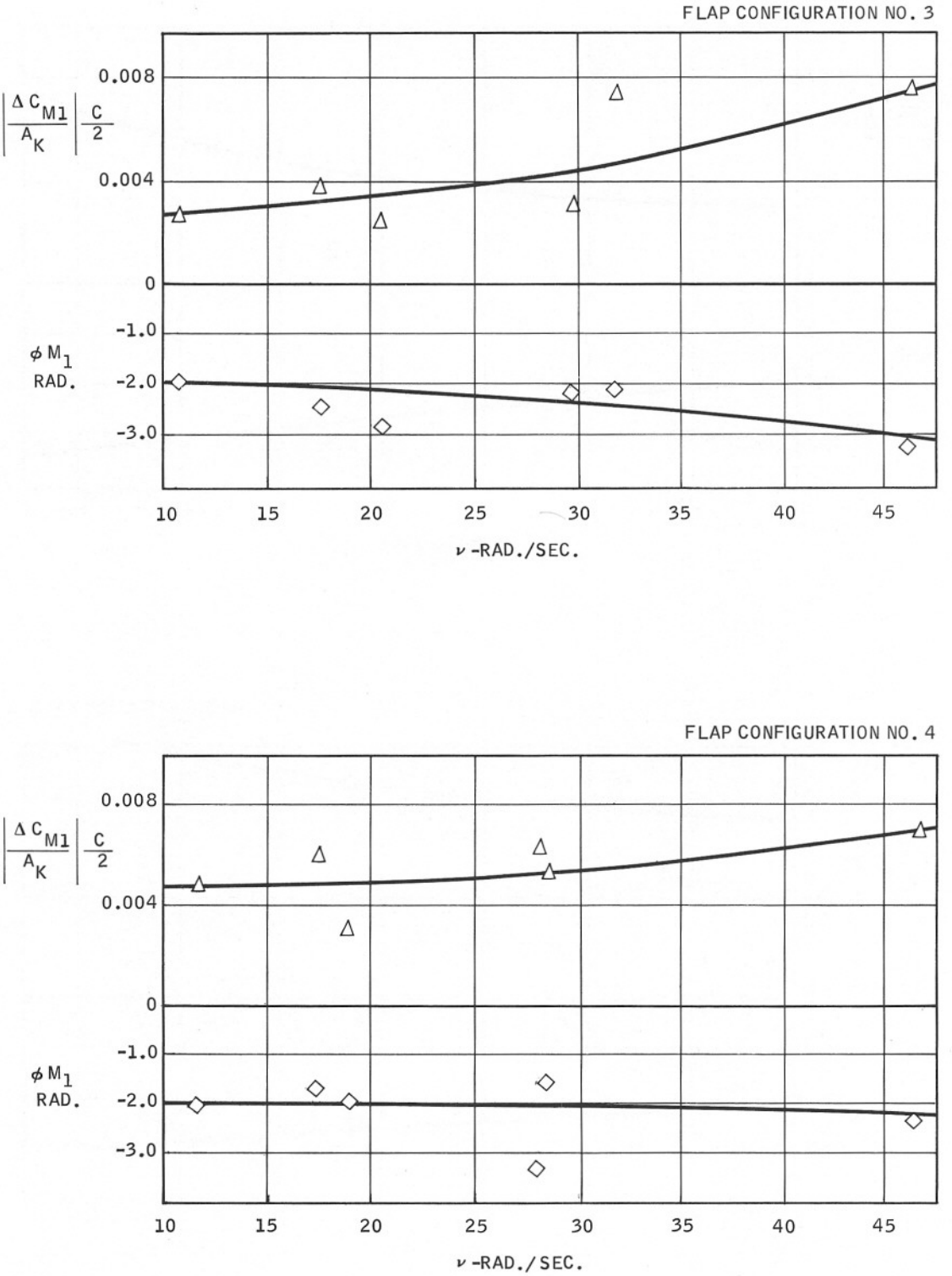


**Figure 20. Pitching Moment Frequency Response, Following Seas, Flaps Fixed**

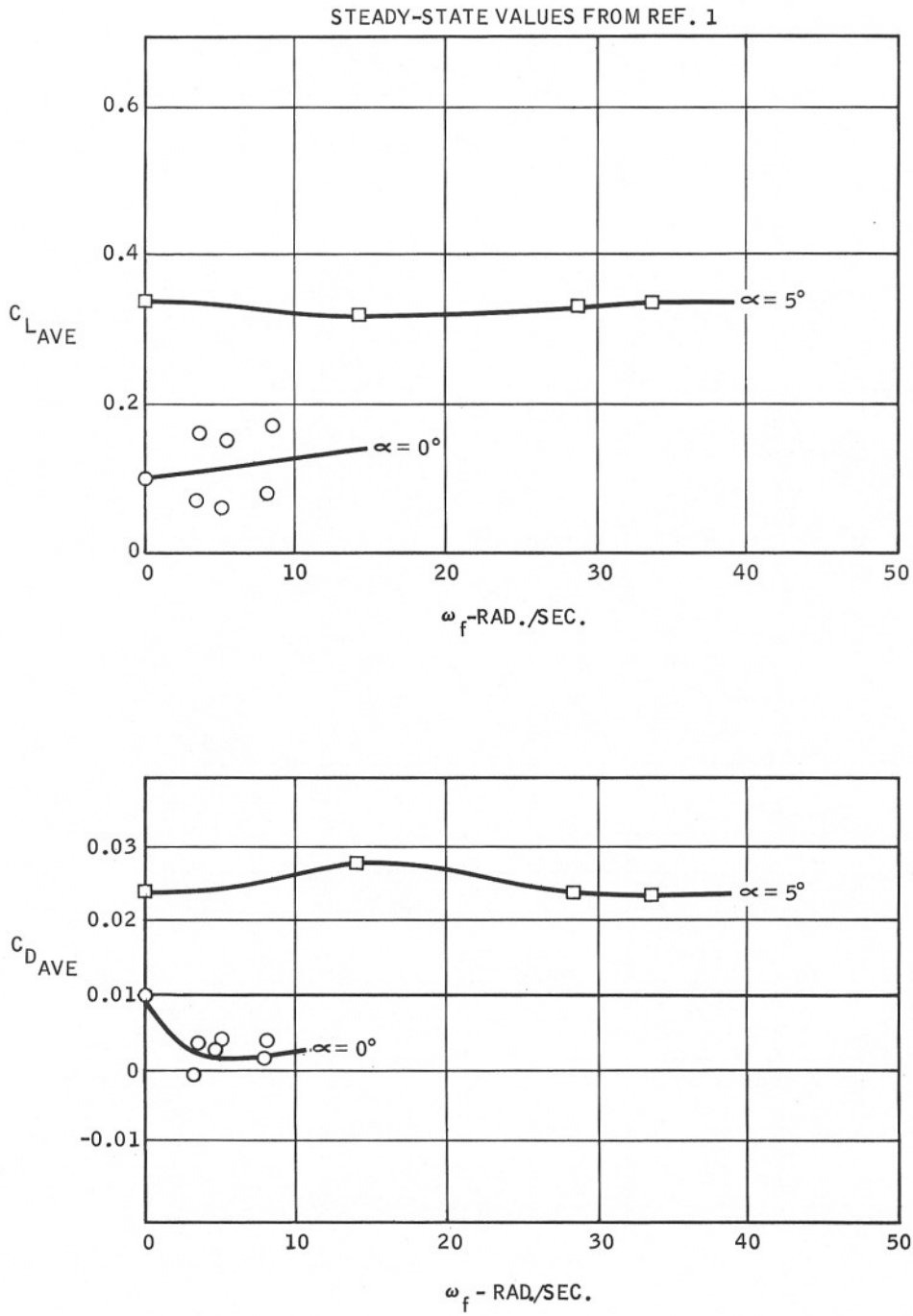


Figure 21. Flaps Configuration 1 — Mean Values of Force Coefficients, Flaps Cycling in Smooth Water

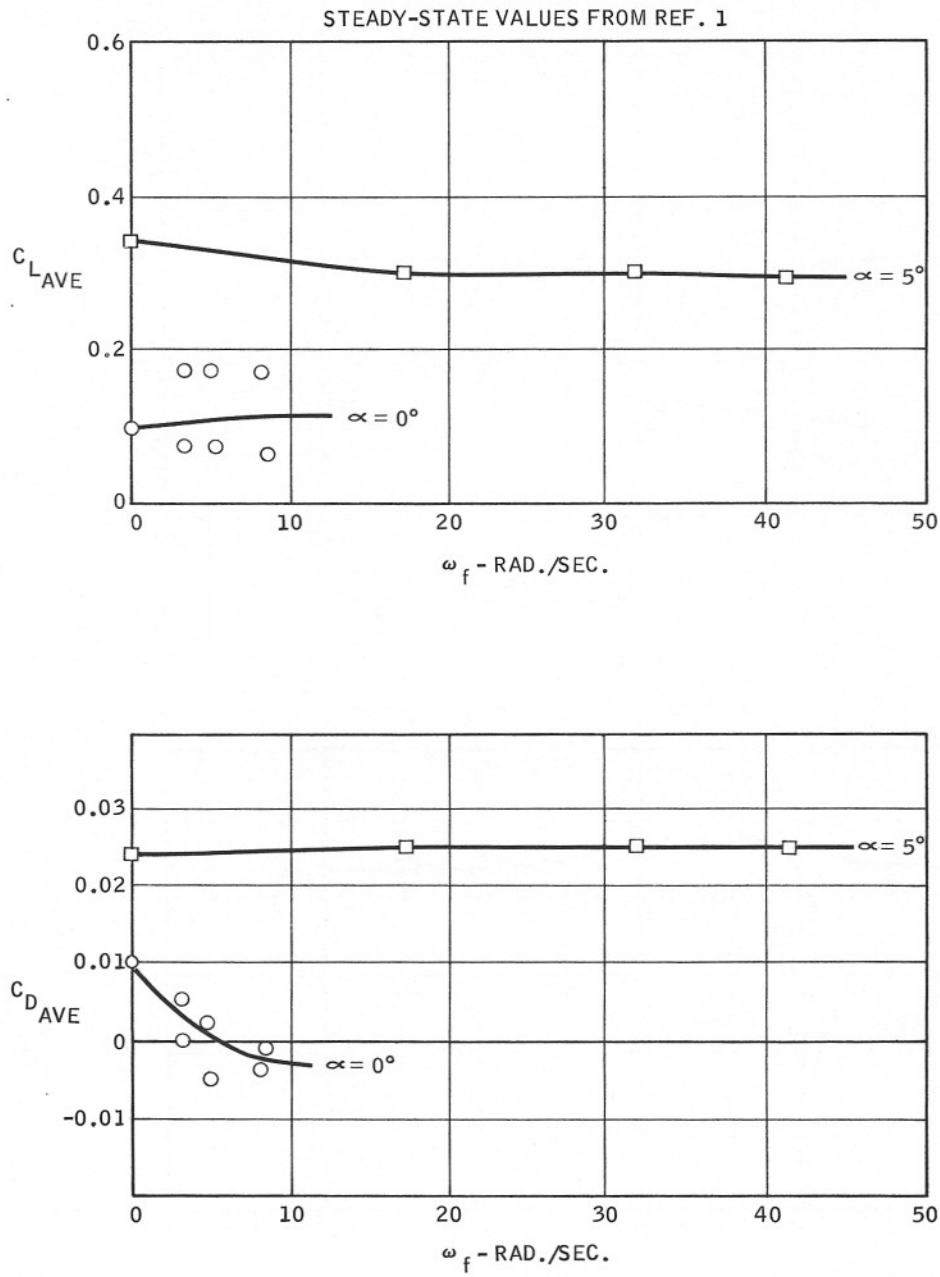


**Figure 22. Flap Configuration 2 — Mean Value of Force Coefficients, Flaps Cycling in Smooth Water**

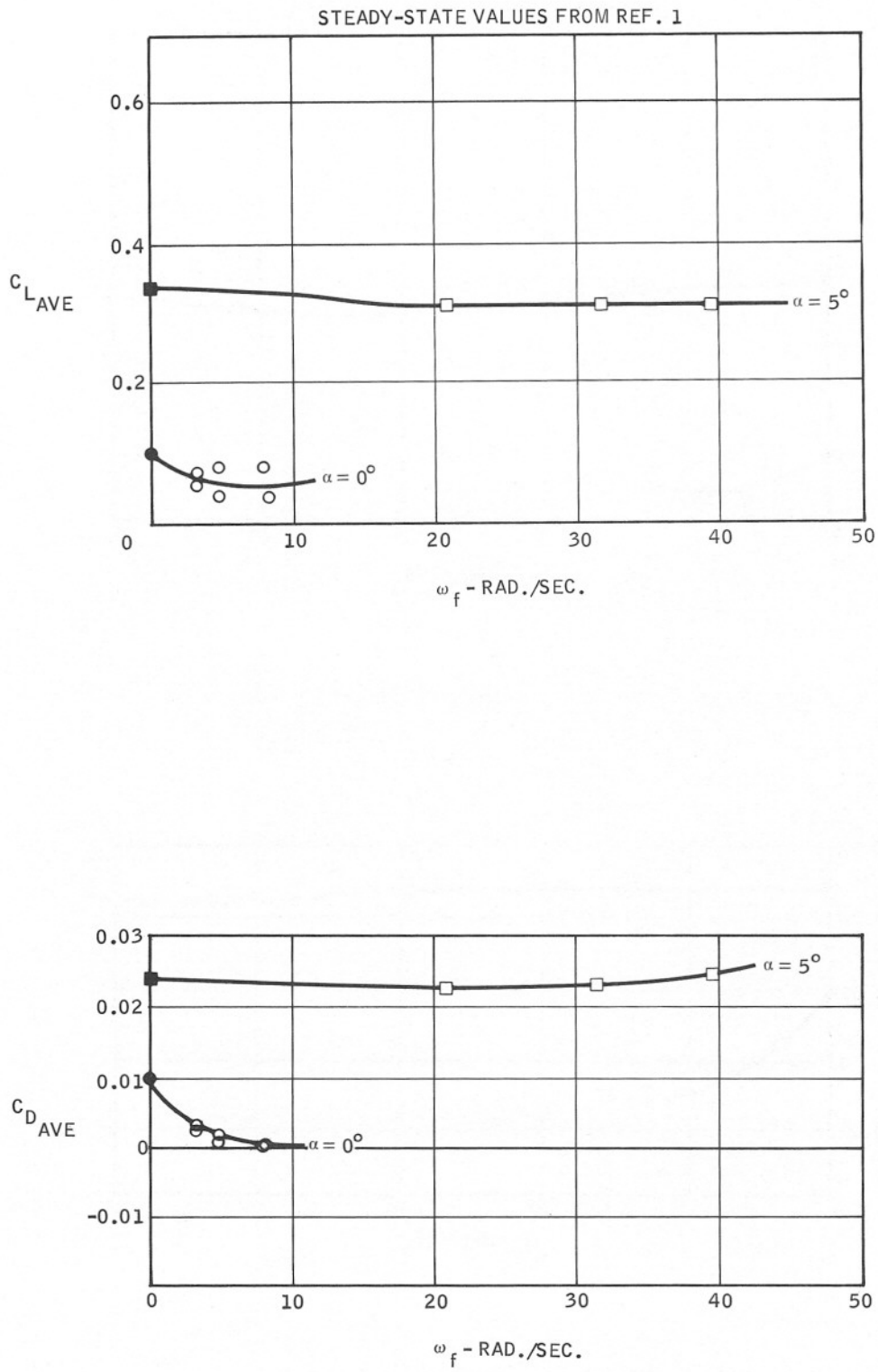


**Figure 23.** Flap Configuration 3 — Mean Values of Force Coefficients, Flaps Cycling in Smooth Water

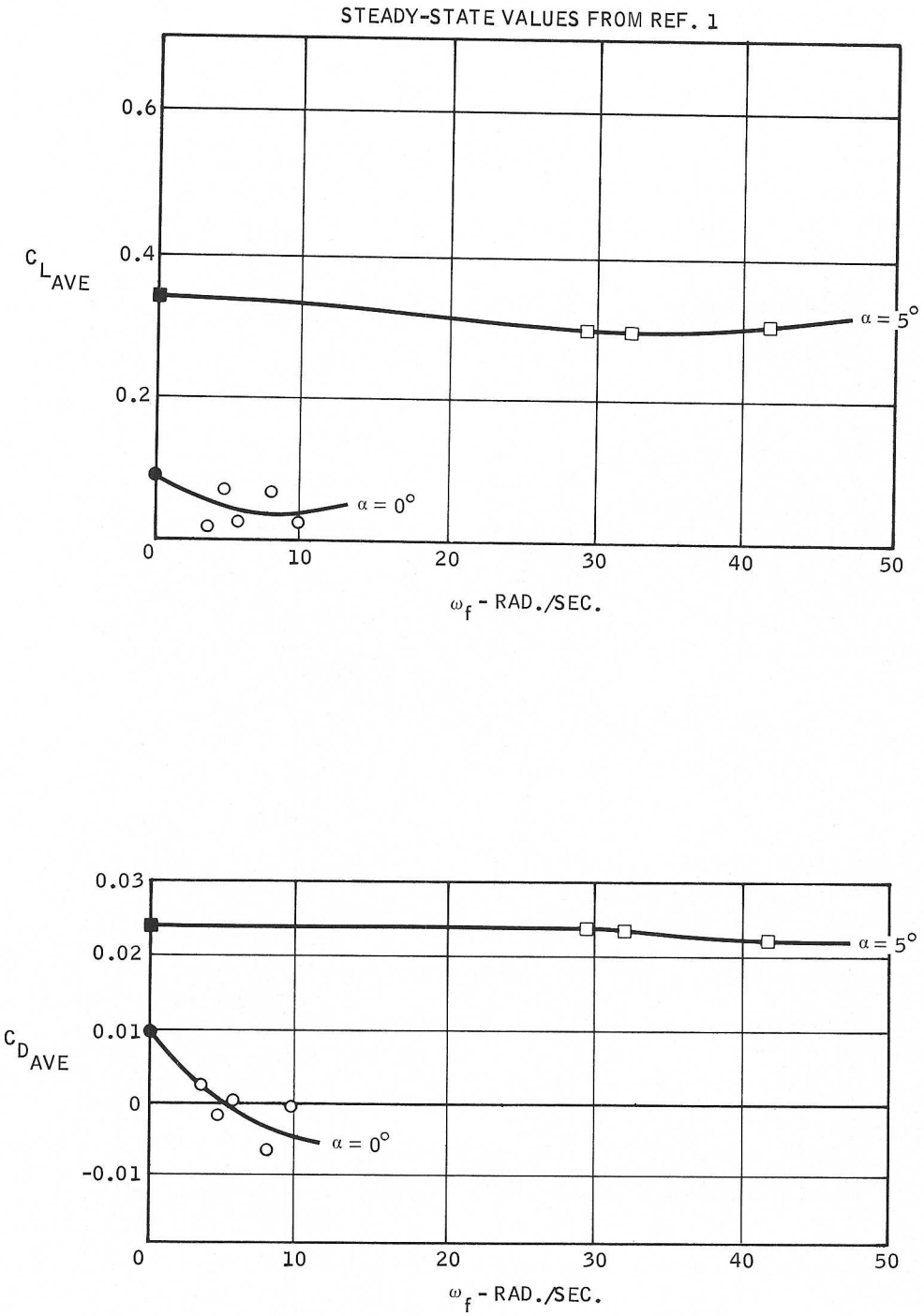


Figure 24. Flap Configuration 4 — Mean Value of Force Coefficients, Flaps Cycling in Smooth Water

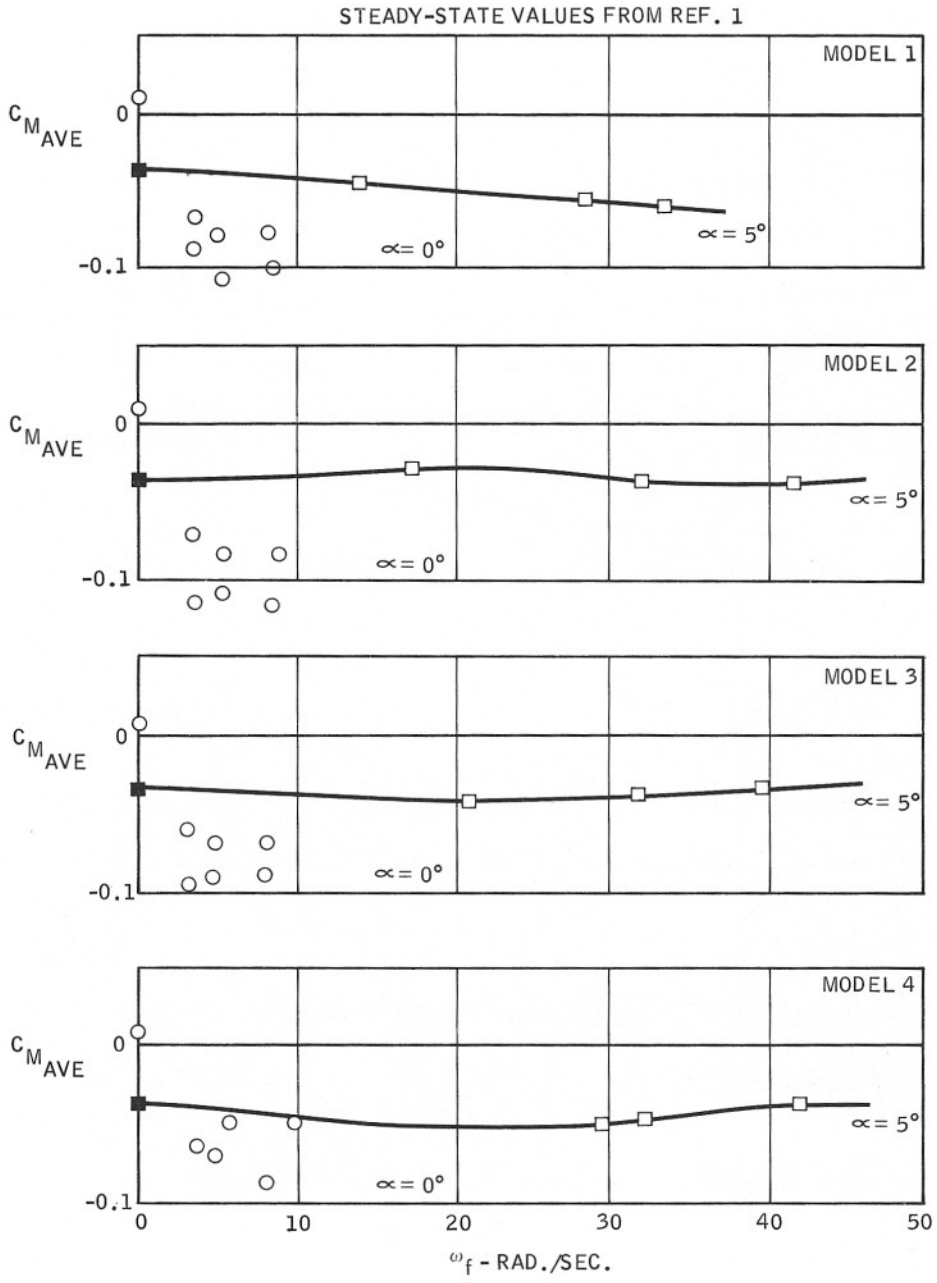


**Figure 25.** Mean Pitching Moment Coefficients — All Models, Flaps Cycling in Smooth Water

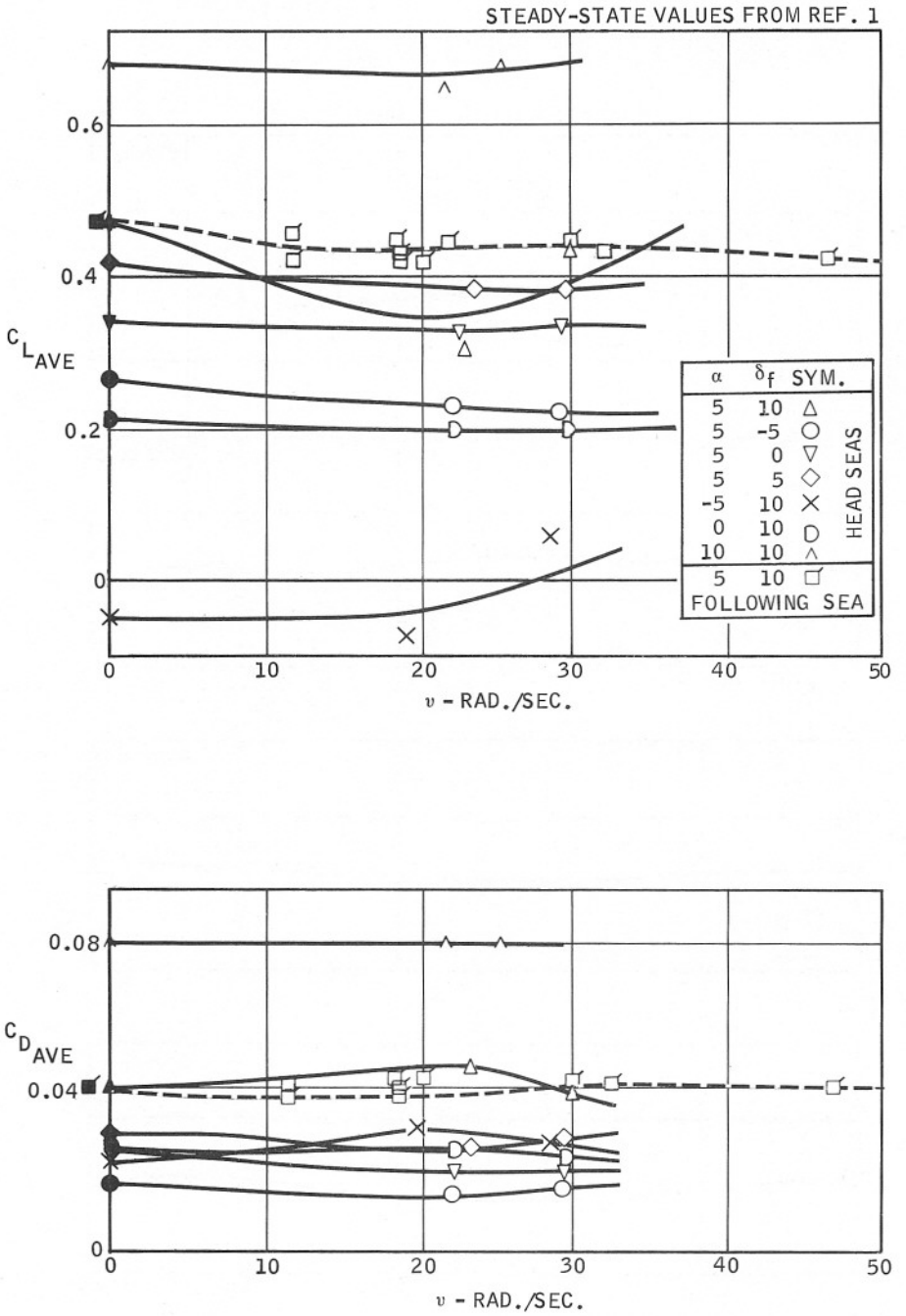


**Figure 26.** Flap Configuration 1 — Mean Value of Force Coefficients, Flaps Fixed in Waves

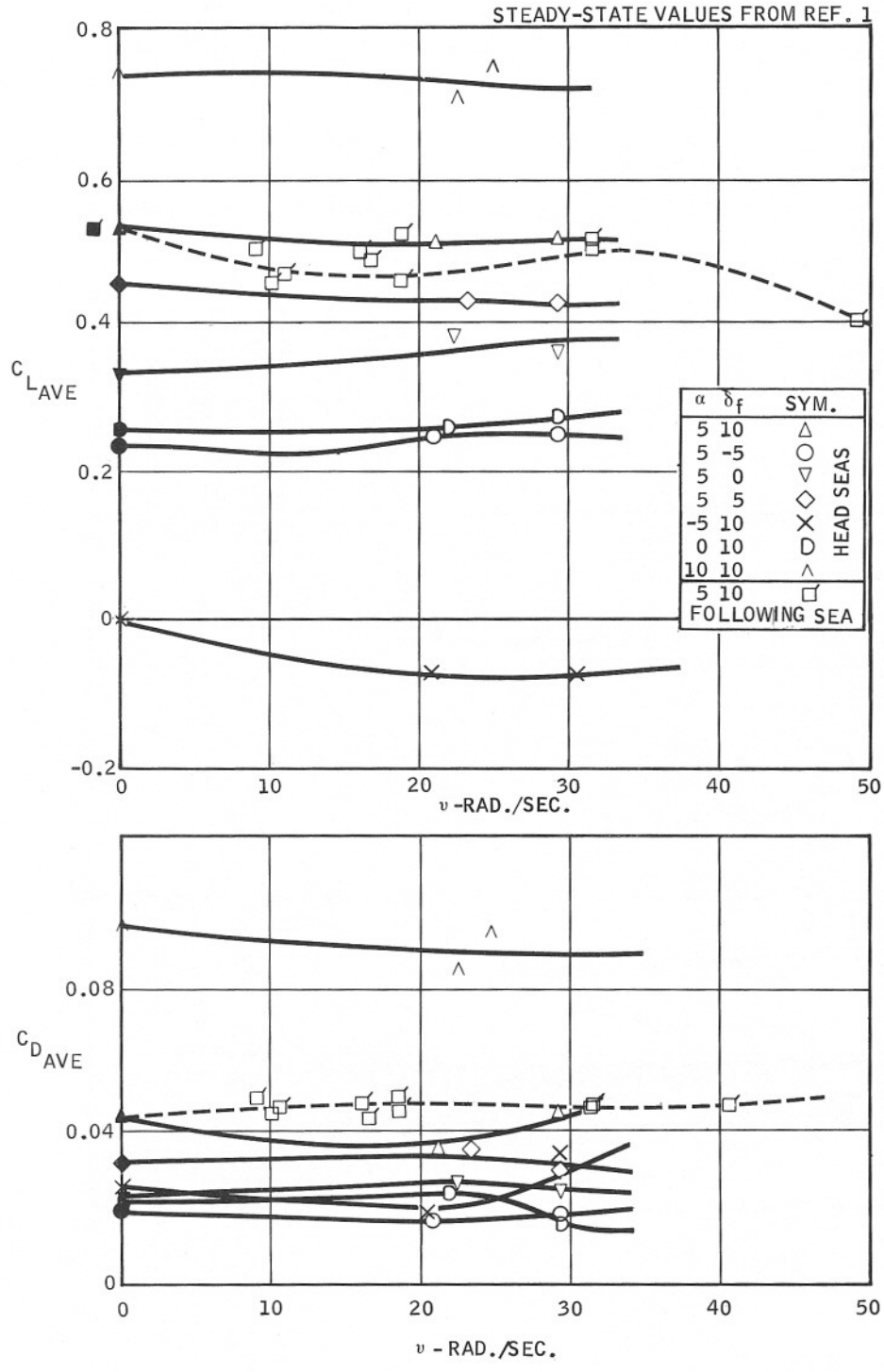


Figure 27. Flap Configuration 2 — Mean Values of Force Coefficients, Flaps Fixed in Waves

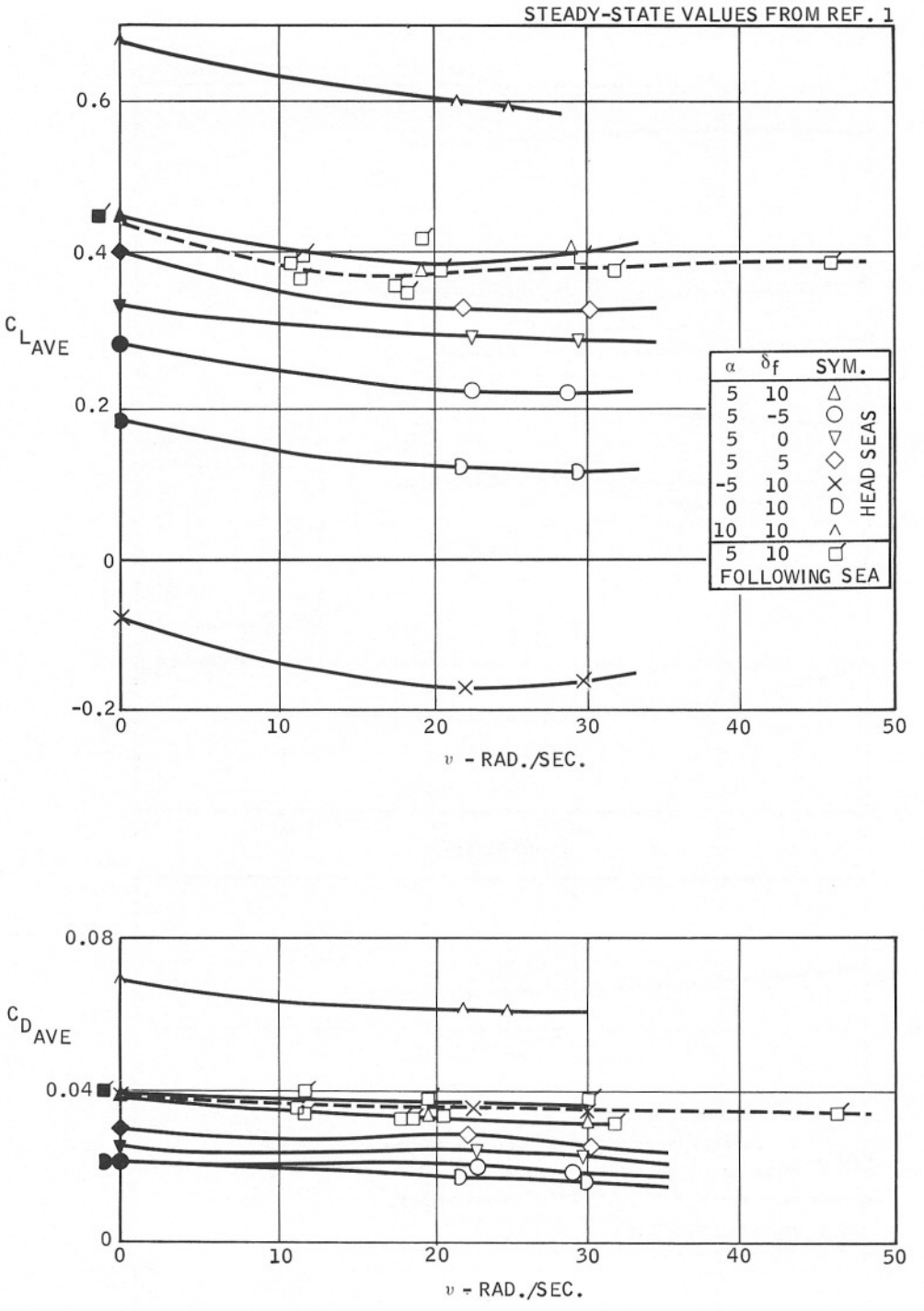


Figure 28. Flap Configuration 3 — Mean Values of Force Coefficients, Flaps Fixed in Waves

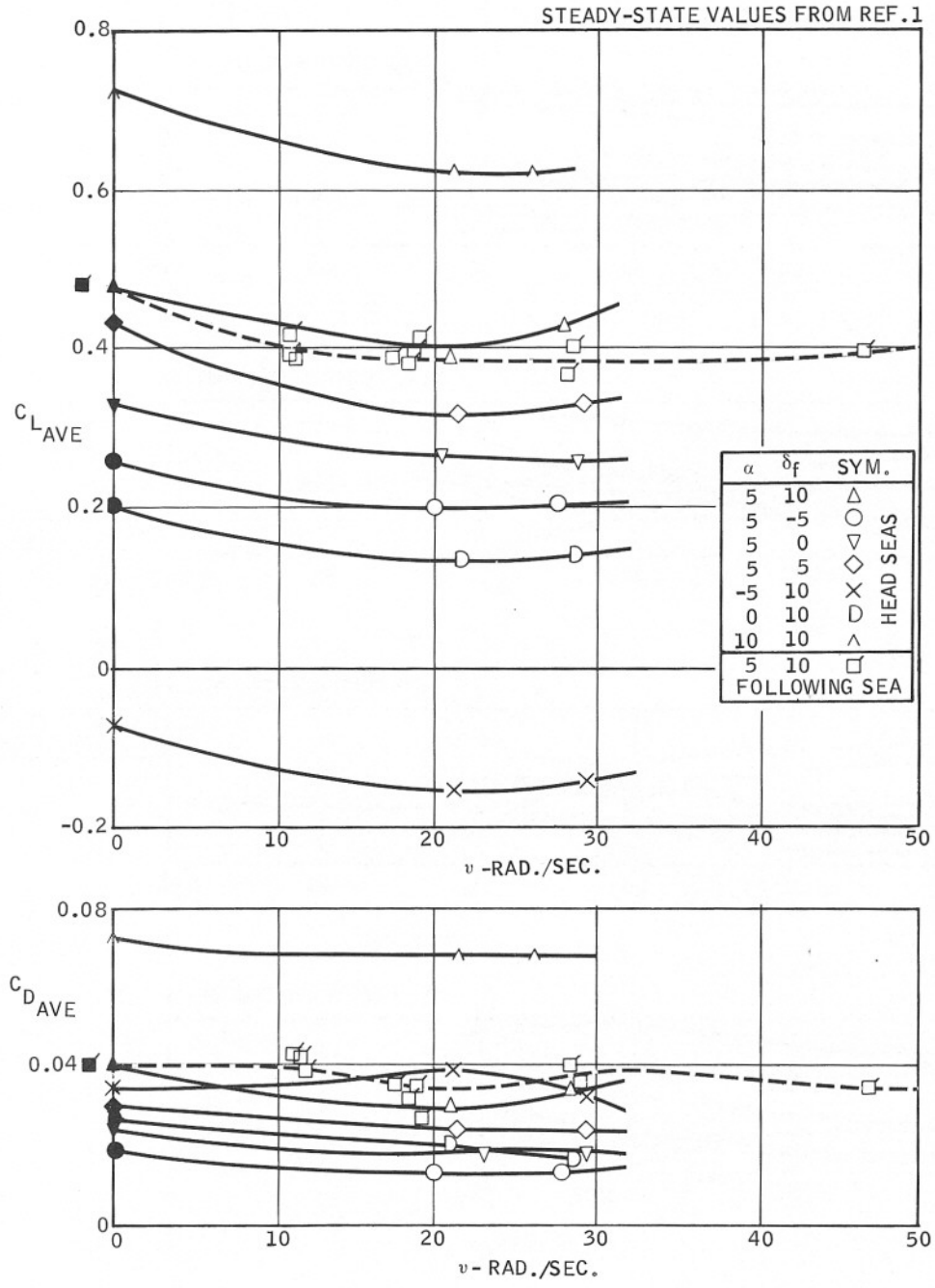


Figure 29. Flap Configuration 4 — Mean Values of Force Coefficients, Flaps Fixed in Waves

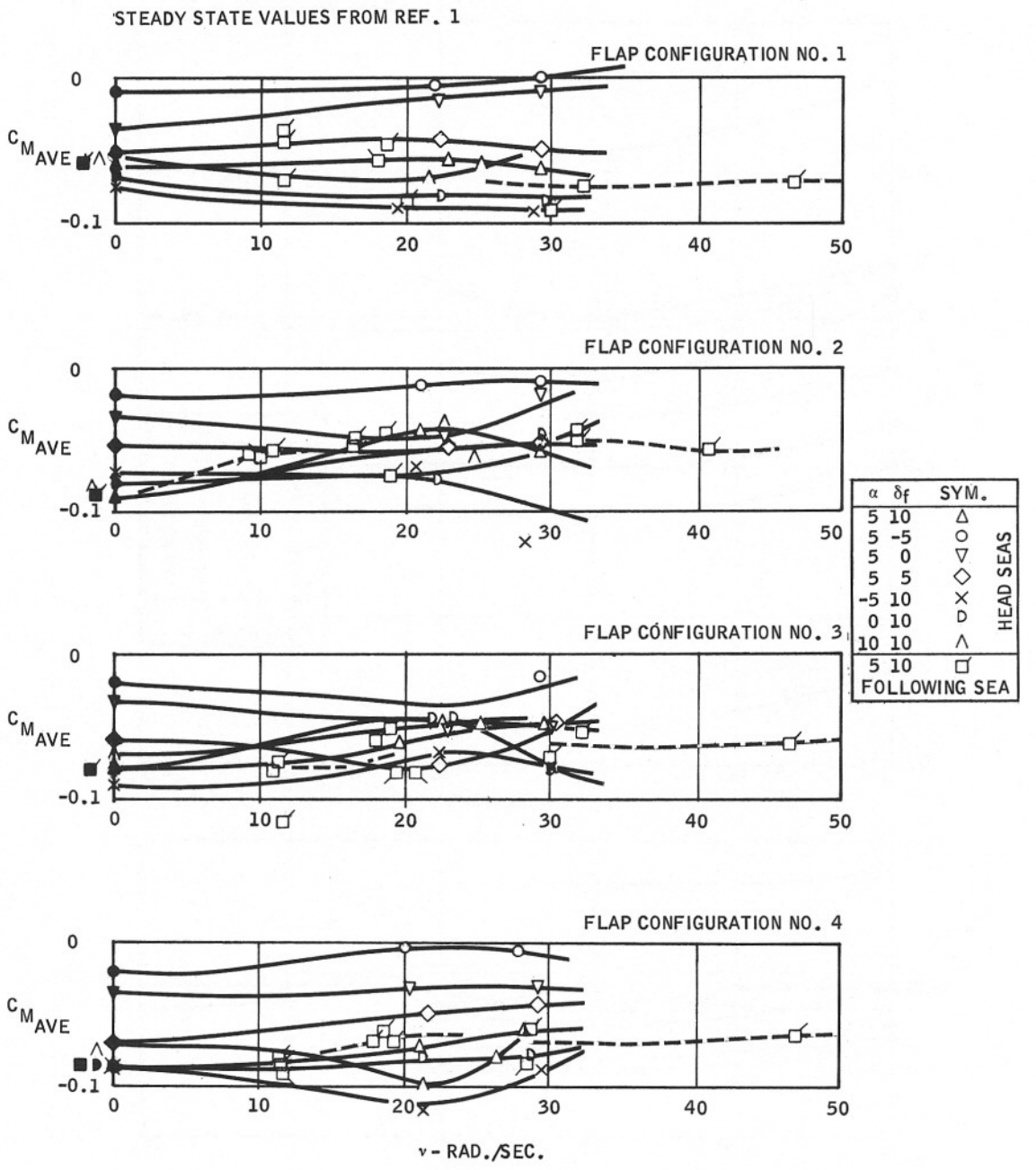


Figure 30. Mean Pitching Moment Coefficients — All Models, Flaps Fixed in Waves

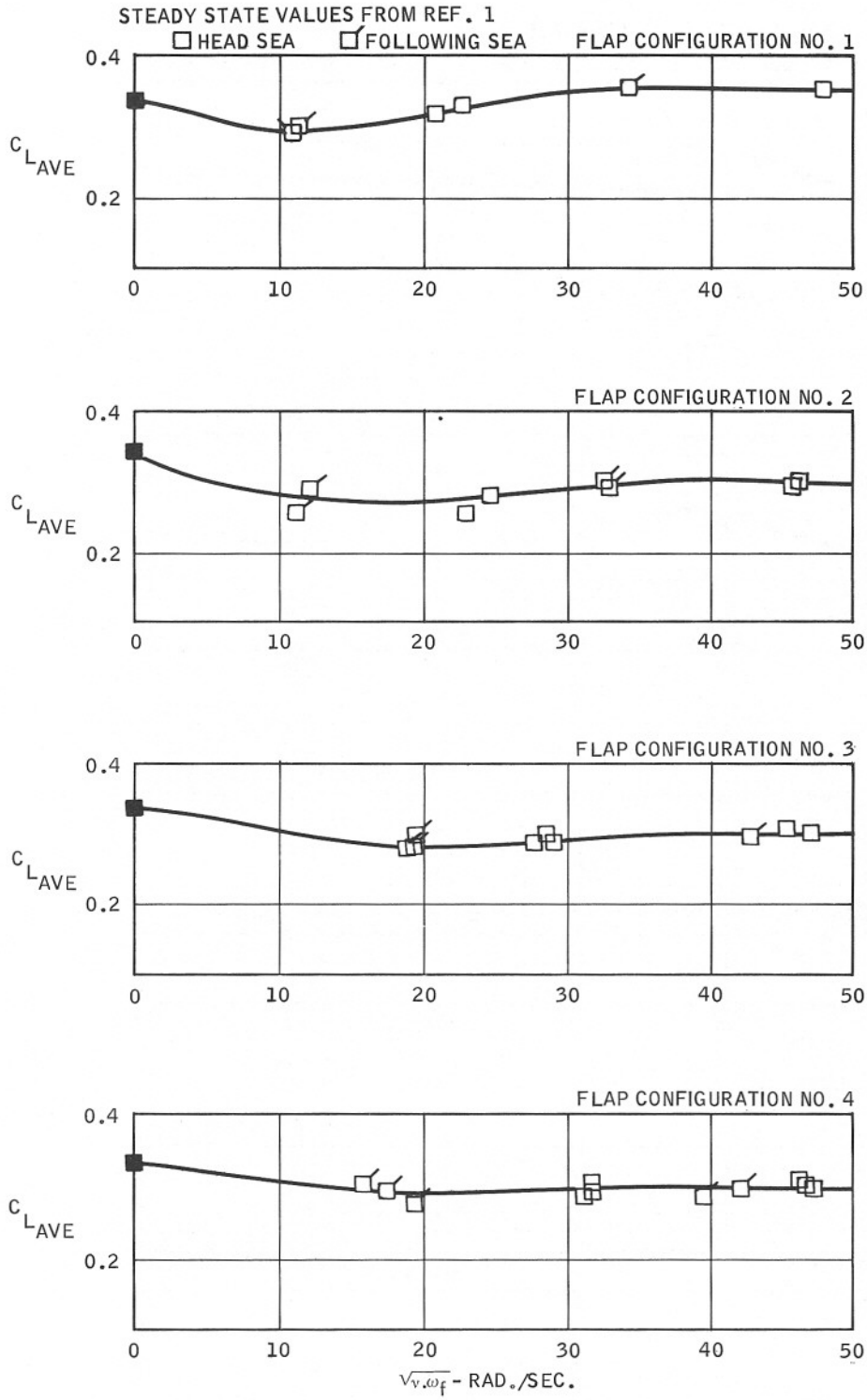


Figure 31. Mean Values of Lift Coefficients — All Models, Flaps Cycling in Waves, $\alpha = 5°$

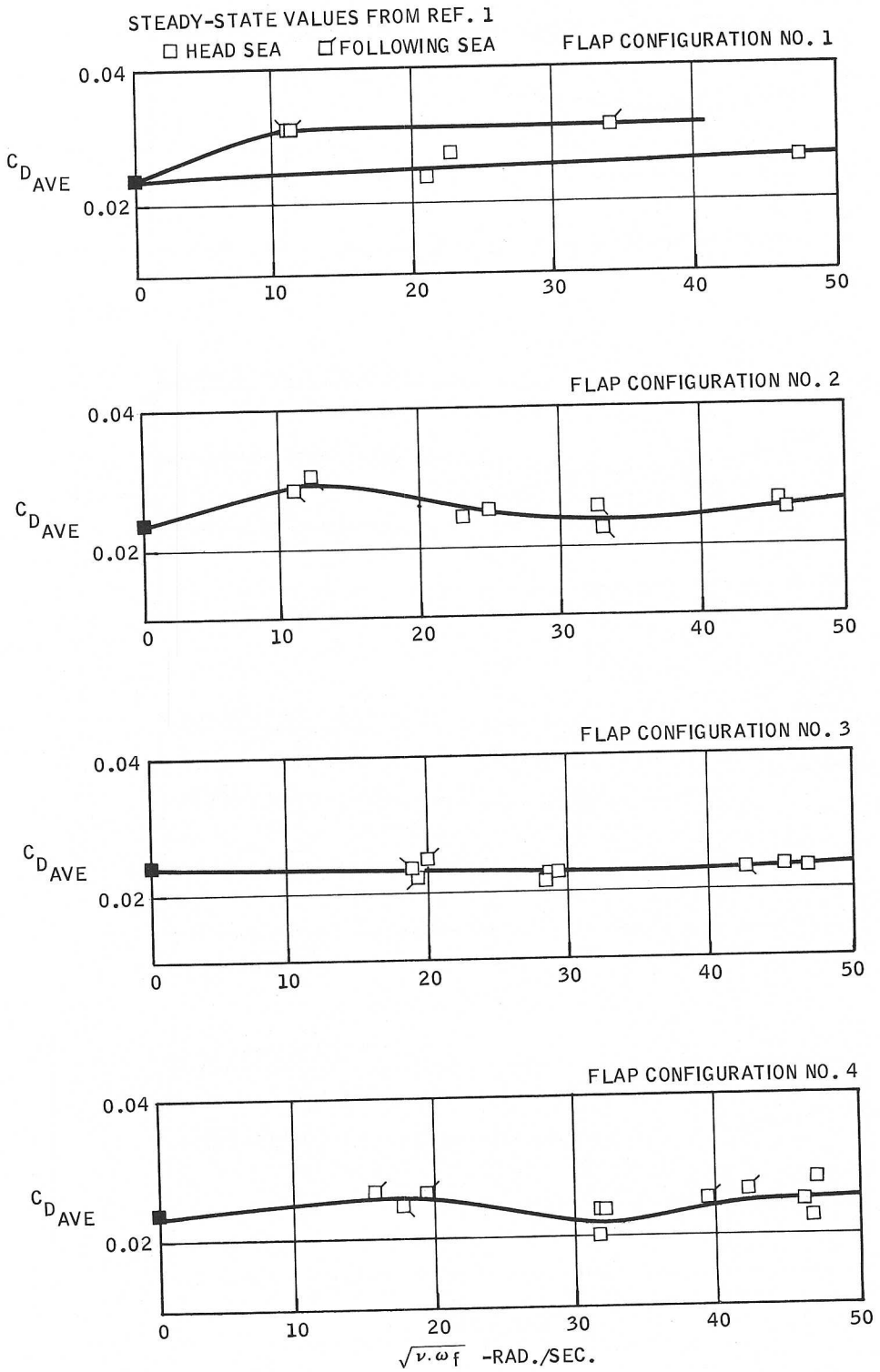


Figure 32. Mean Values of Drag Coefficients — All Models, Flaps Cycling in Waves, $\alpha = 5°$

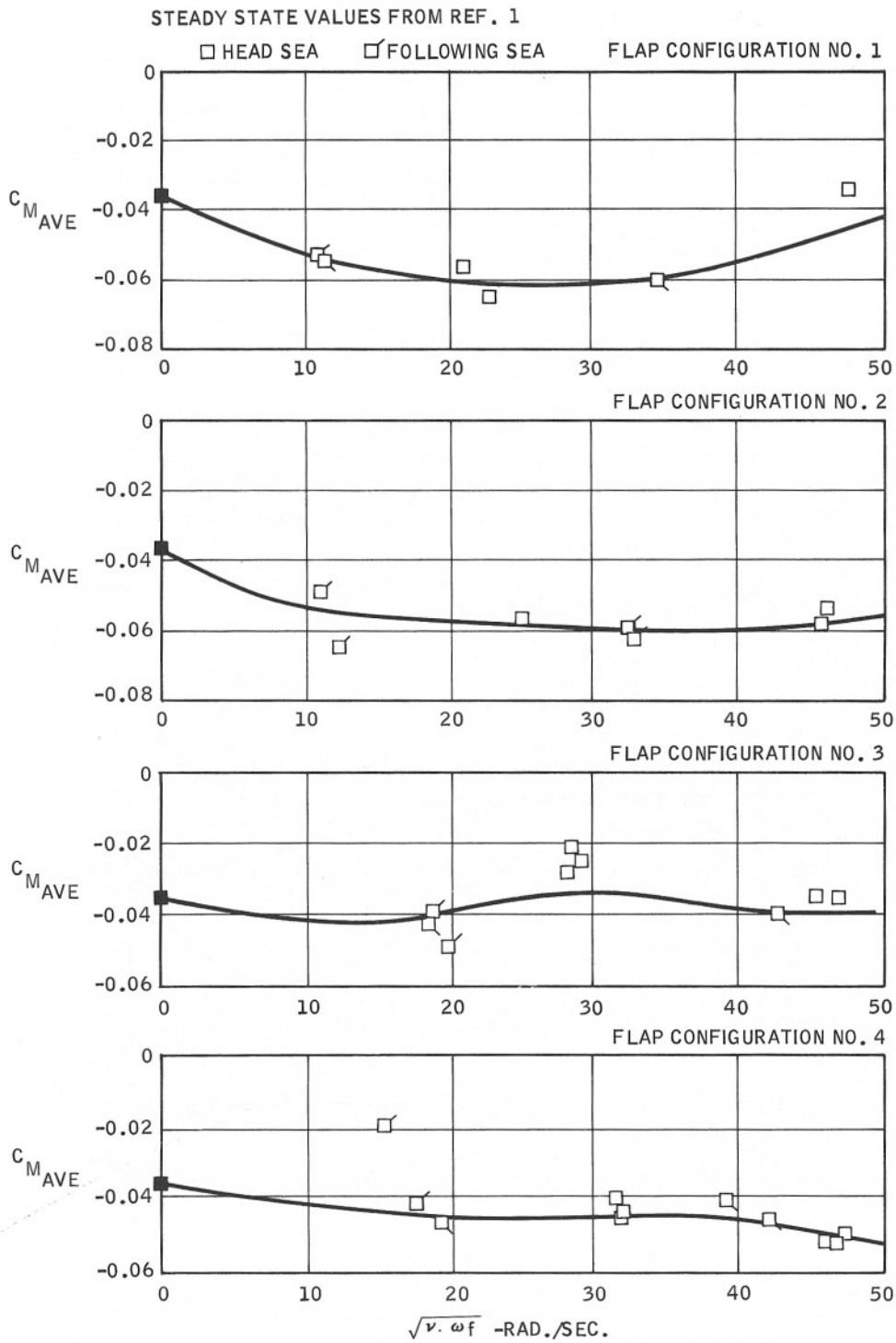


Figure 33. Mean Values of Pitching Coefficients — All Models, Flaps Cycling in Waves, $\alpha$ = 5°

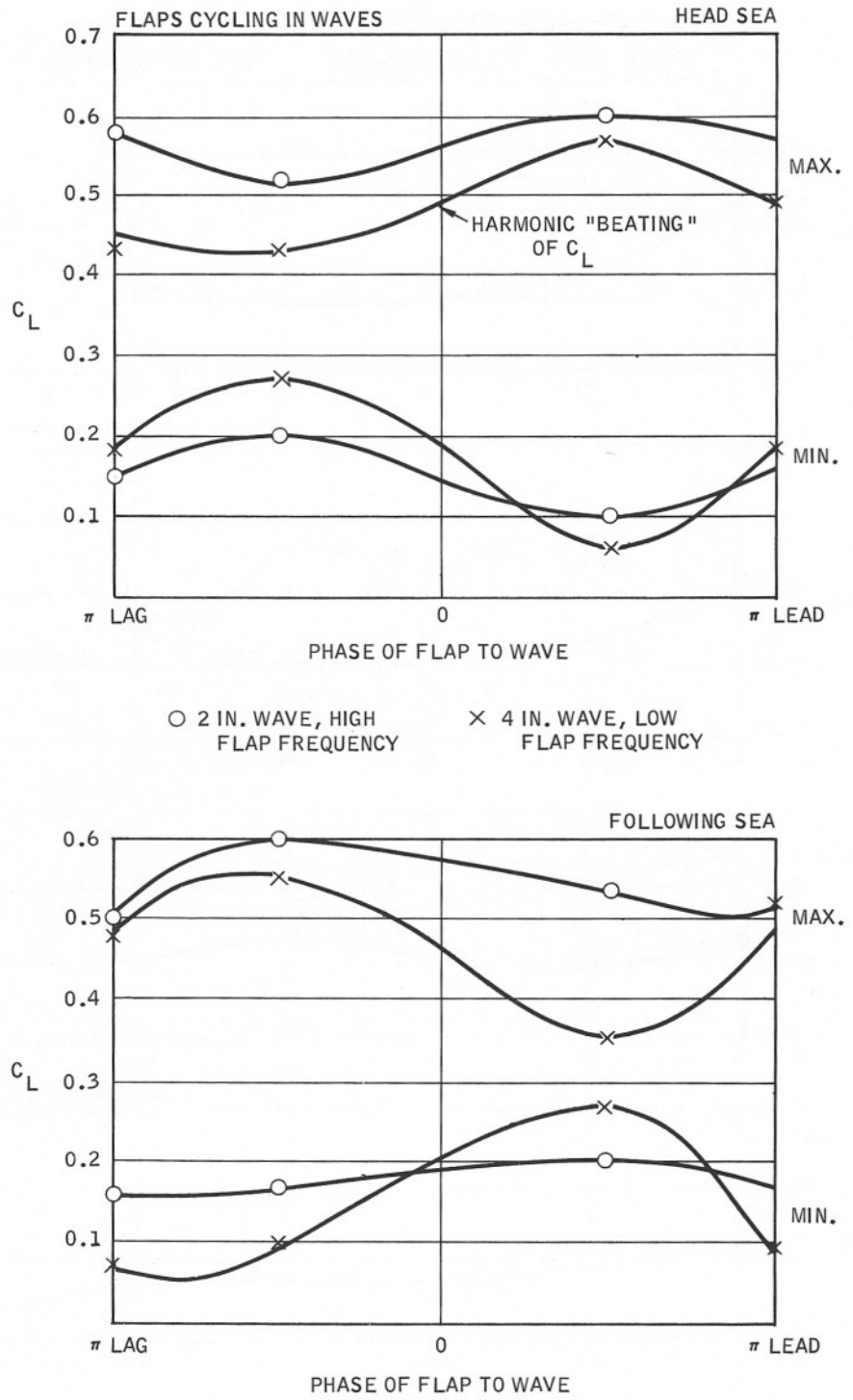


**Figure 34. Flap Configuration 1 — Maximum and Minimum $C_L$ Vs. Phase of Flap to Wave**

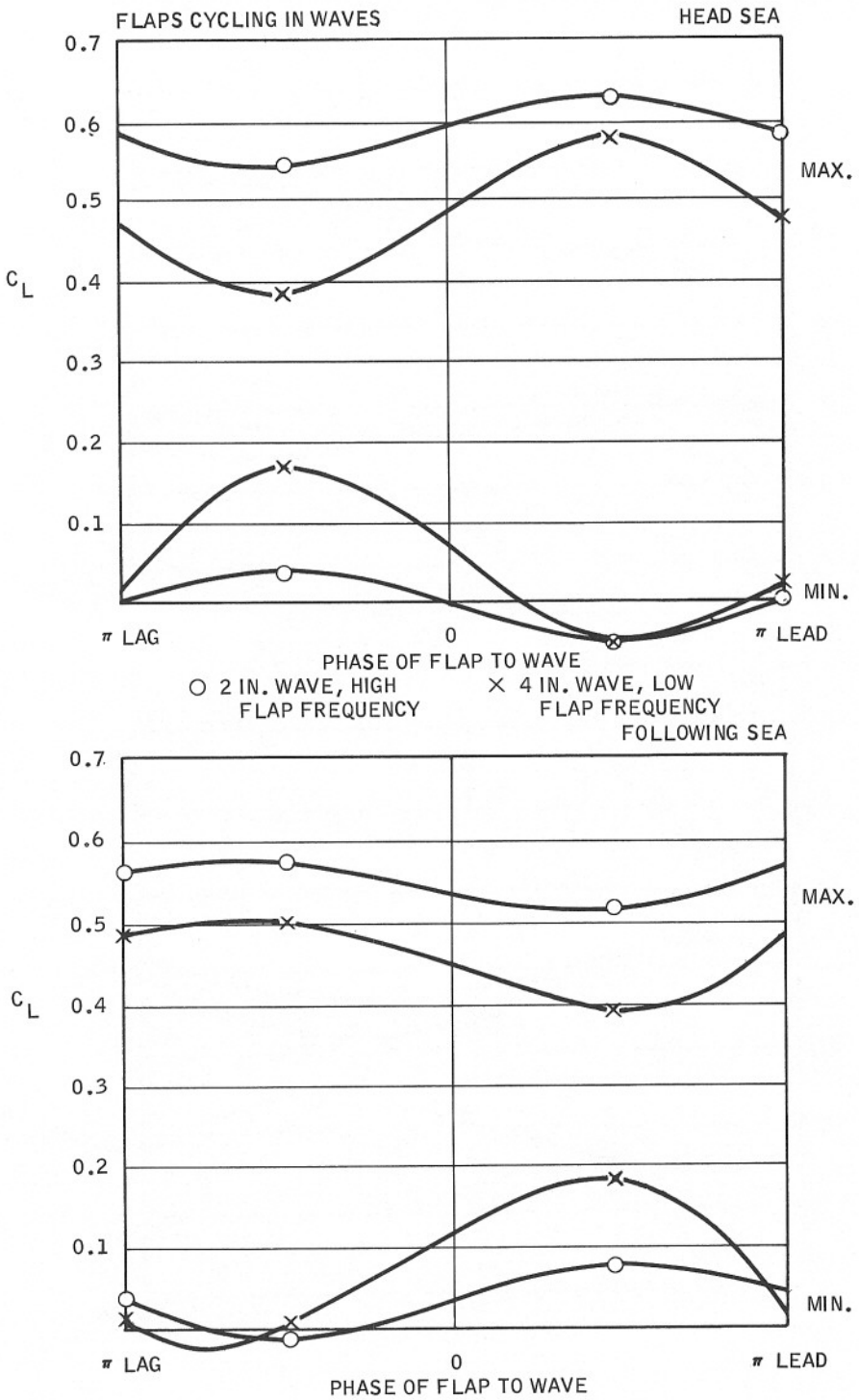


Figure 35. Flap Configuration 2 — Maximum and Minimum $C_L$ Vs. Phase of Flap to Wave

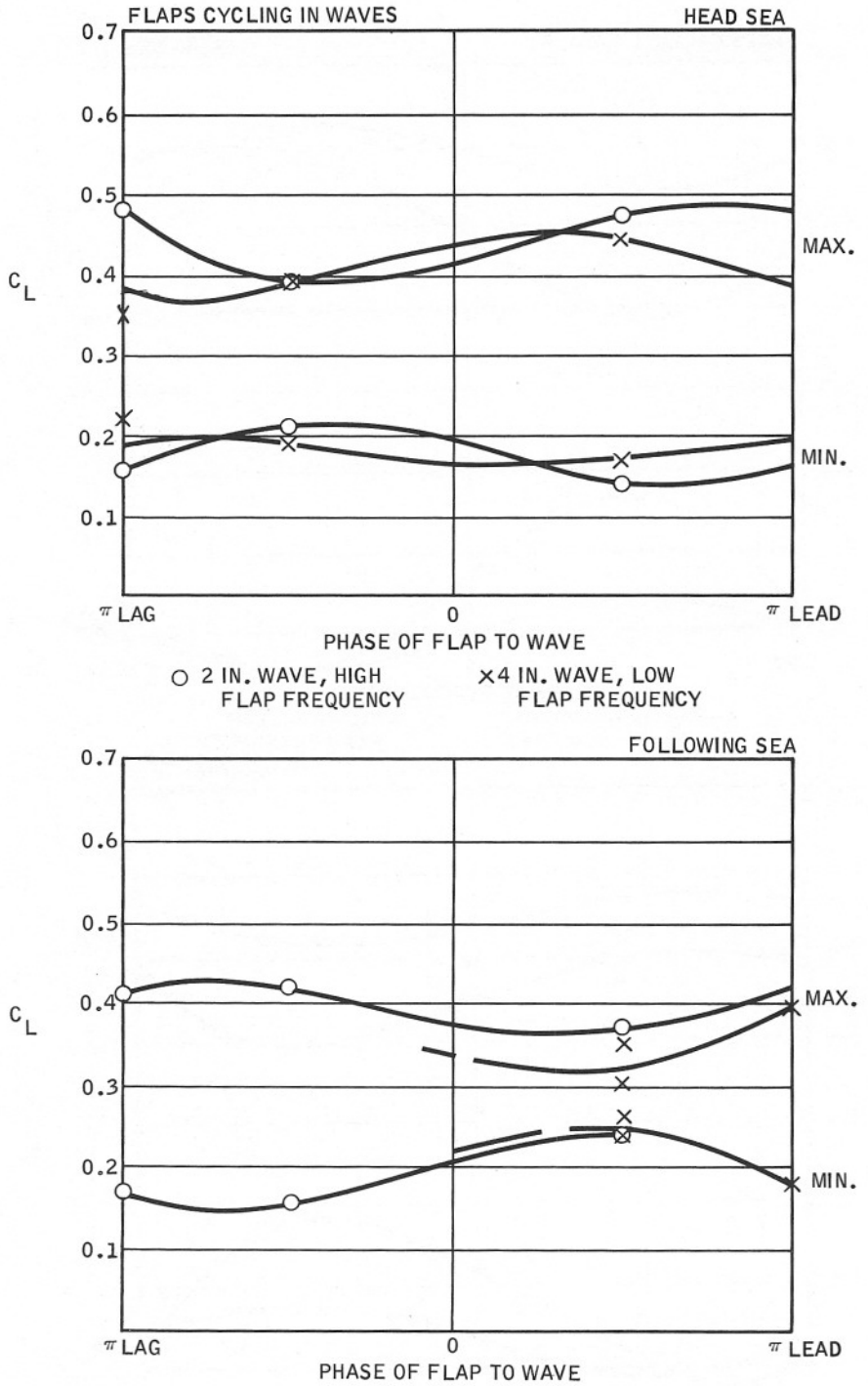


Figure 36. Flap Configuration 3 — Maximum and Minimum $C_L$ Vs. Phase of Flap to Wave

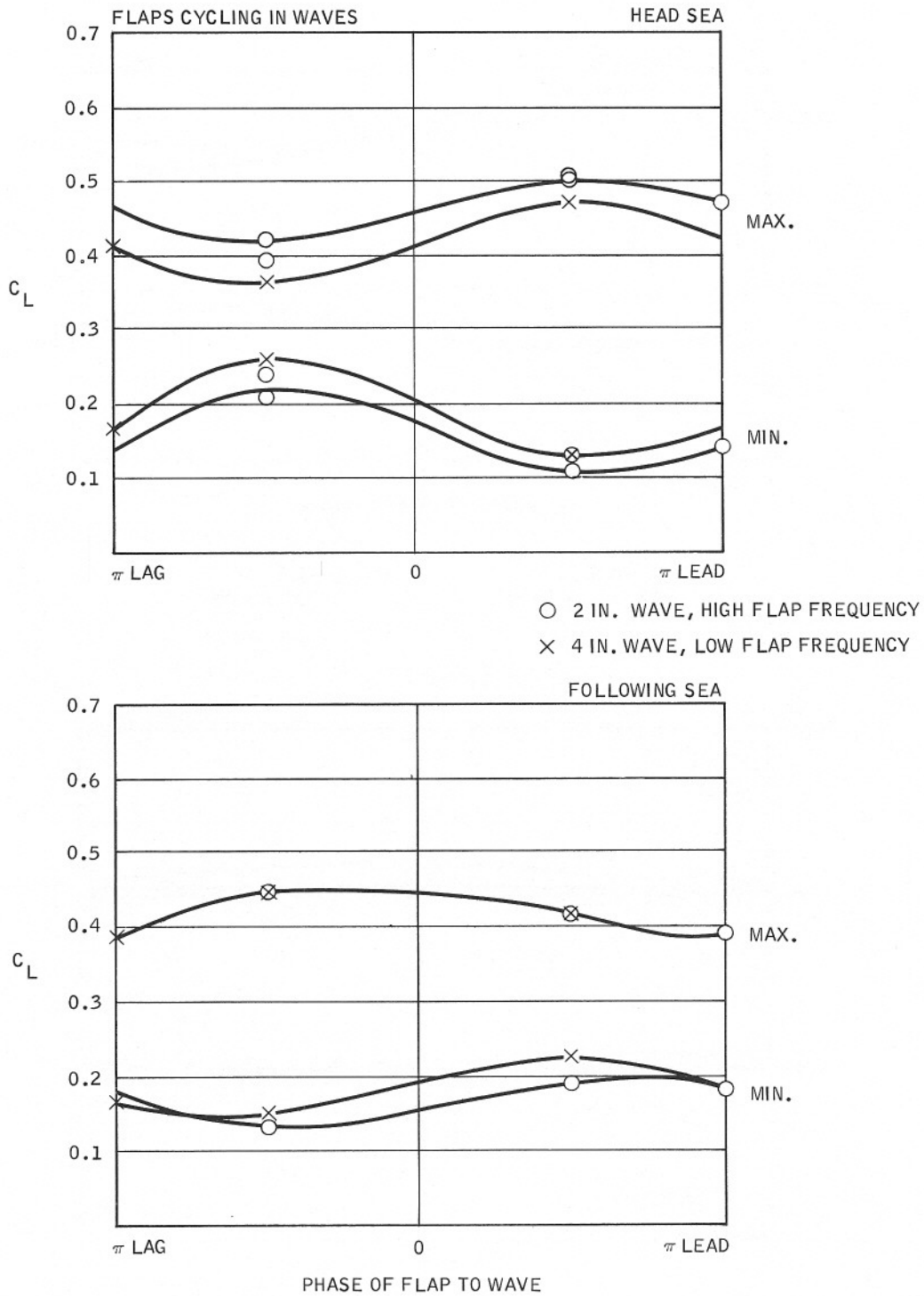


**Figure 37.** Flap Configuration 4 — Maximum and Minimum $C_L$ Vs. Phase of Flap to Wave

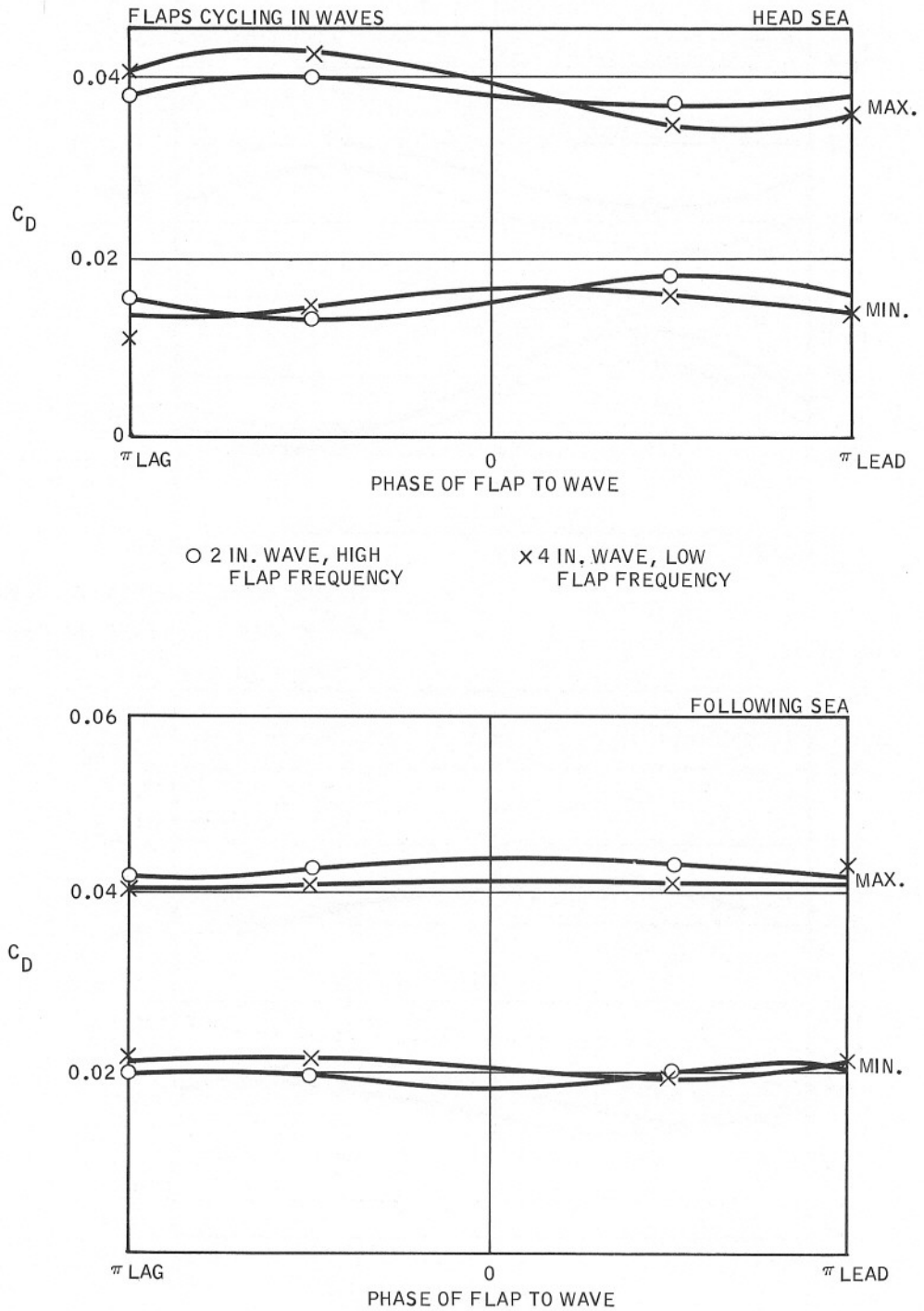


**Figure 38.** Flap Configuration 1 — Maximum and Minimum $C_D$ Vs. Phase of Flap to Wave

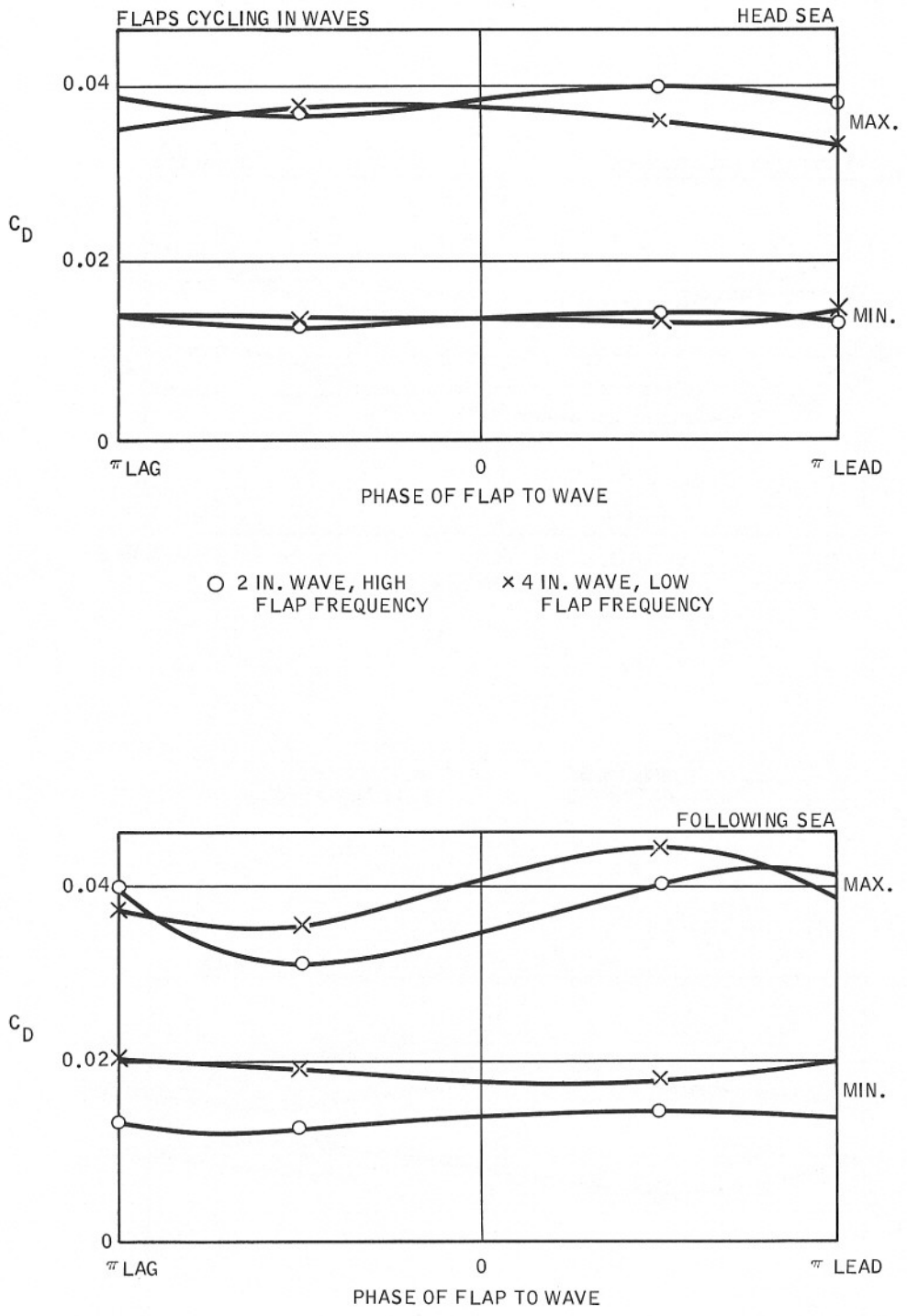


**Figure 39.** Flap Configuration 2 — Maximum and Minimum $C_D$ Vs. Phase of Flap to Wave

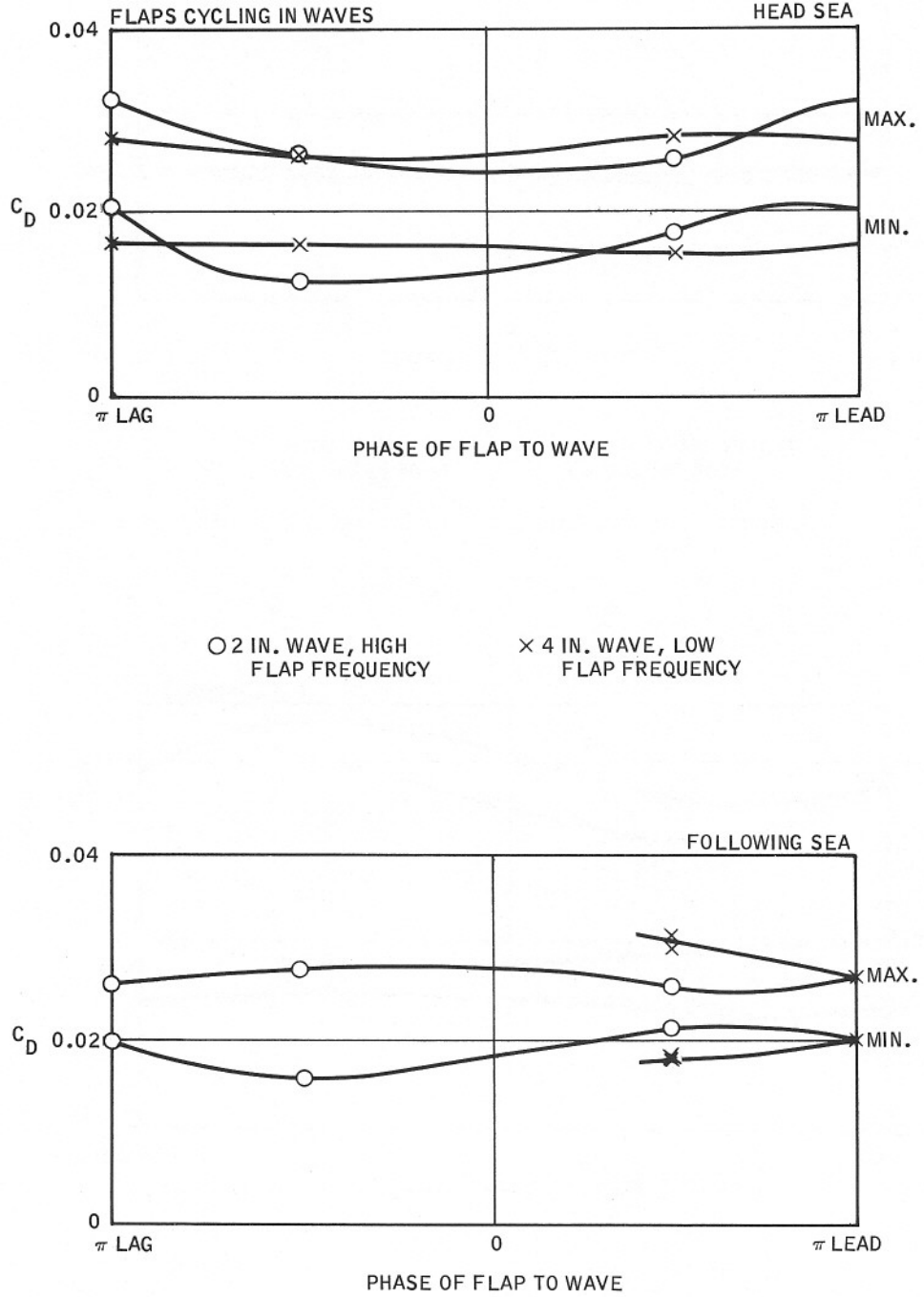


**Figure 40. Flap Configuration 3 — Maximum and Minimum $C_D$ Vs. Phase of Flap to Wave**

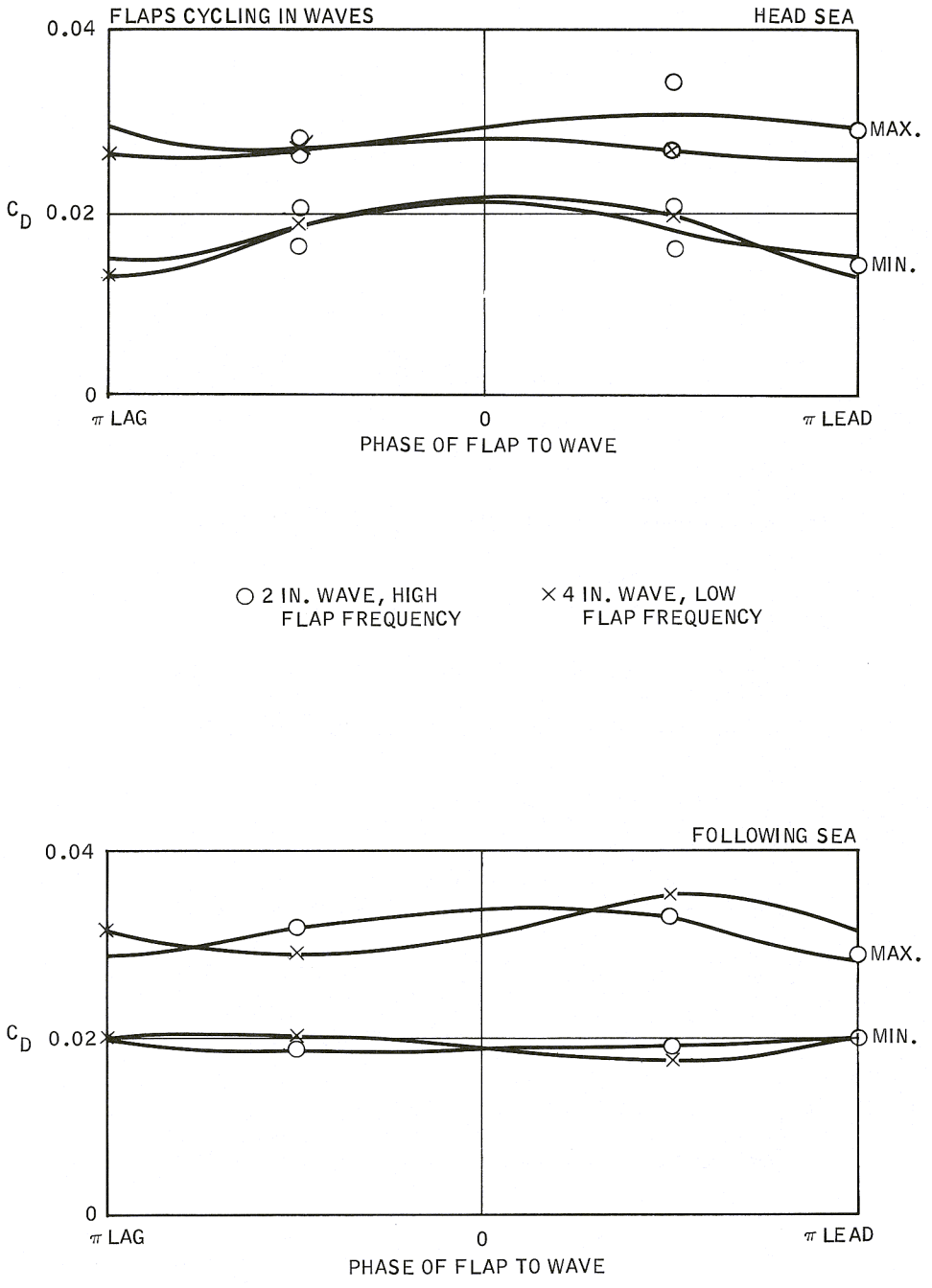


Figure 41. Flap Configuration 4 — Maximum and Minimum $C_D$ Vs. Phase of Flap to Wave

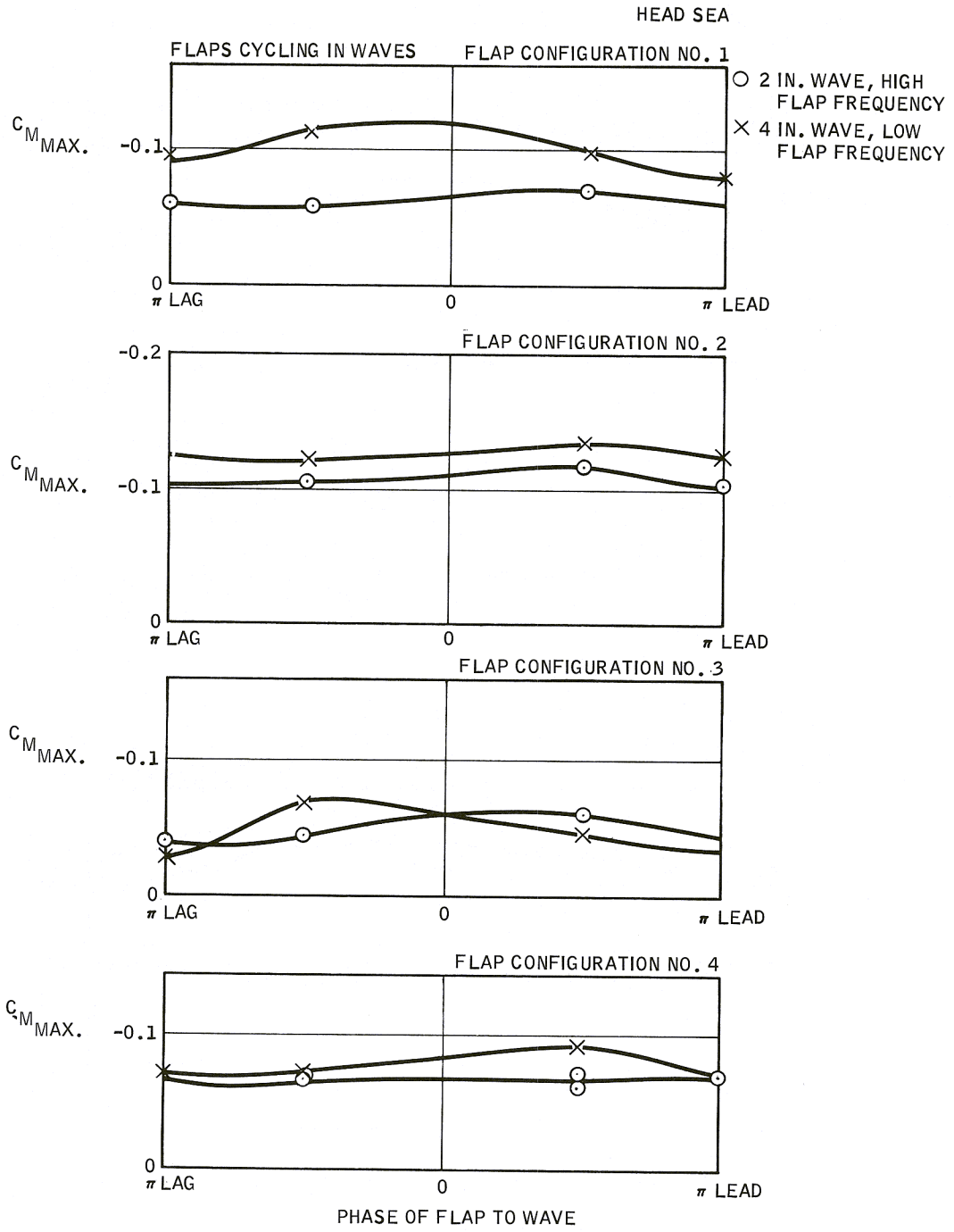


Figure 42. Maximum $-C_M$ Vs. Phase of Flap to Wave

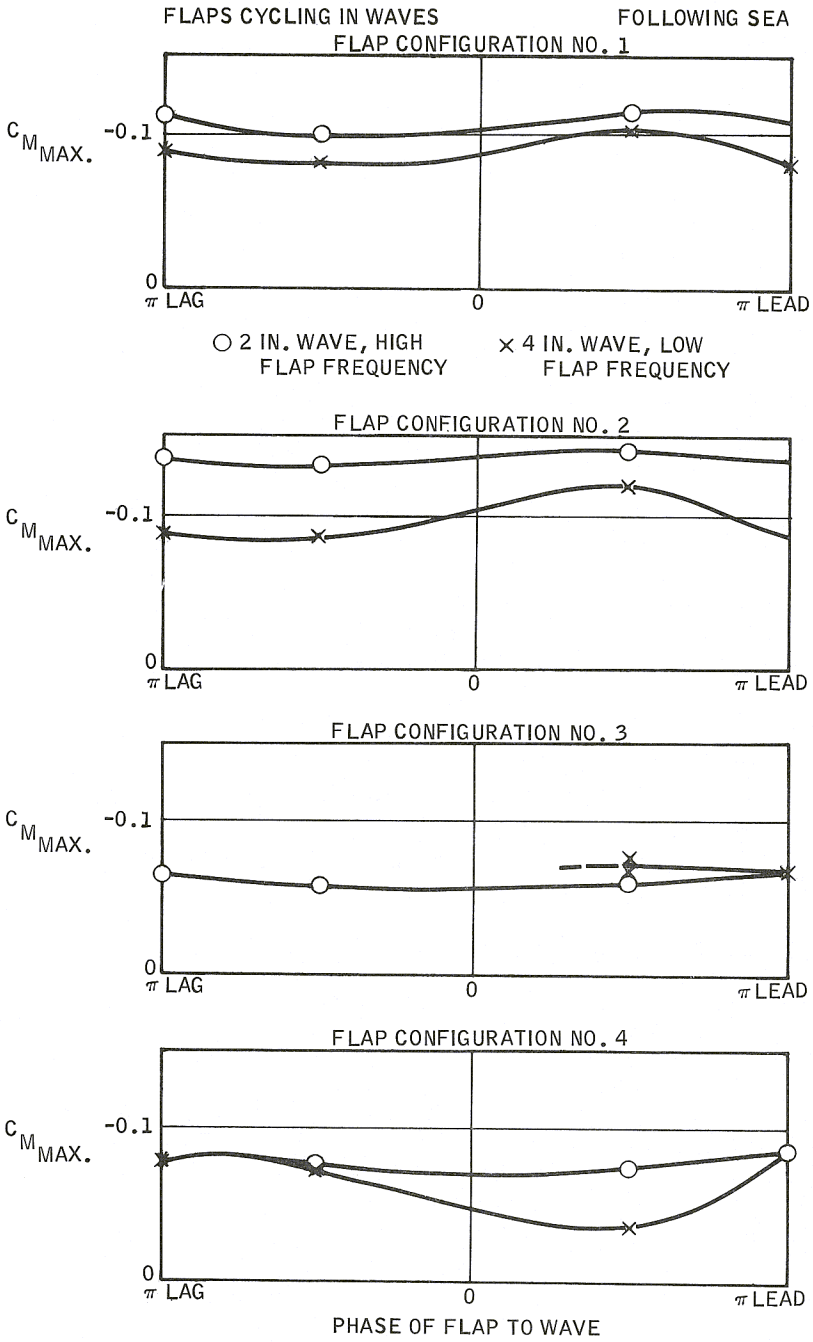


Figure 43. Maximum $-C_M$ Vs. Phase of Flap to Wave

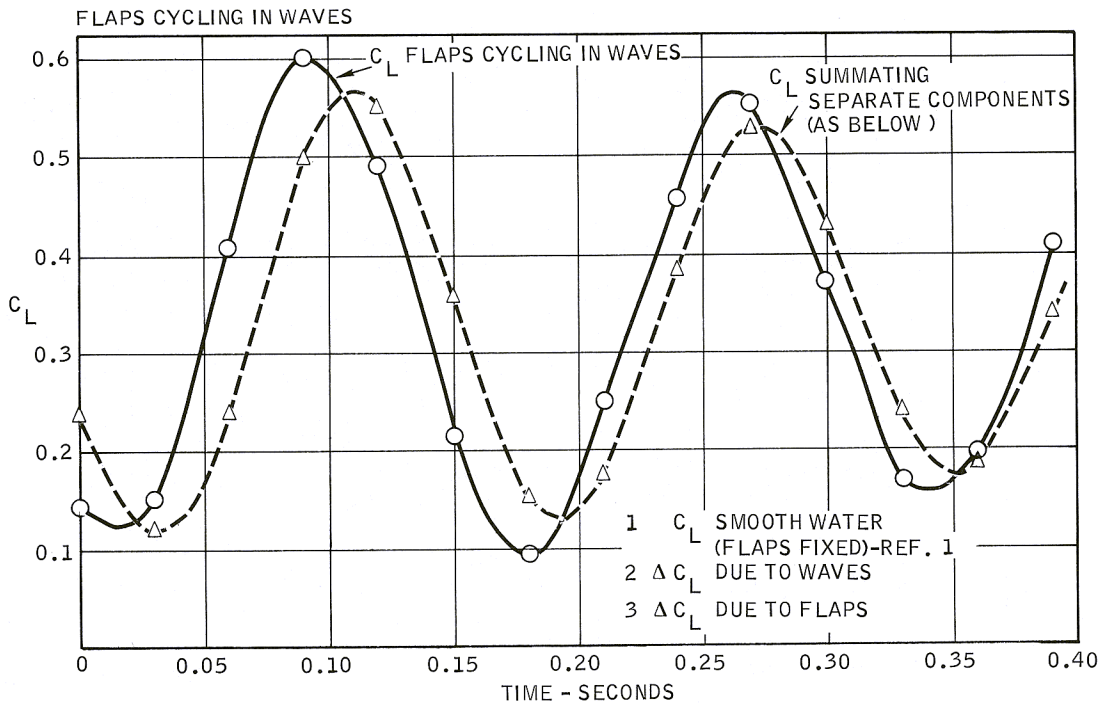


**Figure 44. Run 13191, Flap Configuration 1 — $C_L$ Time History, Following Sea**

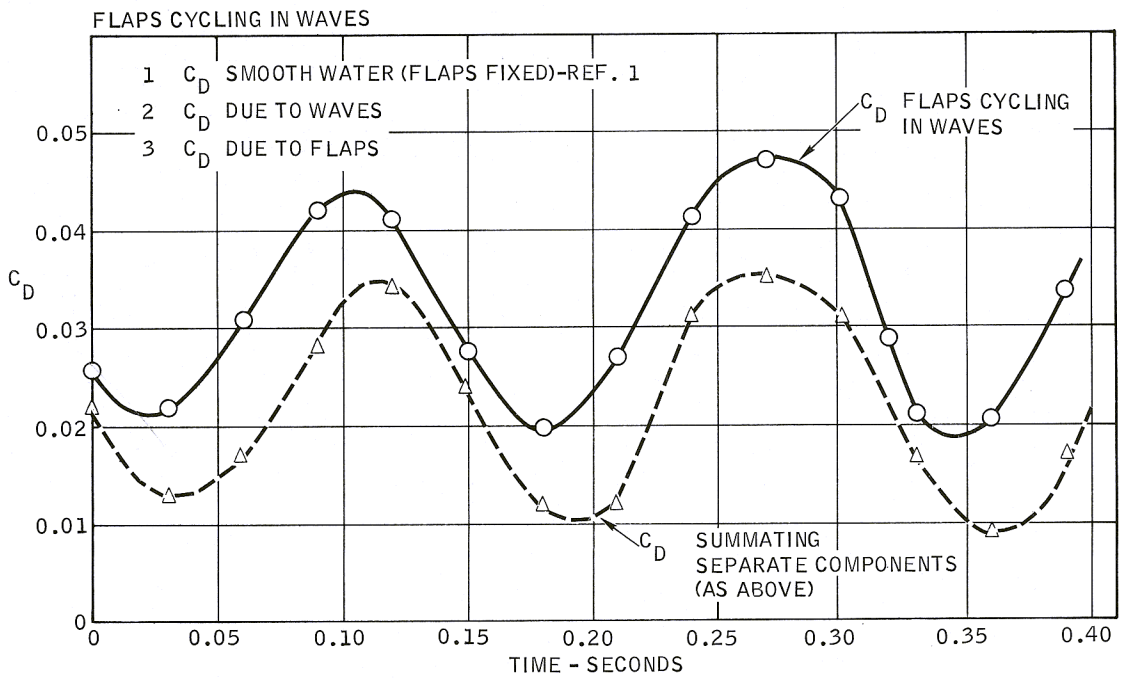


**Figure 45. Run 13191, Flap Configuration 1 — $C_D$ Time History, Following Sea**

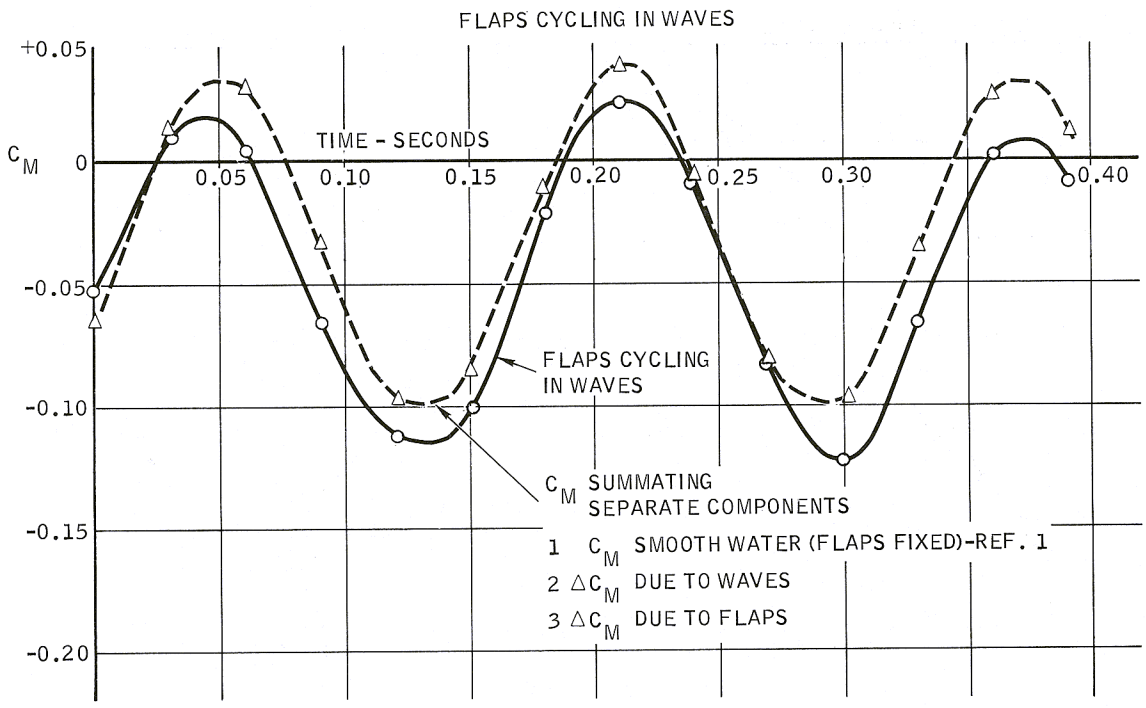


Figure 46. Run 13191, Flap Configuration 1 — $C_M$ Time History, Following Sea

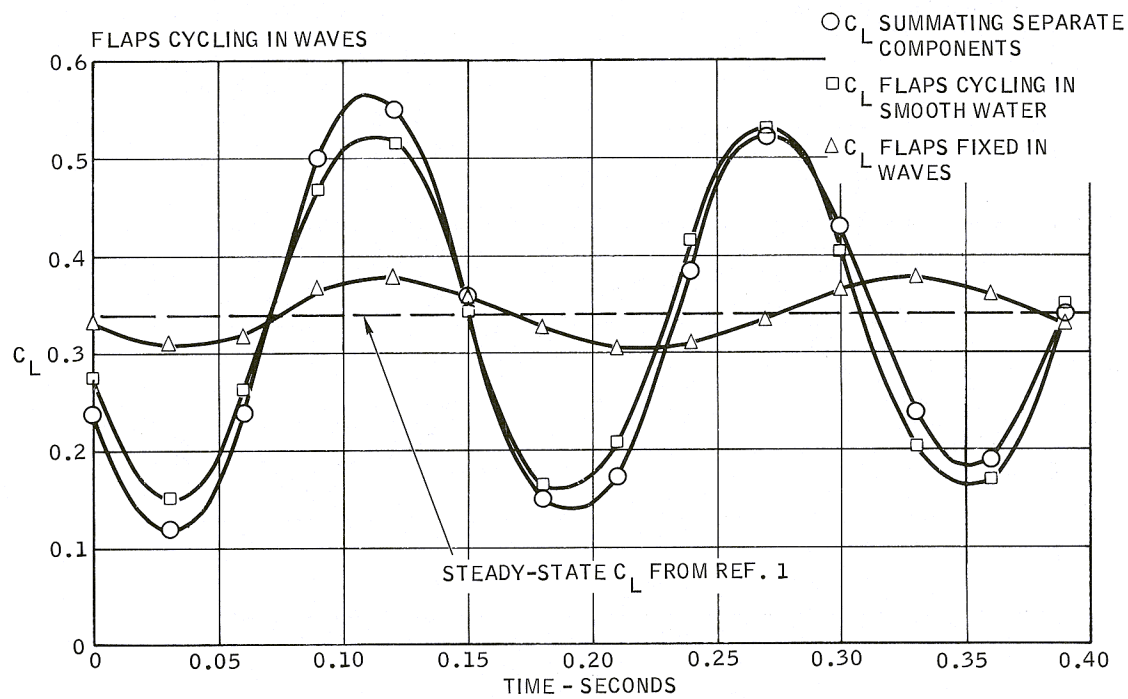


Figure 47. Run 13191, Flap Configuration 1 — $C_L$ Time History, Comparison of Flap and Wave Effects

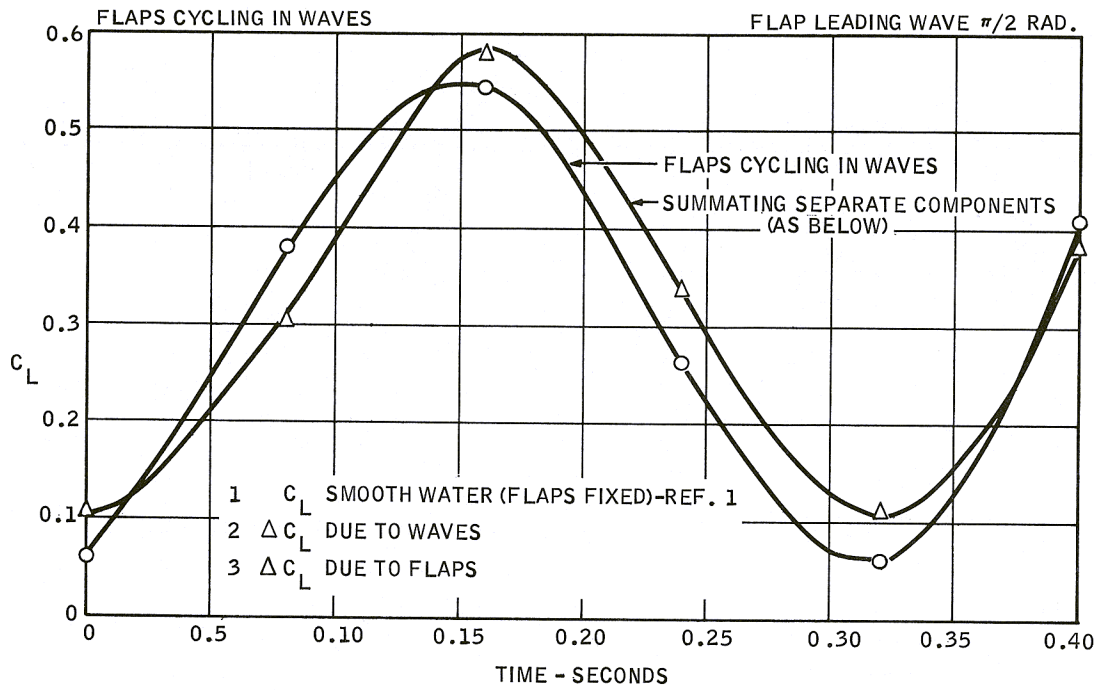


Figure 48. Run 13157, Flap Configuration 1 — $C_L$ Time History, Head Sea

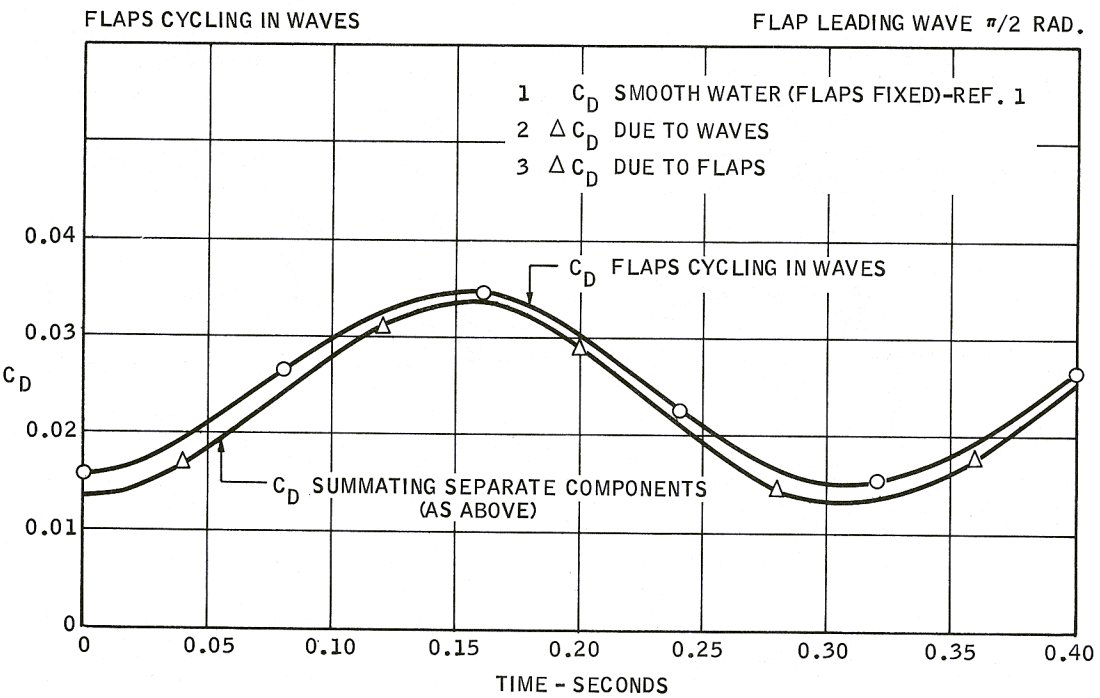


Figure 49. Run 13157, Flap Configuration 1 — $C_D$ Time History, Head Sea

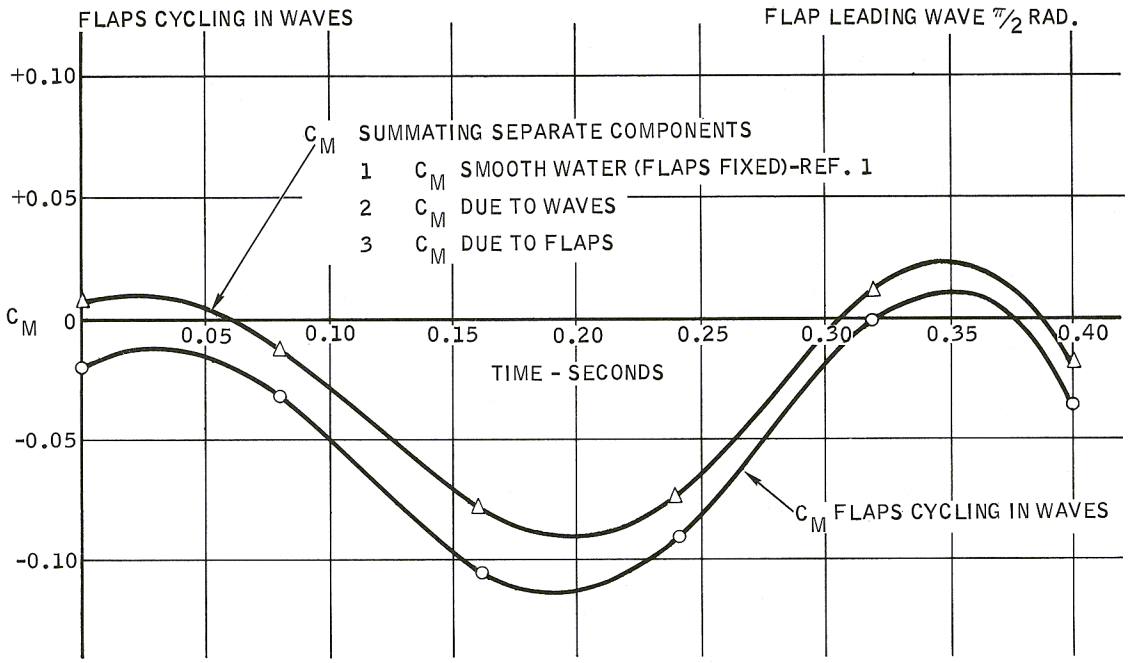


Figure 50. Run 13157, Flap Configuration 1 — $C_M$ Time History, Head Sea

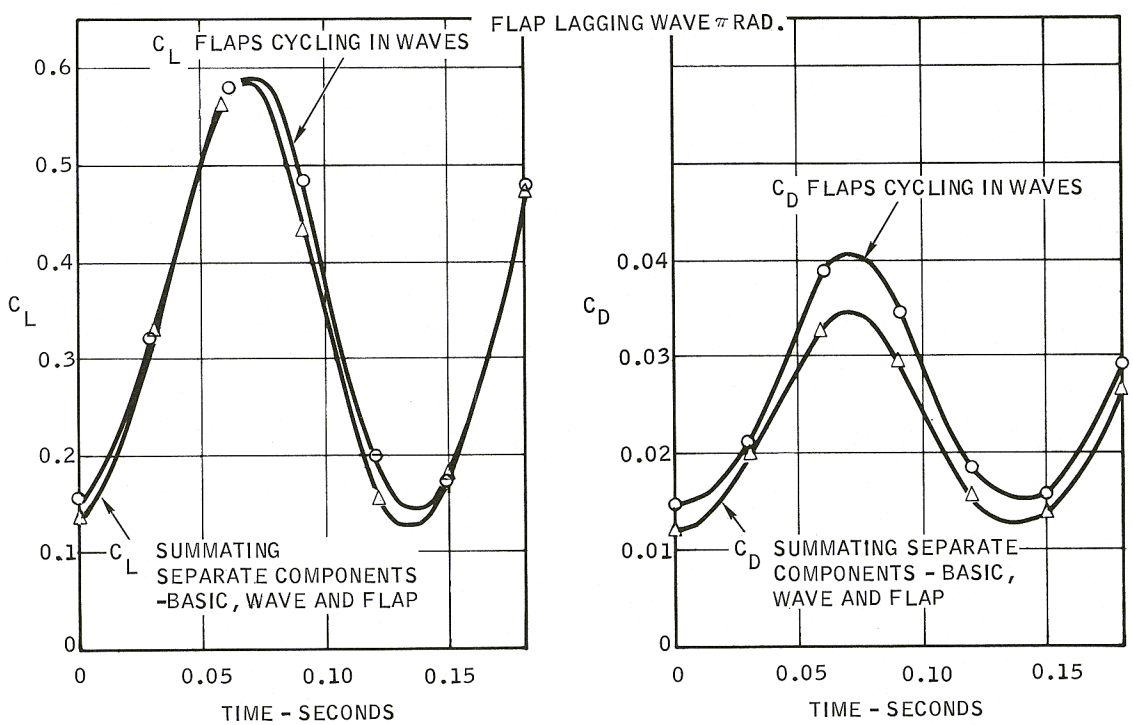


Figure 51. Run 13154, Flap Configuration 1 — $C_L$ and $C_D$ Time History, Head Sea

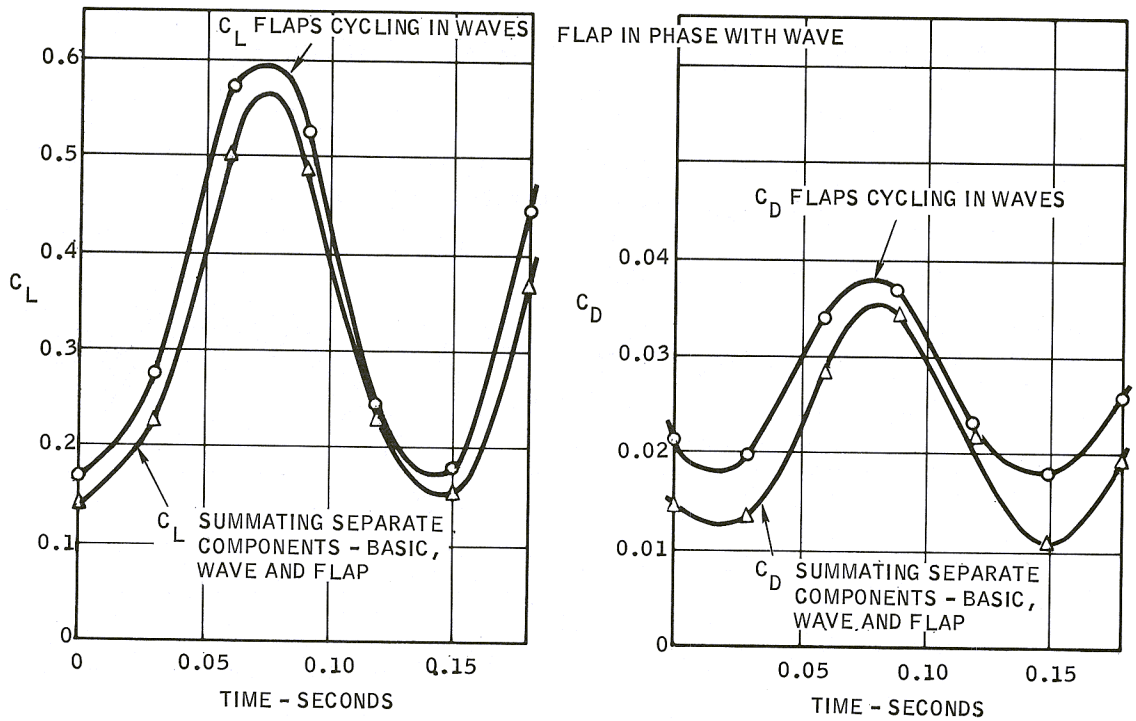


Figure 52. Run 13154, Flap Configuration 1 — $C_L$ and $C_D$ Time History, Head Sea

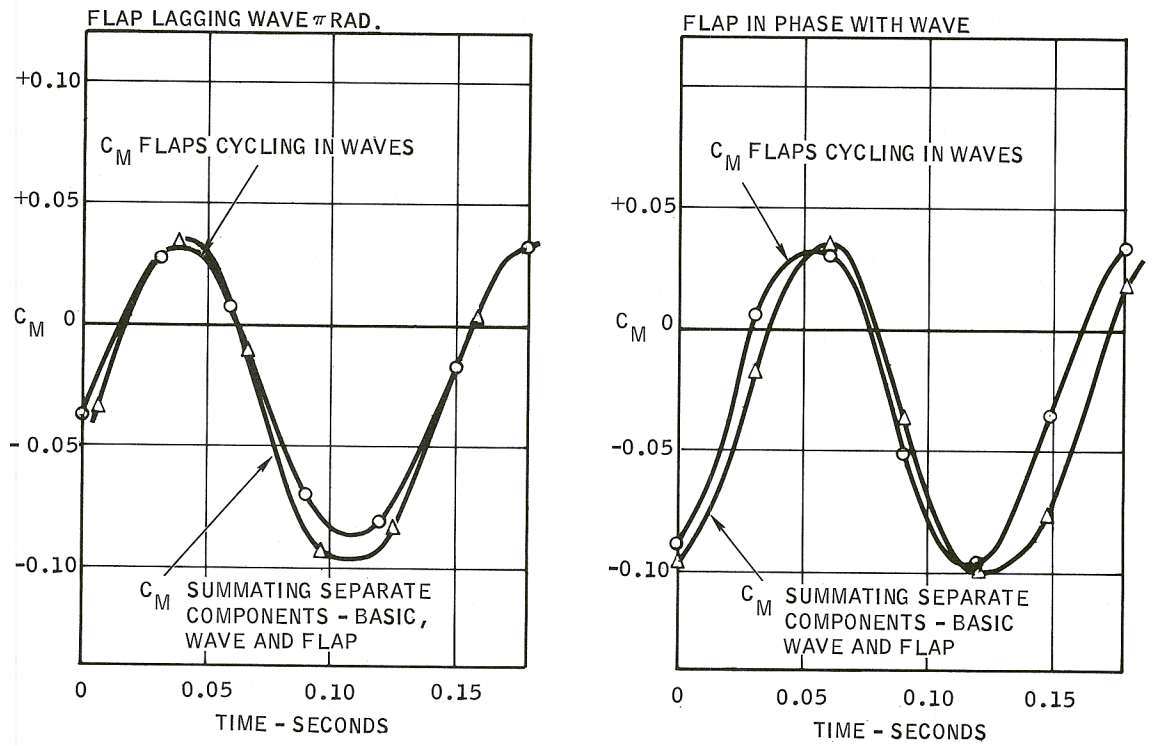


Figure 53. Run 13154, Flap Configuration 1 — $C_M$ Time History, Head Sea

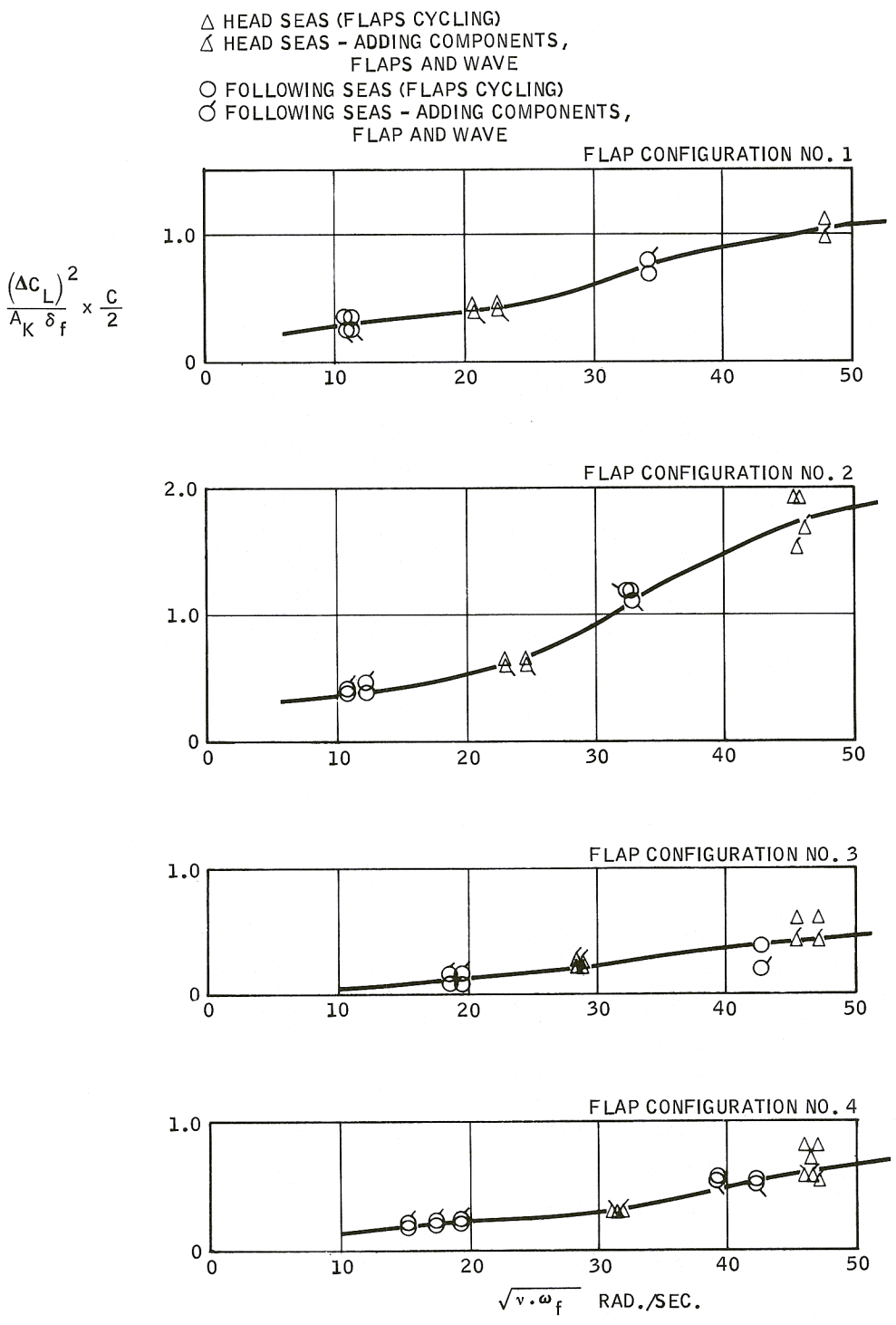


Figure 54. Maximum Lift Frequency Response, Flaps Oscillating in Waves, All Models — Comparisons with Separate Tests

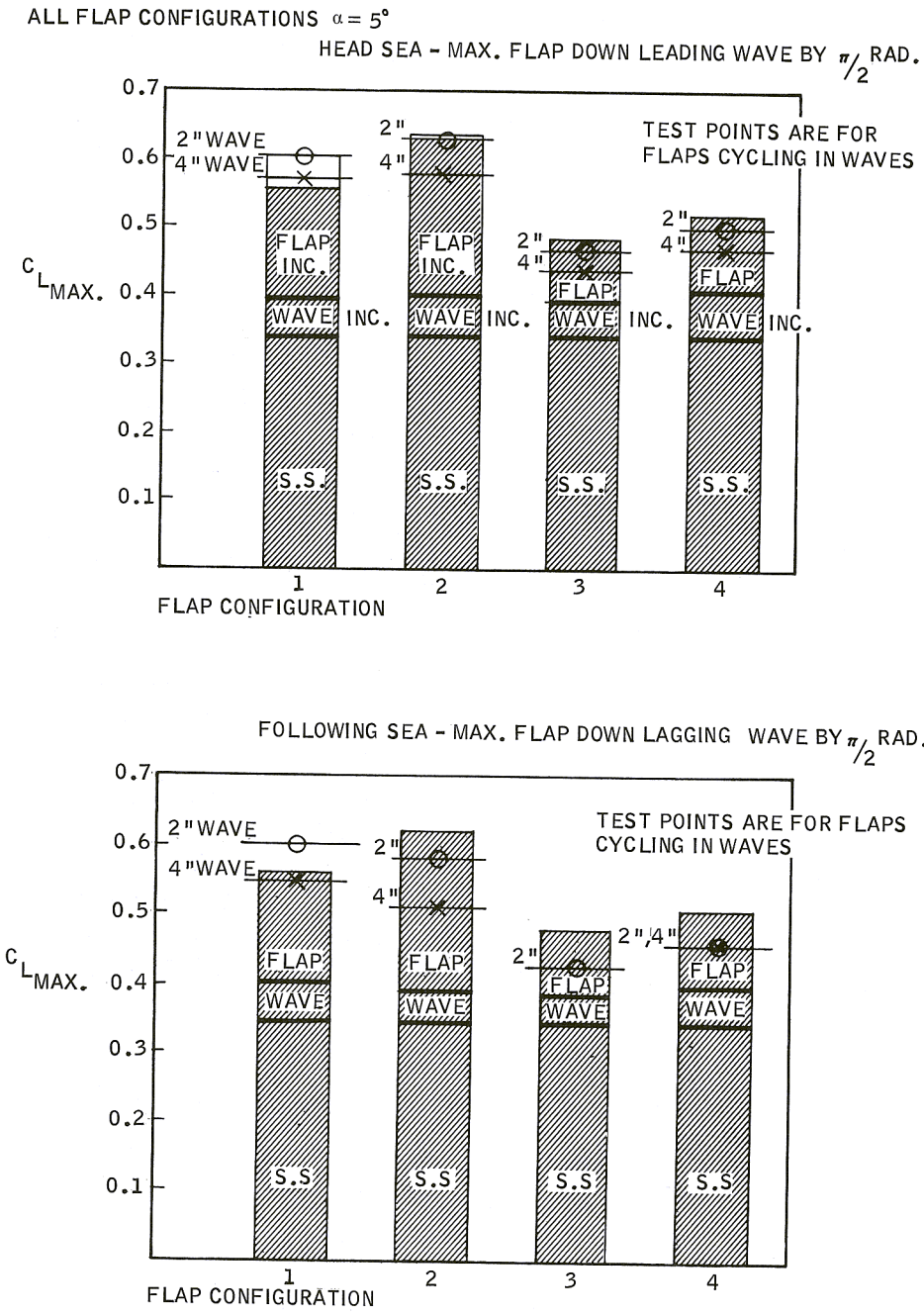


Figure 55. Summary of Flap and Wave Effectiveness

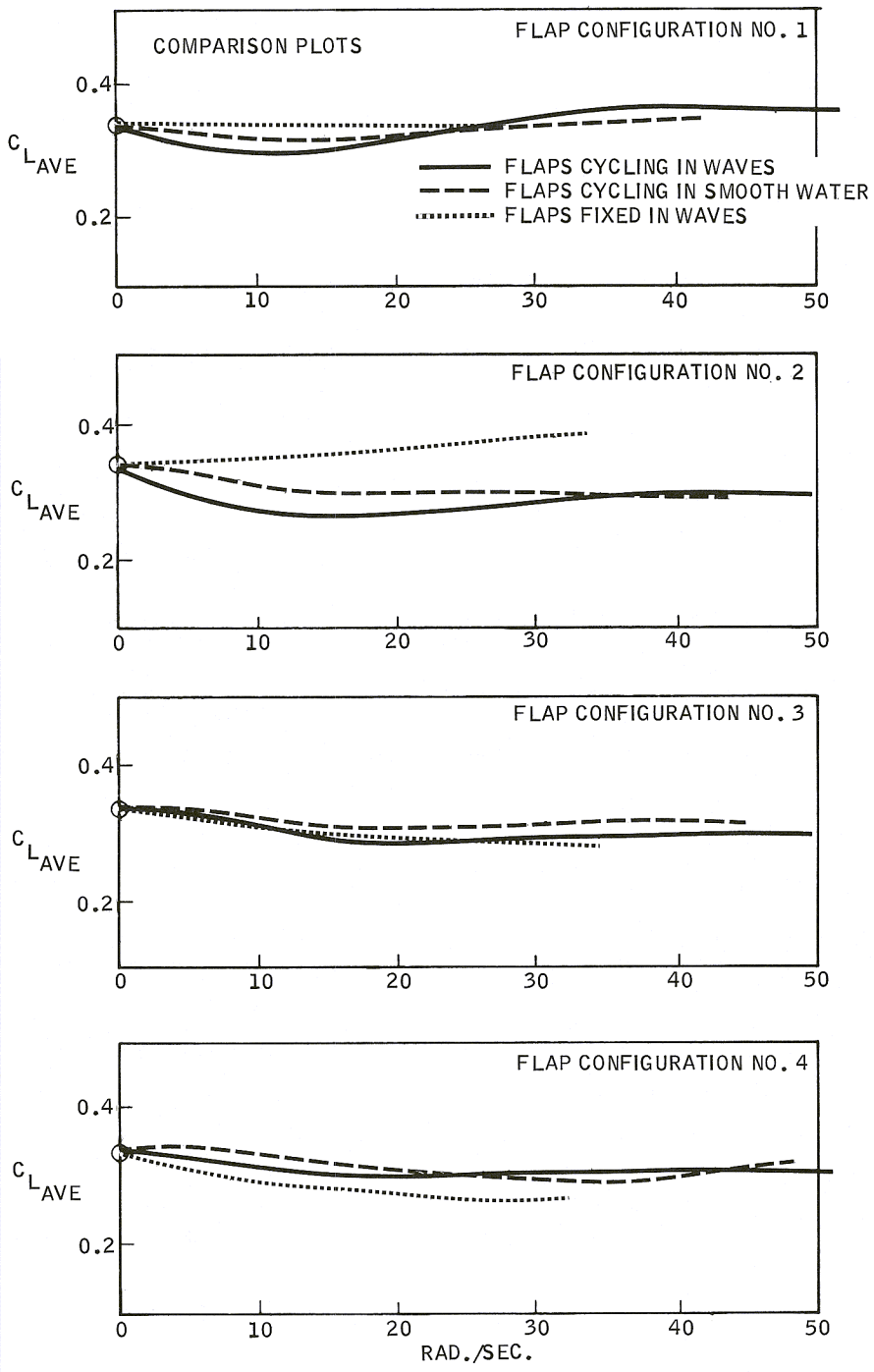


Figure 56. Mean Values of Lift Coefficients — All Models

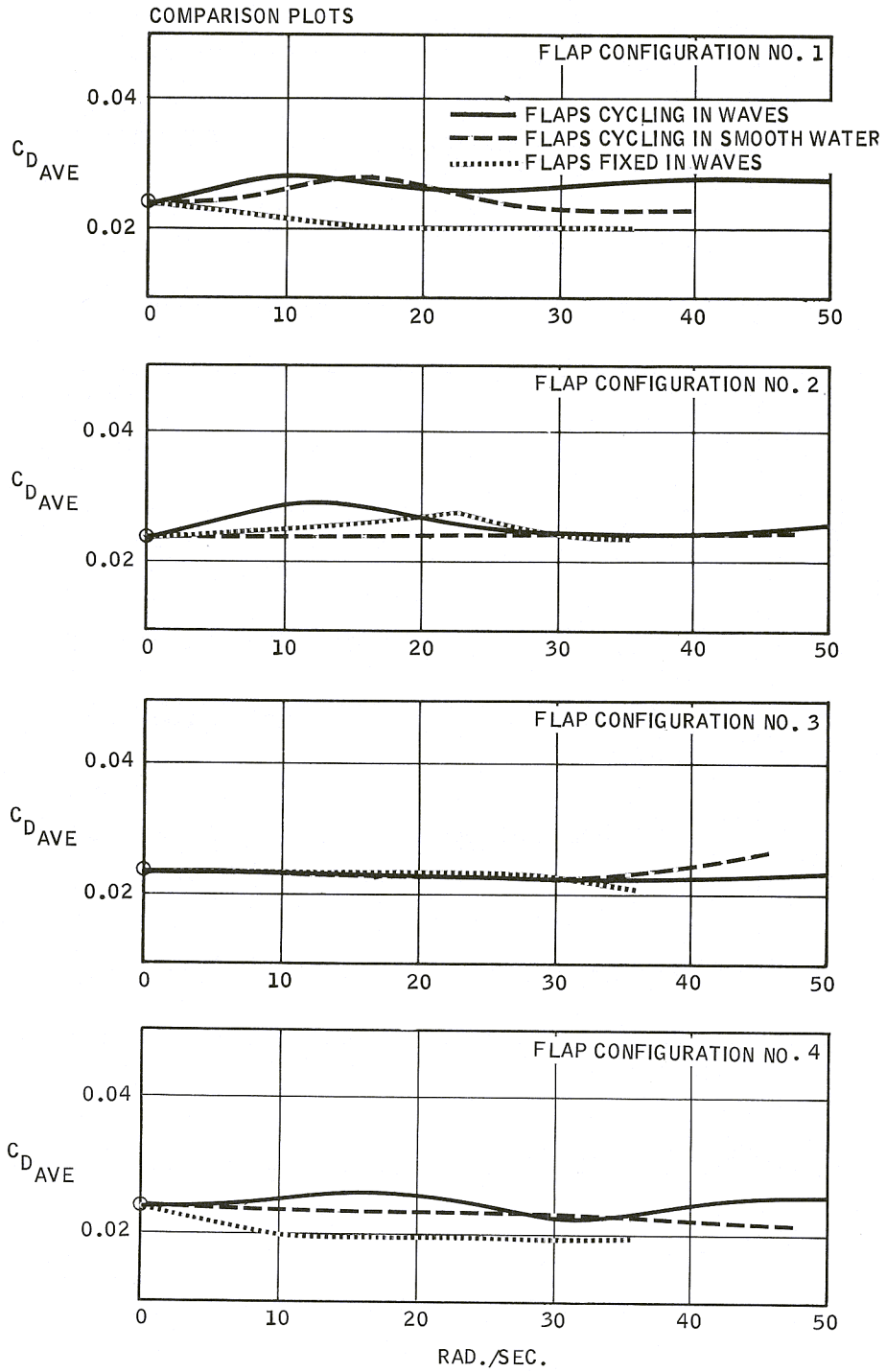


Figure 57. Mean Values of Drag Coefficients — All Models

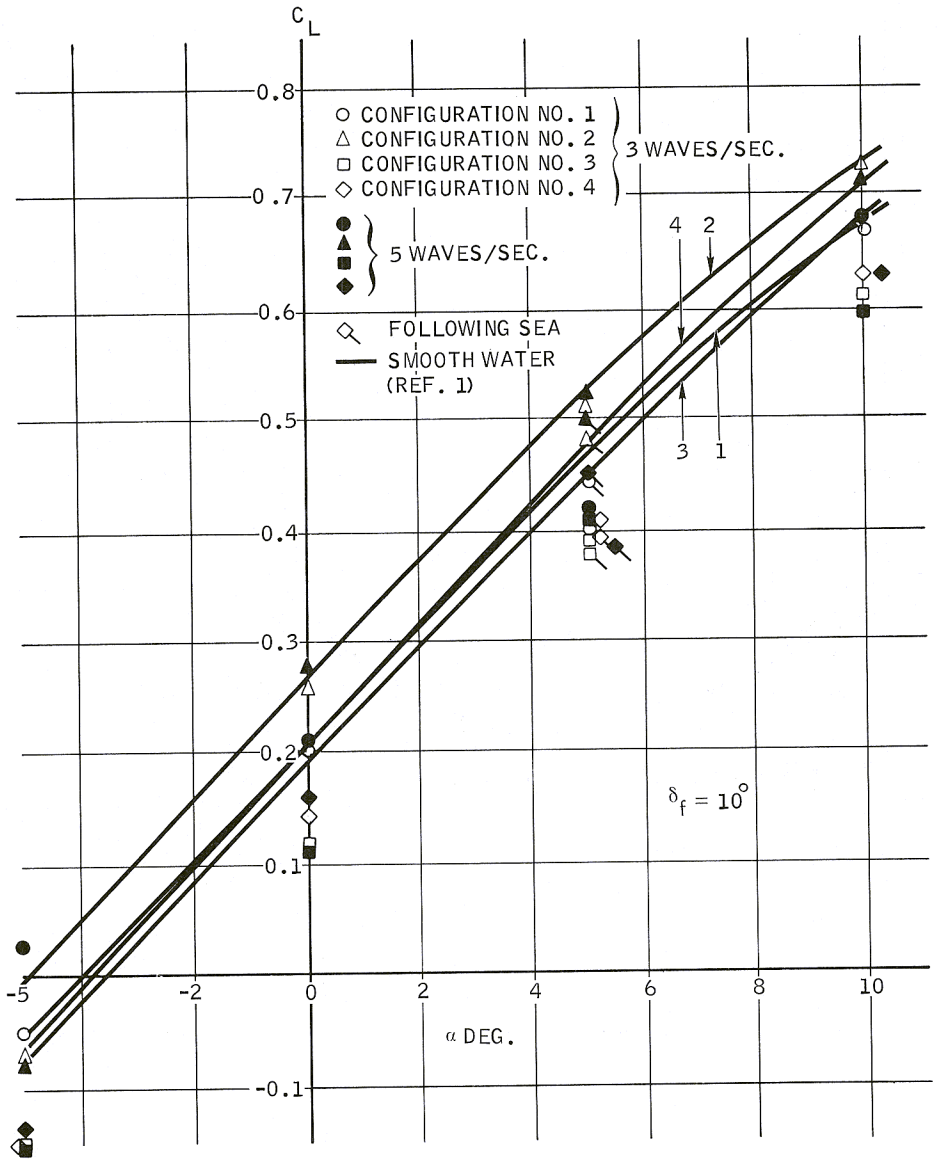


Figure 58. Average $C_L$ Vs. $\alpha$, Flaps Fixed in Waves, and Smooth Water (Ref. 1)

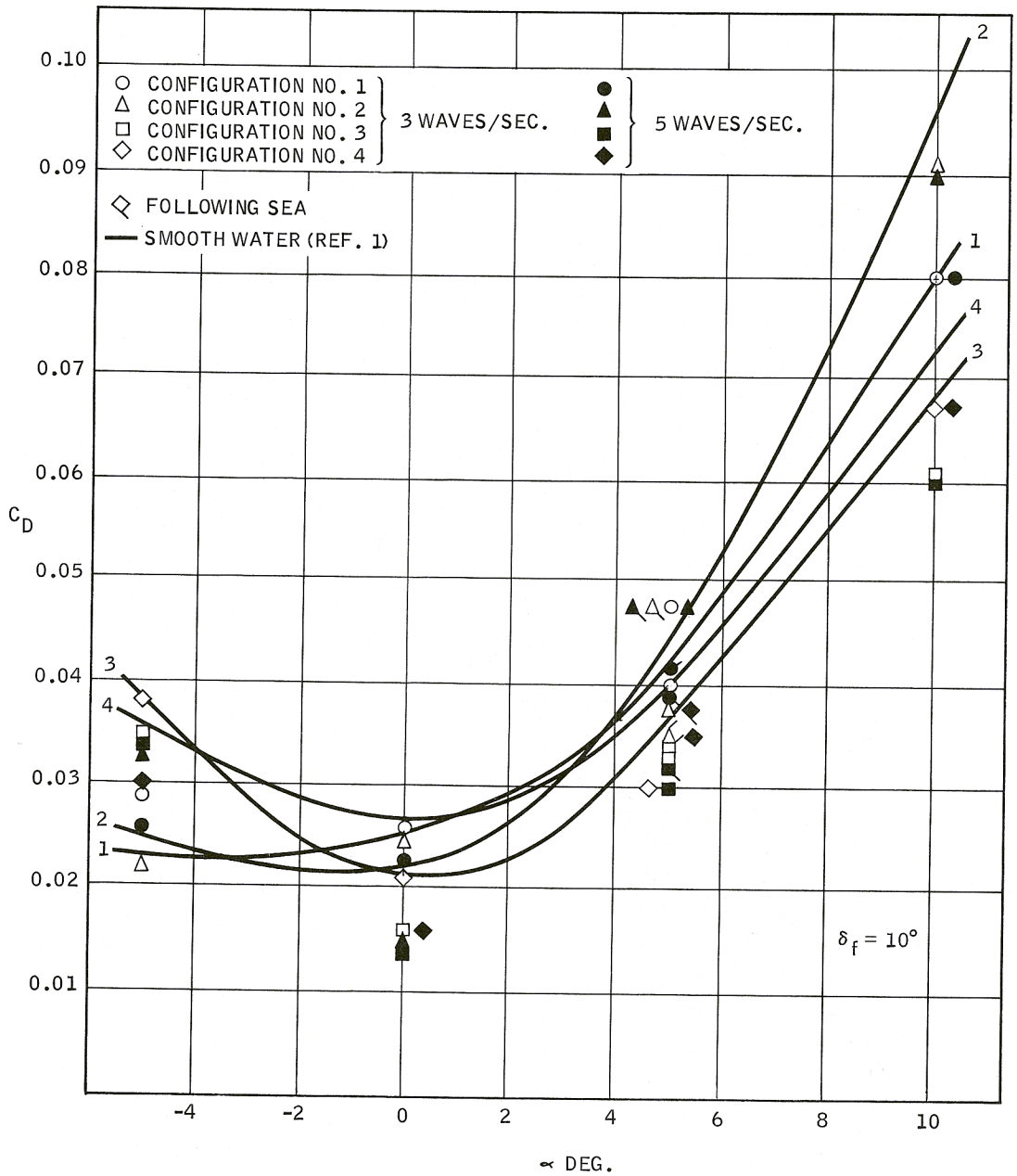


Figure 59. Average $C_D$ Vs. $\alpha$, Flaps Fixed in Waves, and Smooth Water (Ref. 1)

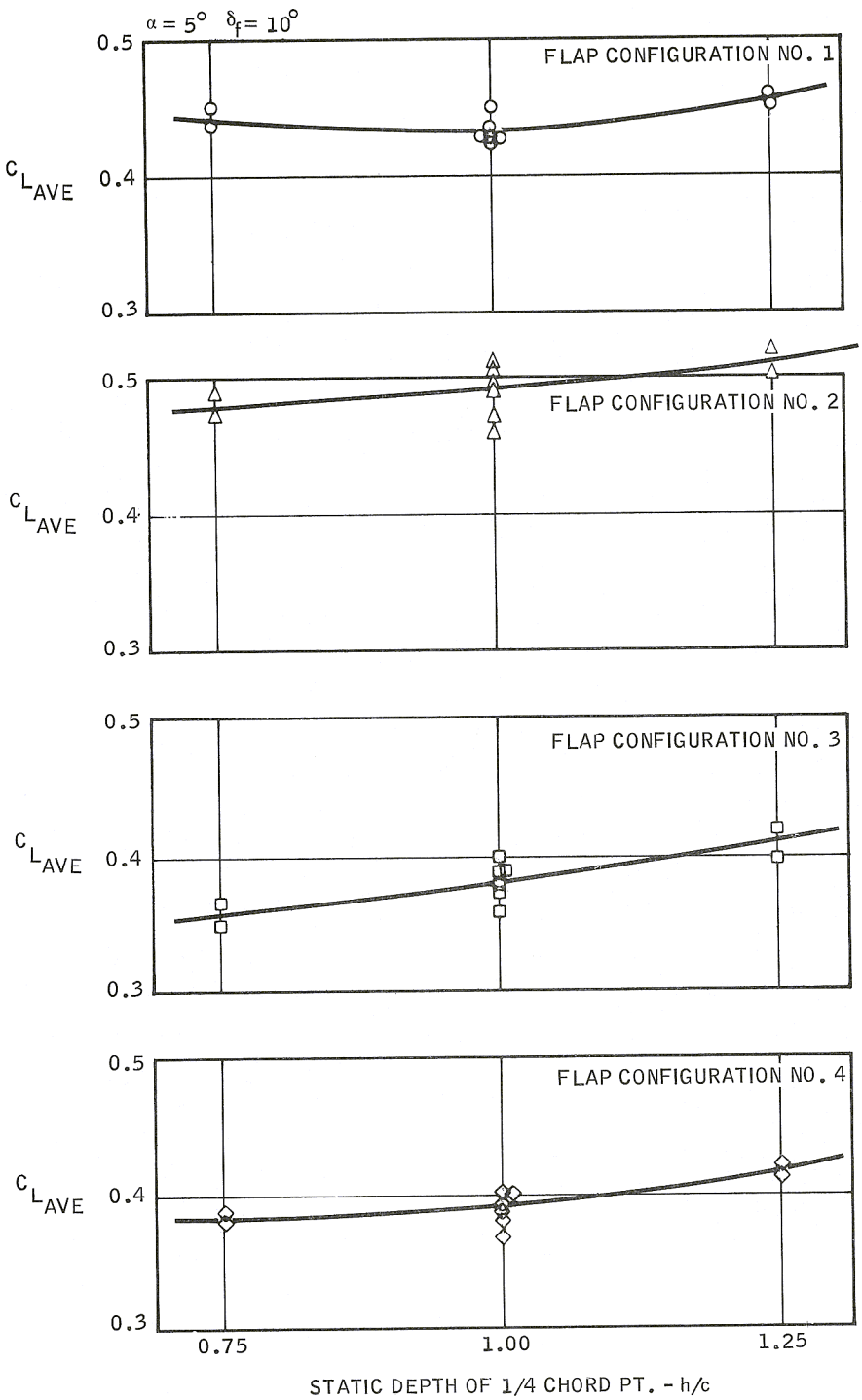


Figure 60. Effect of Depth on Average $C_L$, Flaps Fixed in Waves, Following Sea

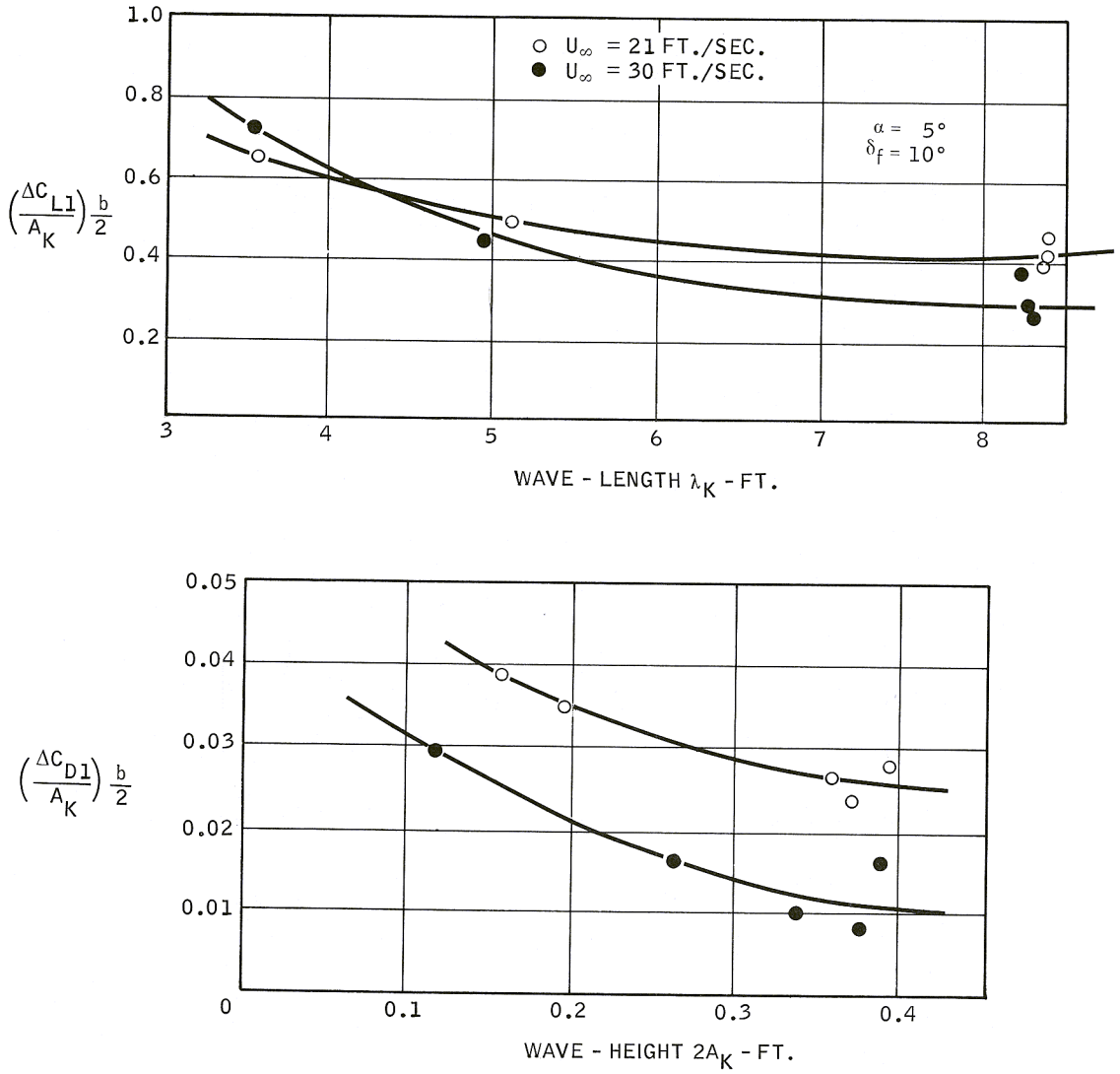


**Figure 61.** Flap Configuration 1 — Oscillatory Lift and Drag Parameters, Flaps Fixed in Waves, Following Sea

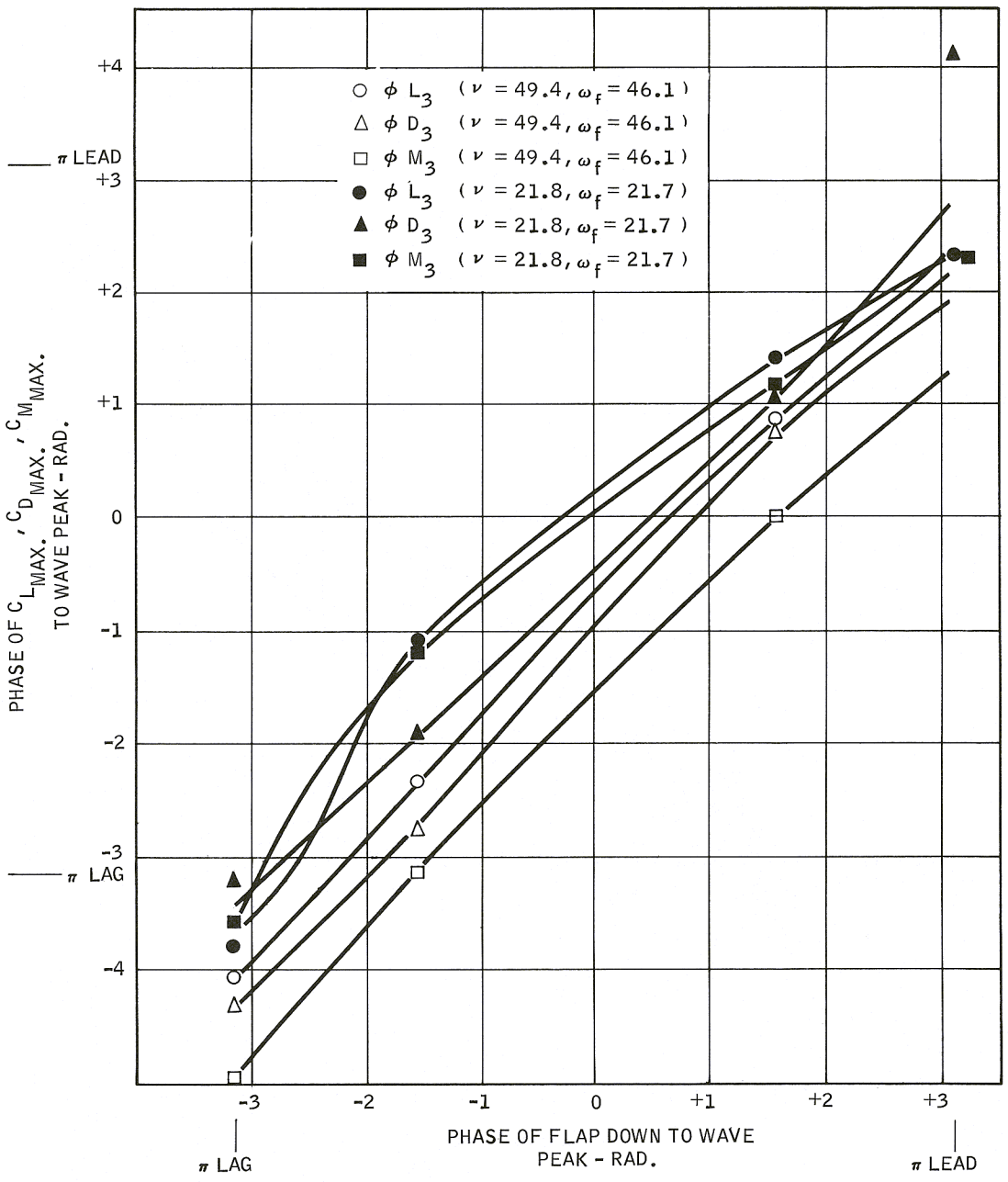


Figure 62. Flap Configuration 1 — Phase Relationships — Flaps Cycling in Waves, Head Sea

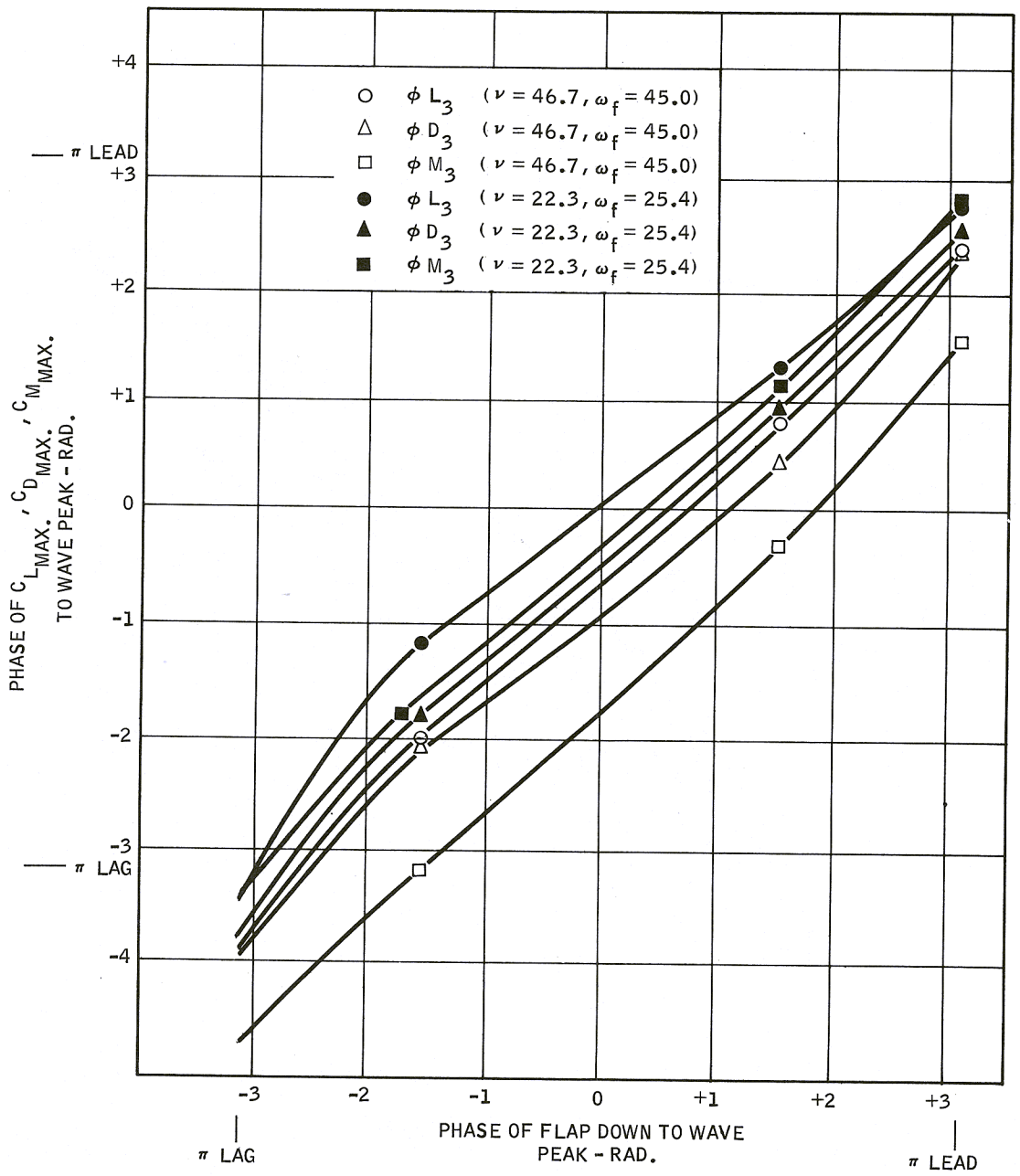


Figure 63. Flap Configuration 2,Phase Relationships — Flaps Cycling in Waves, Head Sea

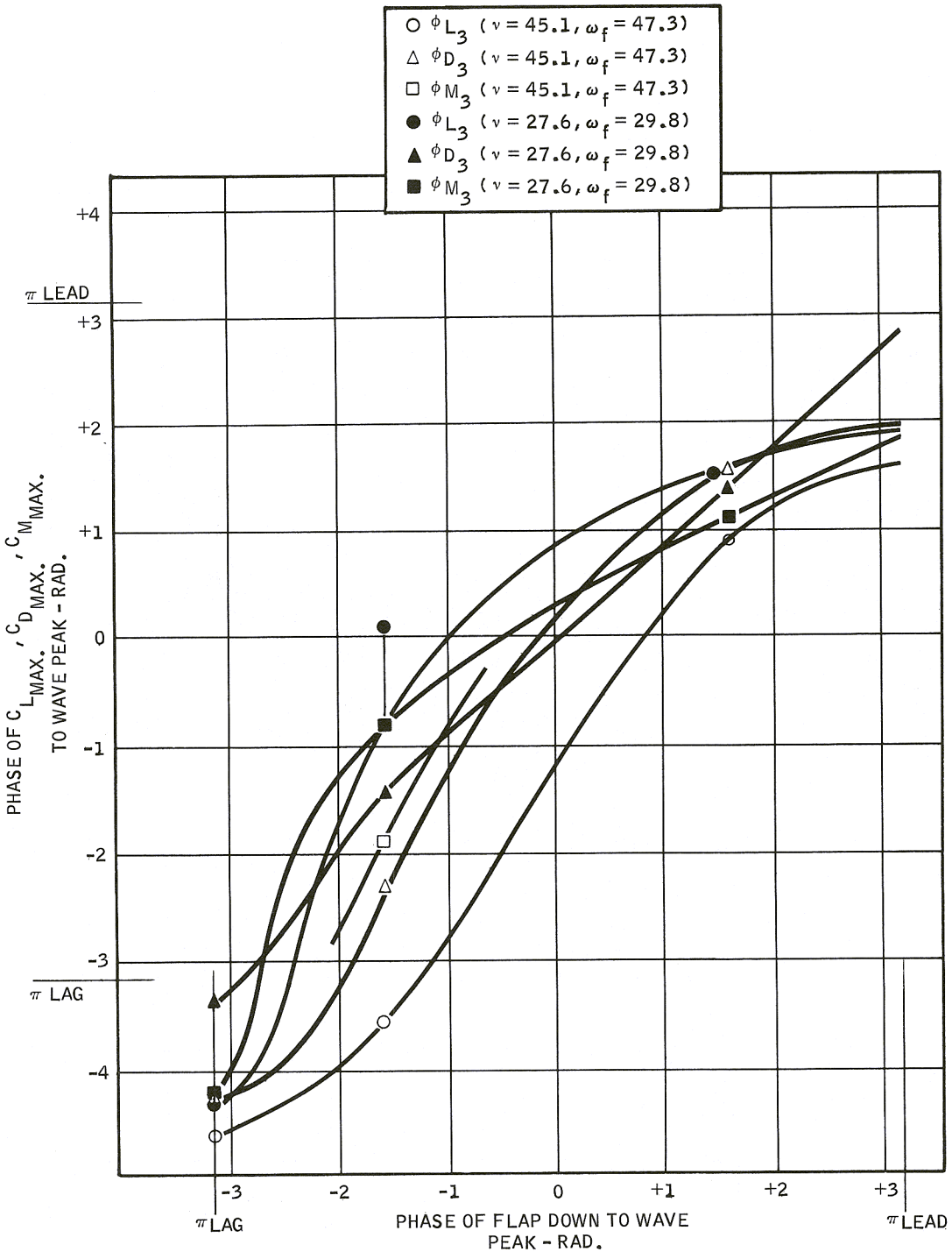


Figure 64. Flap Configuration 3,Phase Relationships — Flaps Cycling in Waves, Head Sea

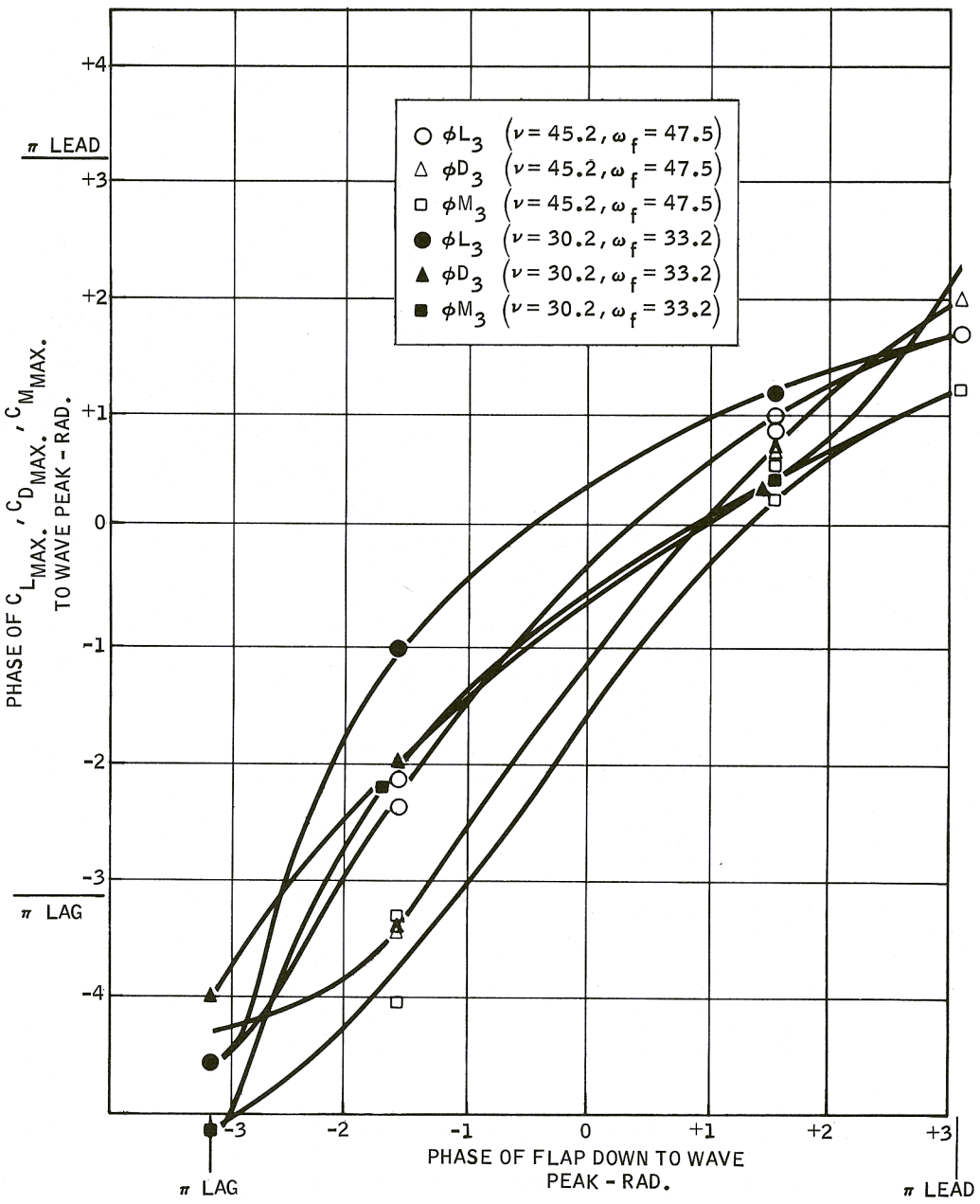


Figure 65. Flap Configuration 4, Phase Relationships — Flaps Cycling in Waves, Following Sea

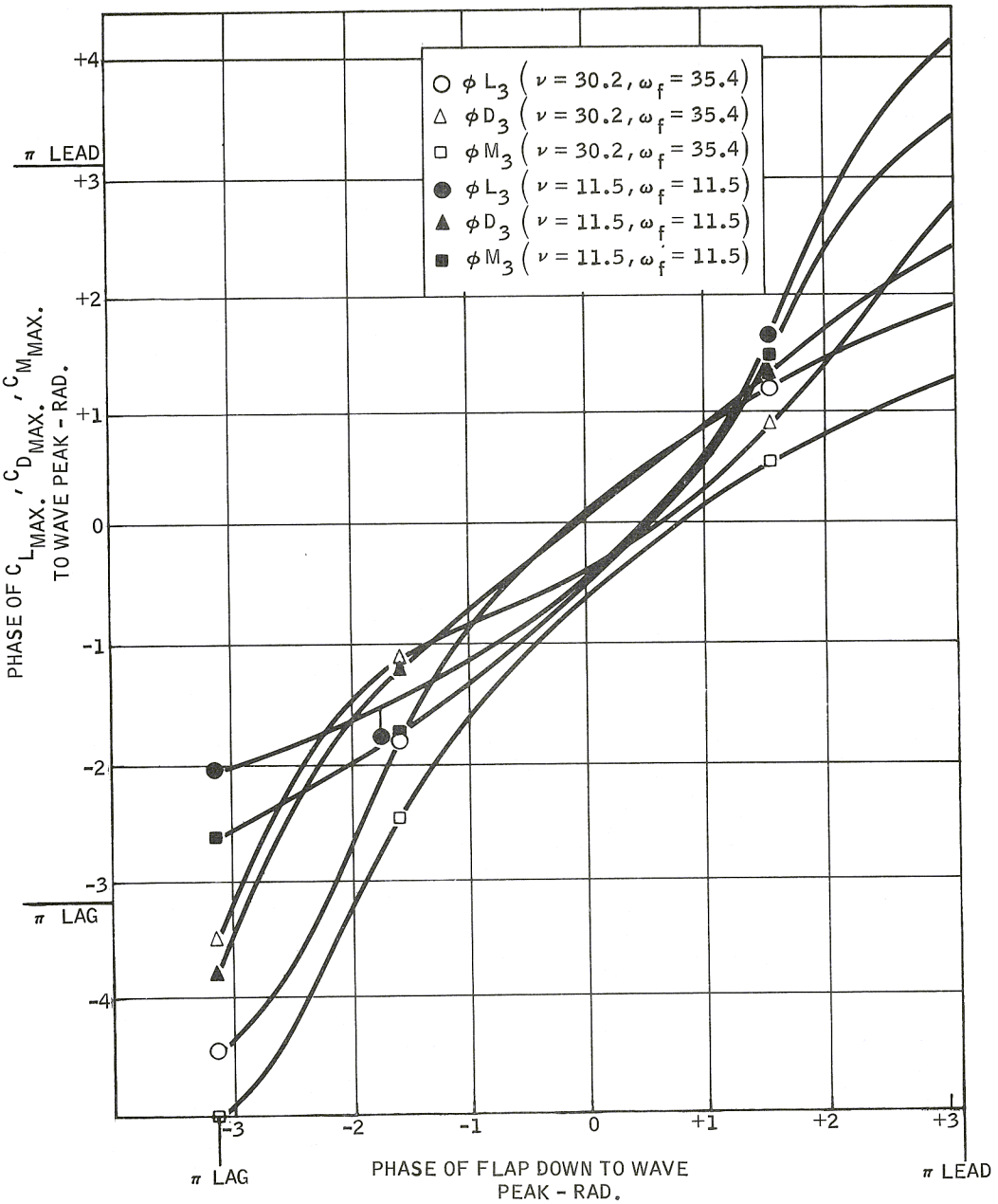


Figure 66. Flap Configuration 2, Phase Relationships — Flaps Cycling in Waves, Following Sea

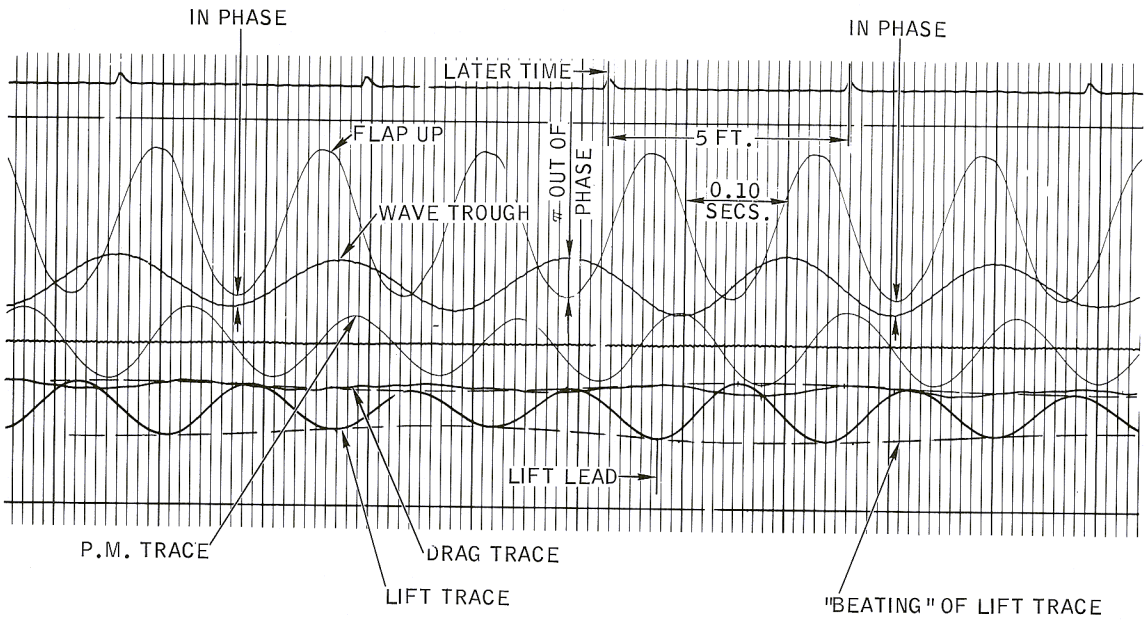


Figure 67. Typical Oscillograph Record, Flaps Cycling in Waves, Following Sea, Run 13191

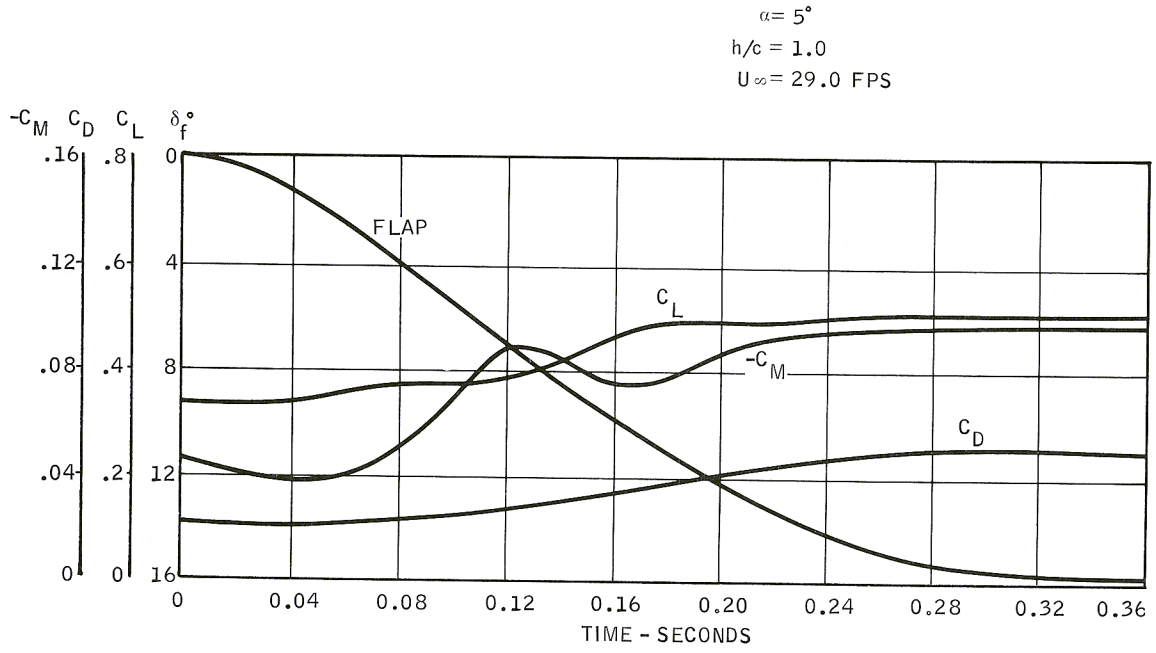


Figure 68. Sudden Flap Deflection, Time History of Force and Moment Build-up — Flap Configuration 1, Run 13125, 16 CPS Flap Cycling Rate

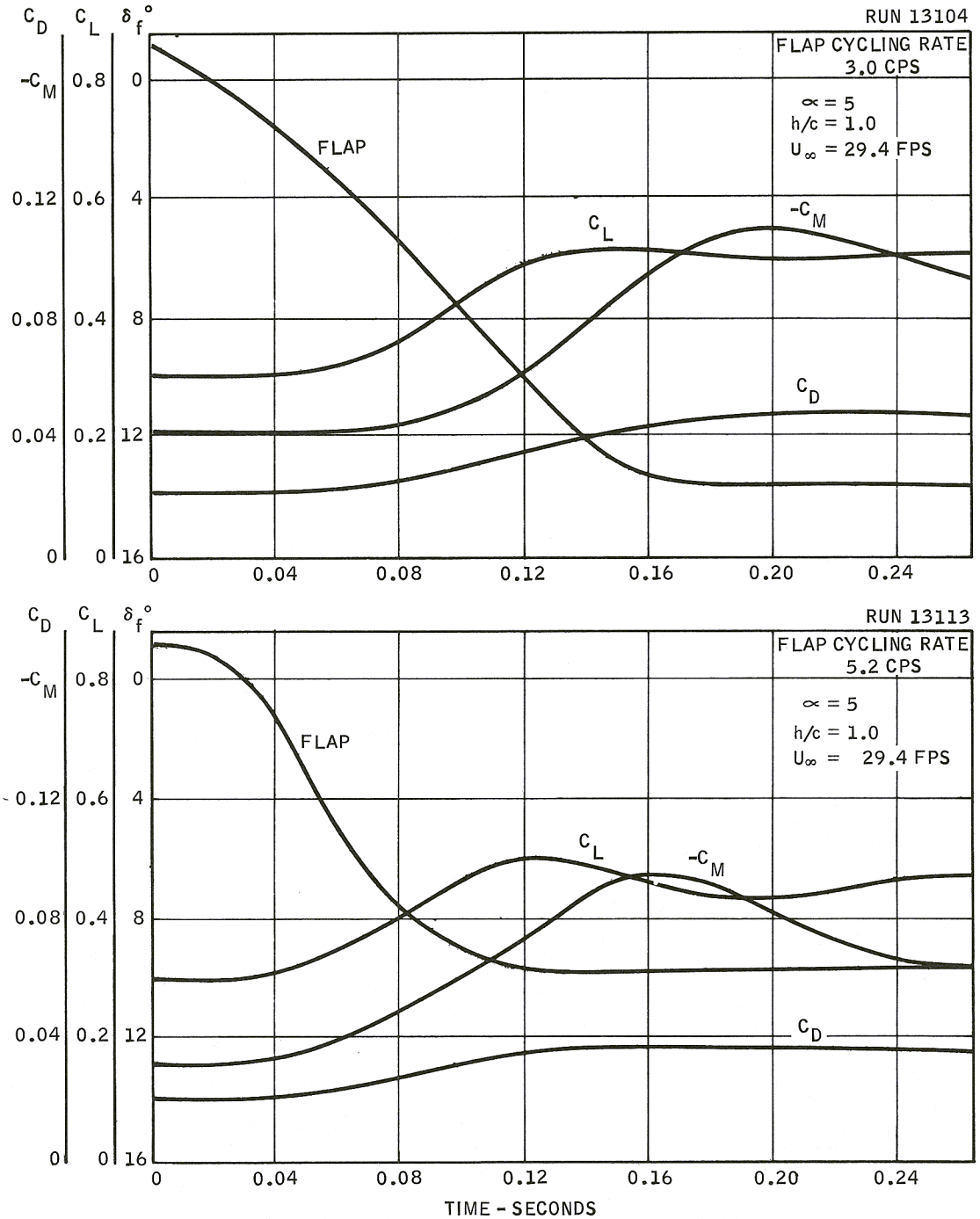


Figure 69. Sudden Flap Deflection, Time History of Force and Moment Build-up — Flap Configuration 1

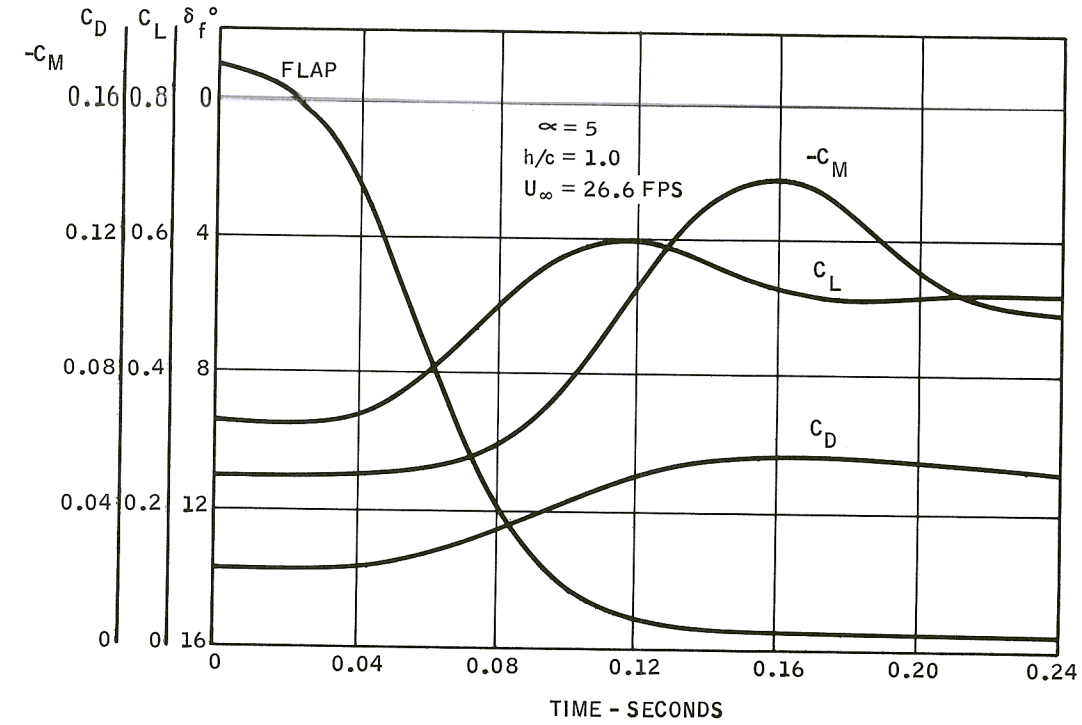


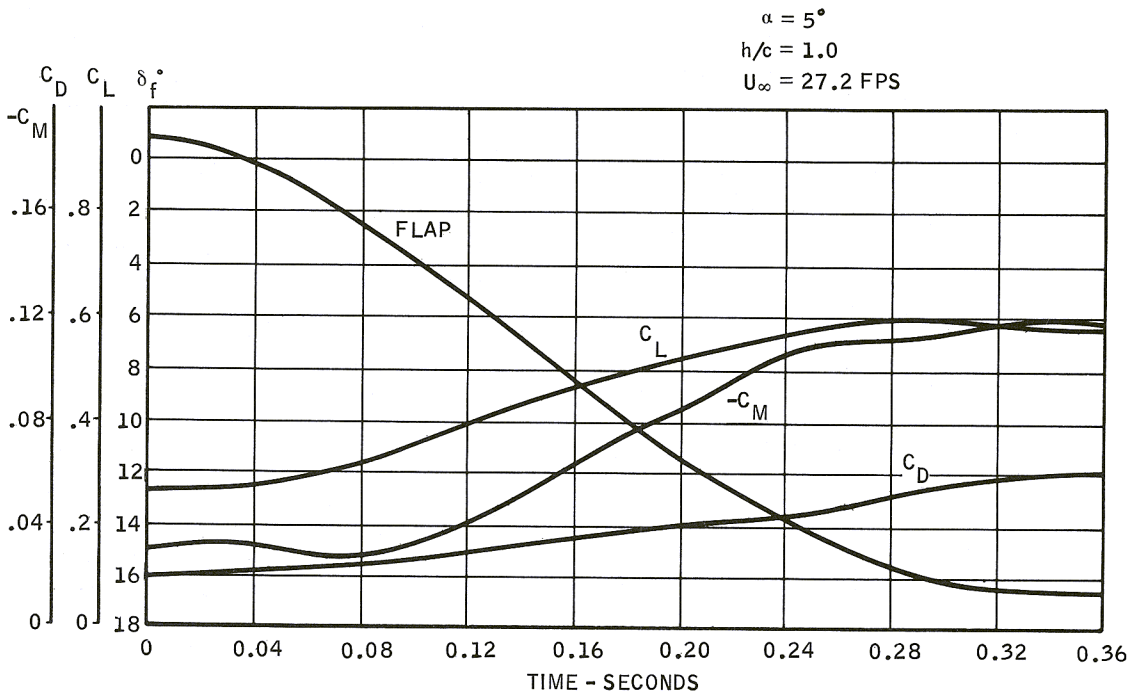


Figure 71. Sudden Flap Deflection, Time History of Force and Moment Build-up - Flap Configuration 2, Run 13230, 1.6 CPS Flap Cycling Rate

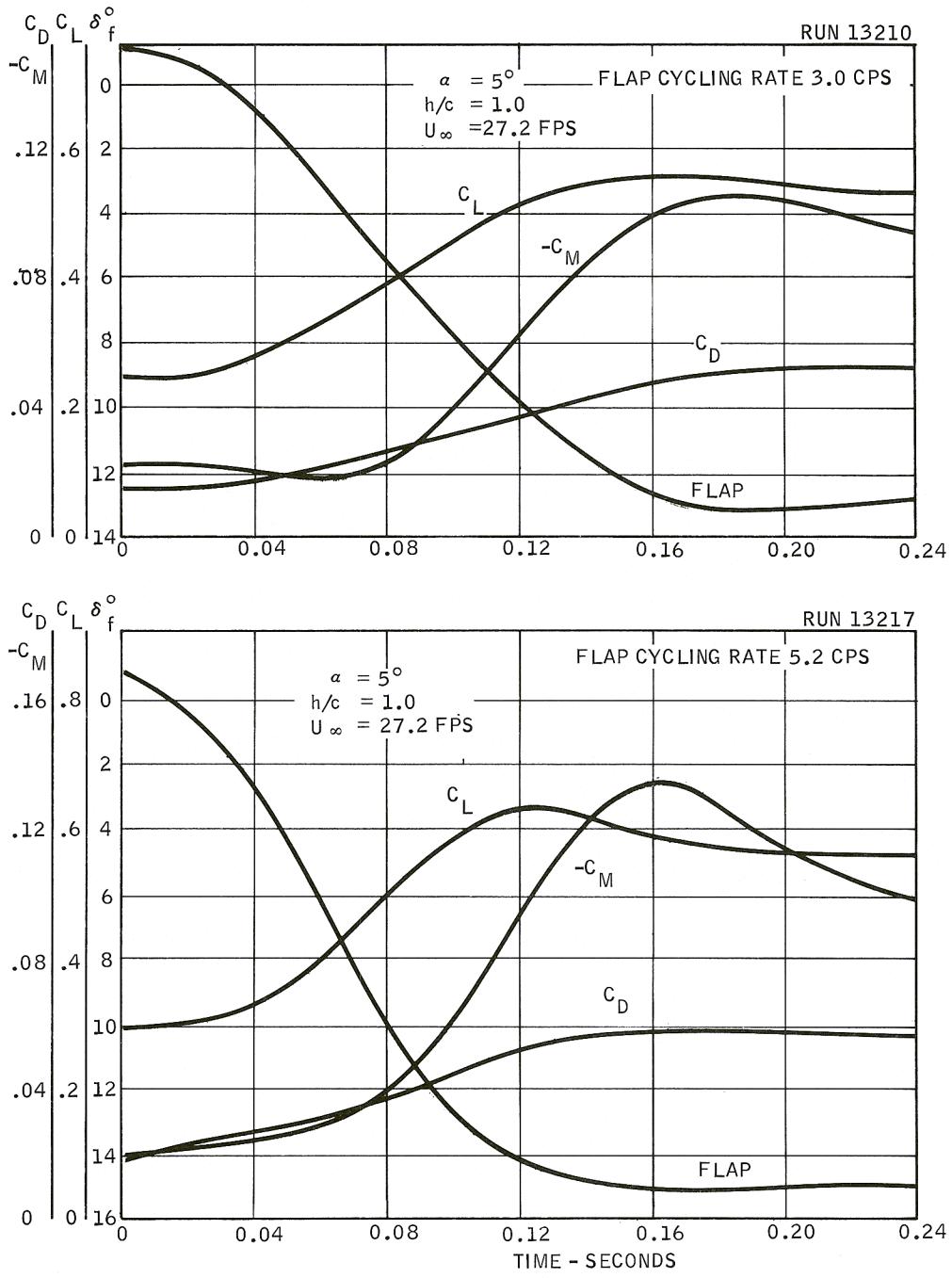


**Figure 72.** Sudden Flap Deflection, Time History of Force and Moment Build-Up — Flap Configuration 2, Run 13210

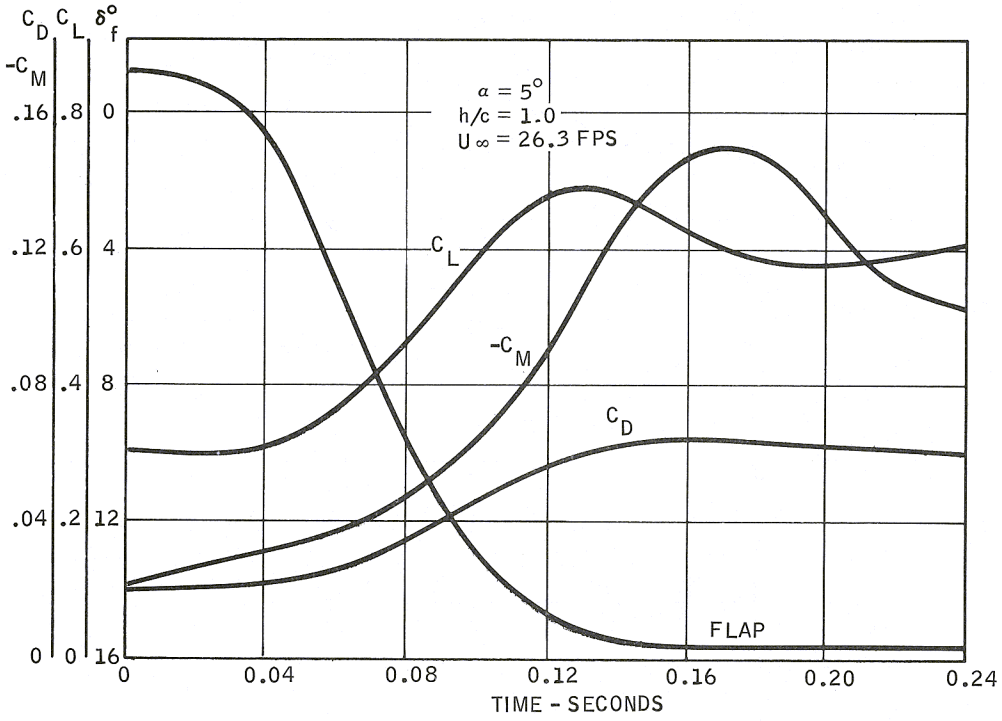


Figure 73. Sudden Flap Deflection, Time History of Force and Moment Build-Up - Flap Configuration 2, Run 13219, 6.5 CPS Flap Cycling Rate

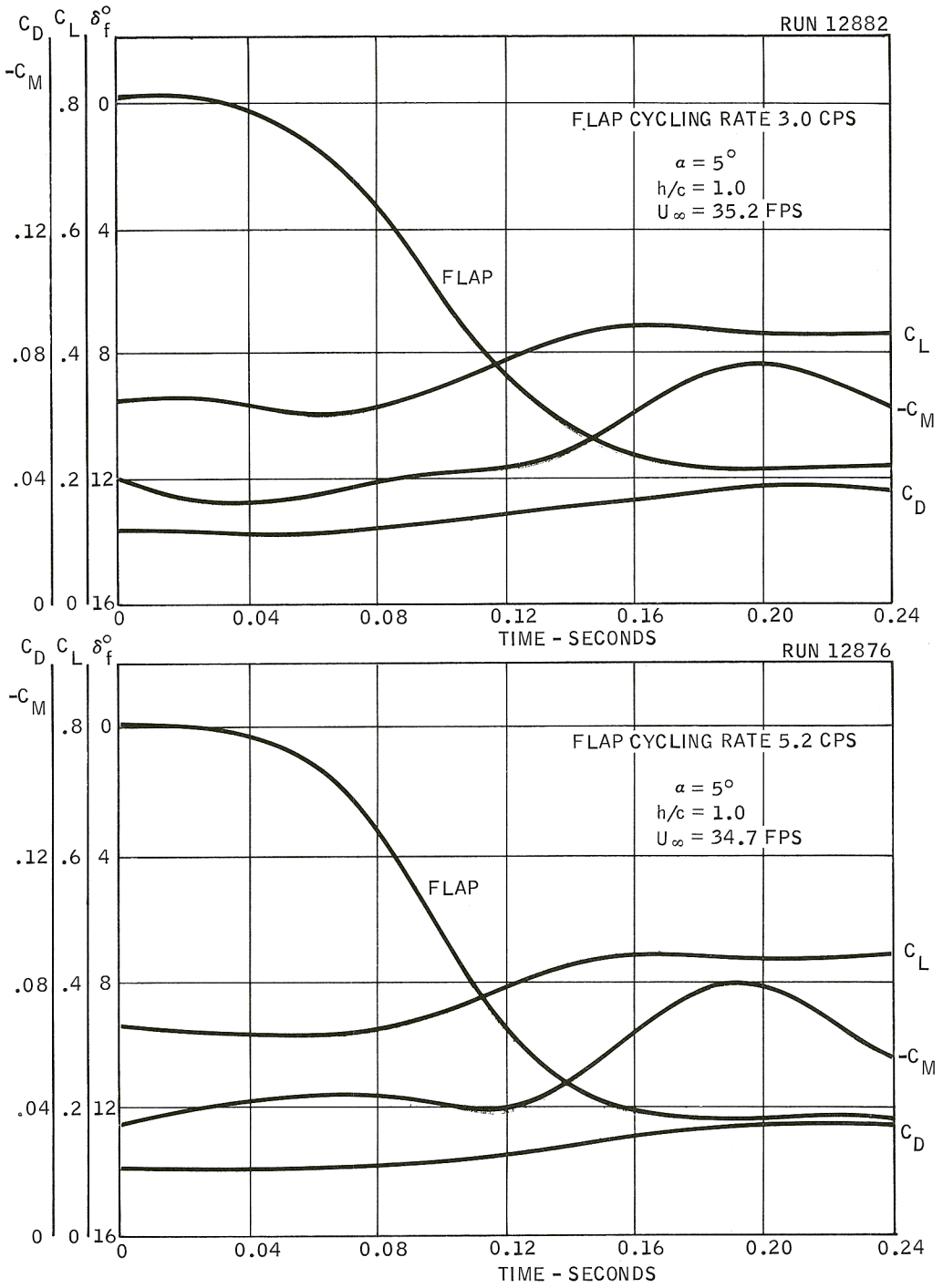


**Figure 74.** Sudden Flap Deflection, Time History of Force and Moment Build-Up — Flap Configuration 3

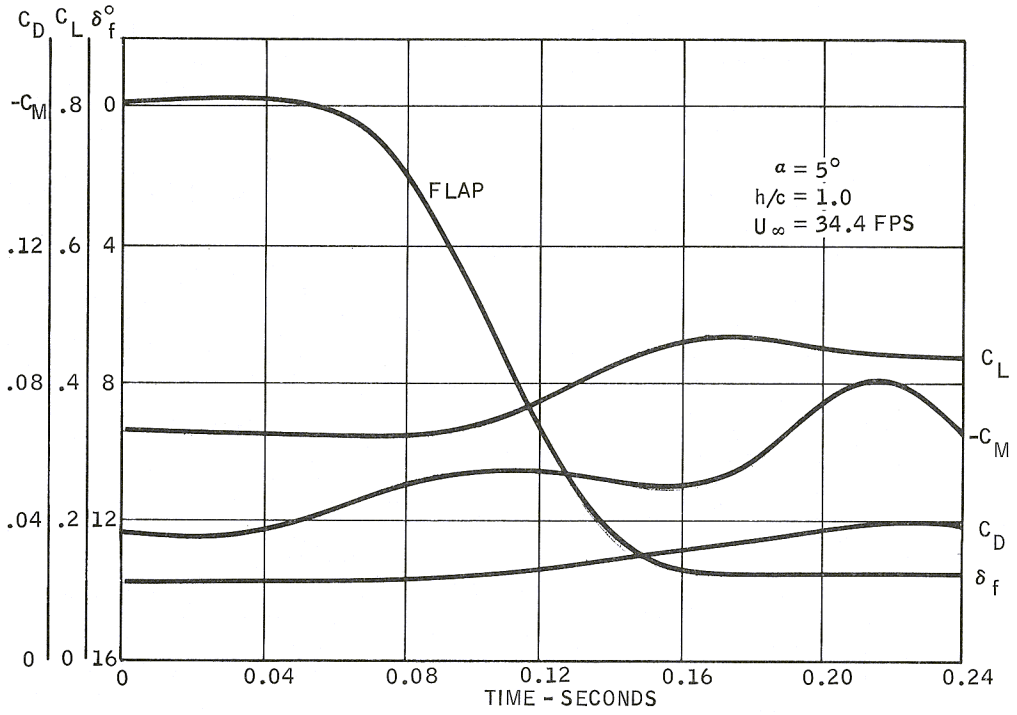


Figure 75. Sudden Flap Deflection, Time History of Force and Moment Build-up — Flap Configuration 3, Run 12878, 6.3 CPS Flap Cycling Rate

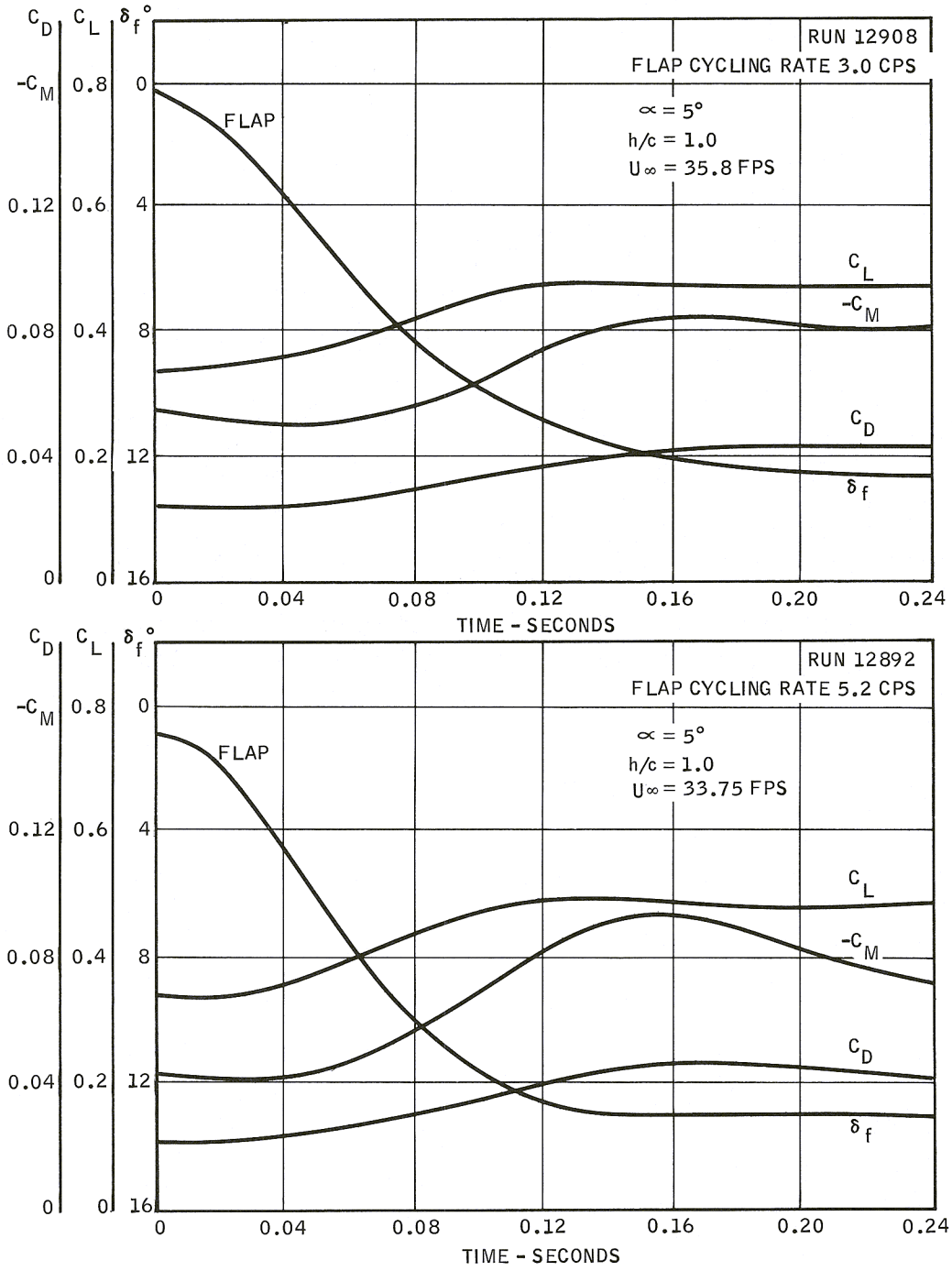


Figure 76. Sudden Flap Deflection, Time History of Force and Moment Build-up — Flap Configuration 4

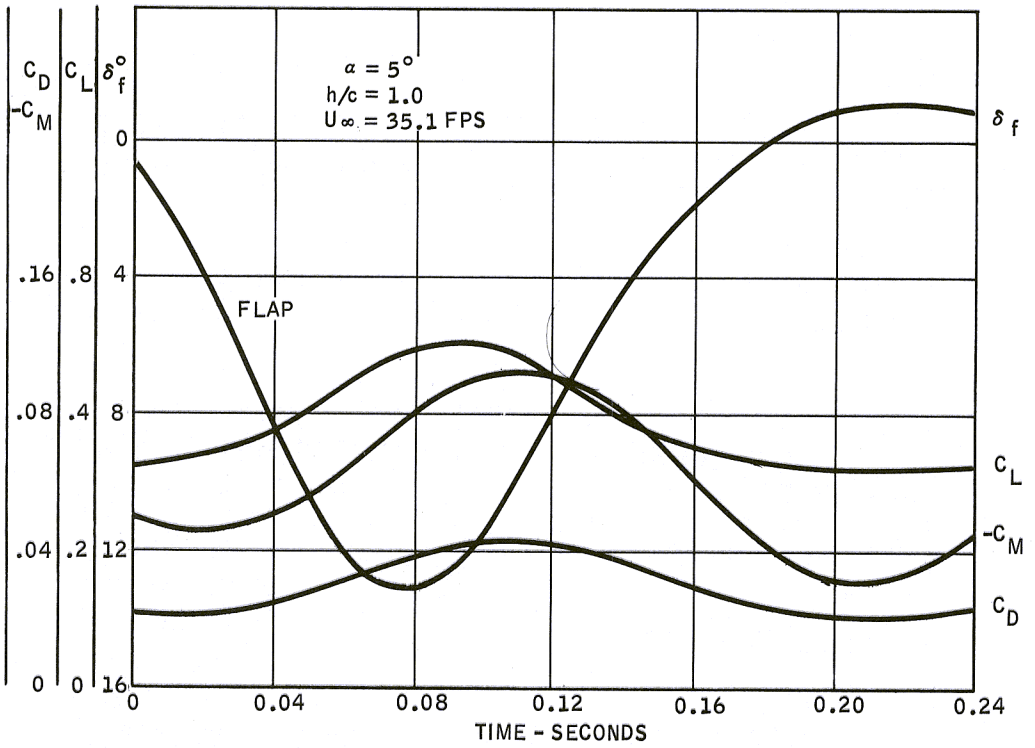


Figure 77. Sudden Flap Deflection, Time History of Force and Moment Build-up — Flap Configuration 4, Run 12895, 6.3 CPS Flap Cycling Rate

# DISTRIBUTION LIST

Copies

3 Chief of Naval Research
Department of the Navy
Washington 25, D.C.
Attn: Code 438
1 Code 461

1 Commanding Officer
Office of Naval Research
Branch Office
495 Summer Street
Boston 10, Massachusetts

1 Commanding Officer
Office of Naval Research
Branch Office
207 West 24th St.
New York 11, New York

1 Commanding Officer
Office of Naval Research
Branch Office
1030 East Green Street
Pasadena, California

1 Commanding Officer
Office of Naval Research
Branch Office
1000 Geary Street
San Francisco 9, California

25 Commanding Officer
Office of Naval Research
Branch Office
Box 39, Navy No. 100
Fleet Post Office
New York, New York

Copies

6 Director
Naval Research Laboratory
Washington 25, D.C.
Attn: Code 2027

Chief, Bureau of Naval Weapons
Department of the Navy
Washington 25, D.C.
1 Attn: Code RUAW-4
1 RRRE
1 RAAD
1 DIS-42

Chief, Bureau of Ships
Department of the Navy
Washington 25, D.C.
1 Attn: Codes 106
310
1 312
1 420
1 421
1 440
1 442
1 449

1 Chief, Bureau of Yards and Docks
Department of the Navy
Washington 25, D.C.
Attn: Code D-400

1 Commanding Officer and Director
David Taylor Model Basin
Washington 7, D.C.
1 Attn: Codes 142
1 500

1 Commanding Officer and Director
David Taylor Model Basin
Washington 7, D.C.
1 Attn: Codes 513
1 520
1 526A
1 530
1 533
1 580
1 585
1 591
1 591A

1 Commander
U.S. Naval Ordnance Test Station
Pasadena Annex
3202 E. Foothill Blvd
Pasadena 8, California

1 Commander
U.S. Naval Ordnance Test Station
China Lake, California
Attn: Code 753

1 Commander
Planning Department
Portsmouth Naval Shipyard
Portsmouth, New Hampshire

1 Commander
Planning Department
Boston Naval Shipyard
Boston 29, Massachusetts

1 Commander
Planning Department
Pearl Harbor Naval Shipyard
Navy 128, Fleet Post Office
San Francisco, California

1 Commander
Planning Department
San Francisco Naval Shipyard
San Francisco 24, California

1 Commander
Planning Department
Mare Island Naval Shipyard
Vallejo, California

1 Commander
Planning Department
New York Naval Shipyard
Brooklyn 1, New York

1 Commander
Planning Department
Puget Sound Naval Shipyard
Bremerton, Washington

1 Commander
Planning Department
Philadelphia Naval Shipyard
U.S. Naval Base
Philadelphia 12, Pennsylvania

1 Commander
Planning Department
Norfolk Naval Shipyard
Portsmouth, Virginia

1 Commander
Planning Department
Charleston Naval Shipyard
U.S. Naval Base
Charleston, South Carolina

1 Commander
Planning Department
Long Beach Naval Shipyard
Long Beach 2, California

1 Commander
Planning Department
U.S. Naval Weapons Laboratory
Dahlgren, Virginia

1 Dr. A. V. Hershey
Computation & Exterior Ballistics Laboratory
U.S. Naval Weapons Laboratory
Dahlgren, Virginia

1 Superintendent
U.S. Naval Academy
Annapolis, Maryland
Attn: Library

1 Superintendent
U.S. Naval Postgraduate School
Monterey, California

1 Commandant
U.S. Coast Guard
1300 E Street, N.W.
Washington, D.C.

1 Secretary Ship Structure Committee
U.S. Coast Guard Headquarters
1300 E Street, N.W.
Washington, D.C.

1 Commander
Military Sea Transportation Service
Department of the Navy
Washington 25, D.C.

U.S. Maritime Administration
GAO Building
441 G Street, N.W.
Washington, D. C.
1 Attn: Division of Ship Design
1 Division of Research

1 Superintendent
U.S. Merchant Marine Academy
Kings Point, Long Island, New York
Attn: Capt. L.S. McCready (Dept of Engineering)

2 U.S. Army Transportation Research & Development Command
Fort Eustis, Virginia
Attn: Marine Transport Division

1 Director of Research
National Aeronautics and Space Administration
1512 H Street, N.W.
Washington 25, D.C.

2 J. B. Parkinson
National Aeronautics & Space Administration
Langley Aeronautical Laboratory
Langley Field, Virginia

1 Director
Engineering Sciences Division
National Science Foundation
1951 Constitution Avenue, N.W.
Washington 25, D.C.

Director
National Bureau of Standards
Washington 25, D.C.
Attn: Fluid Mechanics Division
1 (Dr. G. B. Schubauer)
1 Dr. G. H. Keulegan

10 Armed Services Technical Information Agency
Arlington Hall Station
Arlington 12, Virginia

1 Office of Technical Services
Department of Commerce
Washington 25, D.C.

California Institute of Technology
Pasadena 4, California
1 Attn: Professor M. S. Plesset
1 Prof. T. Y. Wu
1 Prof. A. J. Acosta

3 University of California
Berkeley 4, California
Attn: Division of Engineering

1 University of California
Department of Engineering
Los Angeles 24, California
Attn: Dr. A. Powell

1 Director
Scripps Institute of Oceanography
University of California
La Jolla, California

1 Professor M. L. Albertson
Department of Civil Engineering
Colorado A&M College
Fort Collins, Colorado

1 Professor J. E. Cermak
Department of Civil Engineering
Colorado State University
Fort Collins, Colorado

1 Professor W. R. Sears
Graduate School of Aeronautical
Engineering
Cornell University
Ithaca, New York

3 State University of Iowa
Iowa Institute of Hydraulic Research
Iowa City, Iowa

Harvard University
Cambridge 38, Massachusetts
1 Attn: Prof. G. Birkhoff (Dept of
Mathematics)
1 Prof. G. F. Carrier (Dept
of Mathematics)

Massachusetts Institute of
Technology
Cambridge 39, Massachusetts
1 Attn: Department of Naval
Architecture and Marine
Engineering
1 Prof. A. T. Ippen

University of Michigan
Ann Arbor, Michigan
2 Attn: Prof. R. B. Couch (Dept of
Naval Architecture)
1 Prof. W. W. Willmarth
(Aero Engr Department)
1 Prof. M. S. Uberoi
(Aero Engr Department)

1 Dr. L. G. Straub, Director
St. Anthony Falls Hydraulic
Laboratory
University of Minnesota
Minneapolis 14, Minnesota

1 Professor J. J. Foody
Engineering Department
New York State University
Maritime College
Fort Schulyer, New York

New York University
Institute of Mathematical Sciences
25 Waverly Place
New York 3, New York
1 Attn: Prof. J. Keller
1 Prof. J. J. Stoker
1 Prof. R. Kraichnan

The Johns Hopkins University
Department of Mechanical Engineering
Baltimore 18, Maryland
1 Attn: Prof. S. Corrsin
2 Prof. O. M. Phillips

1 Massachusetts Institute of Technology
Department of Naval Architecture and Marine Engineering
Cambridge 39, Massachusetts
Attn: Prof. M. A. Abkowitz, Head

1 Dr. G. F. Wislicenus
Ordnance Research Laboratory
Pennsylvania State University
University Park, Pennsylvania

1 Professor R. C. DiPrima
Department of Mathematics
Rensselaer Polytechnic Institute
Troy, New York

Stevens Institute of Technology
Davidson Laboratory
Castle Point Station
Hoboken, New Jersey
1 Attn: Mr. J. P. Breslin
1 Mr. D. Savitsky

1 Webb Institute of Naval Architecture
Crescent Beach Road
Glen Cove, New York
Attn: Technical Library

1 Director
Woods Hole Oceanographic Institute
Woods Hole, Massachusetts

Hamburgische Schiffbau-Versuchsanstalt
Bramfelder Strasse 164
Hamburg 33, Germany
1 Attn: Dr. O. Grim
1 Dr. H. W. Lerbs

1 Institut für Schiffbau der Universität Hamburg
Berliner Tor 21
Hamburg 1, Germany
Attn: Prof. G. P. Weinblum, Director

1 Max-Planck Institut für Strömungsforschung
Bottingerstrasse 6/8
Göttingen, Germany

1 Hydro-og Aerodynamisk Laboratorium
Lyngby, Denmark
Attn: Prof. Carl Prohaska

1 Skipsmodelltanken
Trondheim, Norway
Attn: Prof. J. K. Lunde

1 Versuchsanstalt für Wasserbau and Schiffbau
Schleuseninsel im Tiergarten
Berlin, Germany

1 Technische Hogeschool
Institut voor Toegepaste Wiskunde
Julianalaan 132
Delft, Netherlands
Attn: Prof. R. Timman

1 Bureau D'Analyse et de Recherche
Appliquees
2 Rue Joseph Sansboeuf
Paris 8, France
Attn: Prof. L. Malavard

1 Netherlands Ship Model Basin
Wageningen, Netherlands
Attn: Dr. Ir. J. D. van Manen

1 Allied Research Associates, Inc.
43 Leon Street
Boston 15, Massachusetts
Attn: Dr. T. R. Goodman

1 General Dynamics/Convair
San Diego 12, California
Attn: R. H. Oversmith

1 Dynamic Developments Inc.
Midway Avenue
Babylon, New York
Attn: W. P. Carl

1 Dr. S. F. Hoerner
148 Busteed Drive
Midland Park, New Jersey

1 Hydronautics, Incorporated
200 Monroe Street
Rockville, Maryland
Attn: Phillip Eisenberg

1 Rand Development Corporation
13600 Deise Avenue
Cleveland 10, Ohio
Attn: Dr. A. S. Iberall

1 U.S. Rubber Company
Research and Development
Department
Wayne, New Jersey
Attn: L. M. White

Technical Research Group, Inc.
2 Aerial Way
Syosset, Long Island, New York
1 Attn: Jack Kotik
Dr. Paul Kaplan

1 C. Wigley
Flat 102
6-9 Charterhouse Square
London, E.C.1, England

1 AVCO Corporation
Lycoming Division
1701 K Street, N.W.
Apt. 904
Washington, D.C.
Attn: T. A. Duncan

1 Mr. J. G. Baker
Baker Manufacturing Company
Evansville, Wisconsin

1 Curtiss-Wright Corporation
Research Division
Turbomachinery Division
Quehanna, Pennsylvania
Attn: George H. Pedersen

1 Hughes Tool Company
Aircraft Division
Culver City, California
Attn: M. S. Harned

2 National Research Council
Montreal Road
Ottawa 2, Canada
Attn: E. S. Turner

1 The RAND Corporation
1700 Main Street
Santa Monica, California
Attn: Blaine Parkin

1 Stanford University
Department of Civil Engineering
Stanford, California
Attn: Dr. Byrne Perry

1 Waste King Corporation
5550 Harbor Street
Los Angeles 22, California
Attn: Dr. A. Schneider

1 Lockheed Aircraft Corporation
California Division
Hydrodynamics Research
Burbank, California
Attn: Mr. Bill East